Abstract

Title:	ENHANCED SOLUBILITY AND TARGETED DELIVERY OF DRUGS USING CUCURBIT[N]URIL-TYPE COMPOUNDS
	Gaya Kamelika Hettiarachchi, Doctor of Philosophy, 2013
Directed By:	Associate Professor: Volker Briken, Doctor of Philosophy Cell Biology and Molecular Genetics

There is a significant decrease in the productivity of the drug development pipeline due to low drug solubility and high toxicity. Promising solutions to these issues are to use solubilizing excipients and targeted drug delivery systems (DDS).

There is a constant demand for an increased diversity of excipients and DDSs because no one host molecule can encapsulate all drugs. Here we study the use of three novel cucurbit[n]uril (CB[n])-type compounds synthesized by Dr. Lyle Isaacs. Motor1 and Motor2 are highly soluble (105 mM and 14 mM) and unique in acyclic structure. The targeted delivery of drugs was explored using biotin functionalized CB[7].

Phase solubility experiments evaluated improvements to drug solubility. Host biocompatibility was assessed both *in vitro* and *in vivo*. *In vitro* bioactivity studies were conducted using Motor1 complexed with several anticancer drugs and biotin functionalized CB[7] complexed with oxaliplatin. Studies with Motor1 were repeated *in vivo* using NUDE mice baring human cervical cancer cell tumors.

Motor1 and 2 significantly increased the solubility of drugs from many different therapeutic fields, such as paclitaxel (anticancer), cinnarizine (antihistamine), and 17a-ethynyl estradiol (hormone). CB[7] and Motor1 were non-toxicity up to 10 mM in human liver and kidney cell lines. Female Swiss Webster mice continued to gain weight and appeared healthy after three intravenous doses of Motor1 up to 1230 mg/kg. Bioactivity assays using anticancer drugs paclitaxel albendazole, camptothecin and PBS-1086 complexed in Motor1 resulted in significant cytotoxicity in HeLa cells. A pilot *in vivo* tumor treatment study showed tumor growth stabilization with these treatments. Biotin functionalized CB[7] showed cytotoxicity specifically in cells overexpressing the biotin receptor upon targeted delivery of oxaliplatin.

The CB-type compounds significantly increased the solubility of a large variety of drugs across therapeutic fields. This coupled with host toxicity and drug bioactivity data indicate that these CB[n]-type compounds may be invaluable contributions to the toolbox of excipients and DDSs currently available.

ENHANCED SOLUBILITY AND TARGETED DELIVERY OF DRUGS

USING CUCURBIT[N]URIL-TYPE COMPOUNDS

by

Gaya Kamelika Hettiarachchi

Dissertation submitted to the Faculty of the Graduate School of the
University of Maryland, College Park in partial fulfillment
Of the requirements for the degree of
Doctor of Philosophy
2013

Advisory Committee:
Chair: Professor Volker Briken, Ph.D.
Professor Srinivasa Raghavan, Ph.D.
Professor Daniel C. Stein, Ph.D.
Professor Peter Swaan, Ph.D.
Professor Xiaoping Zhu, Ph.D.

Dedication

I dedicate this dissertation to:

My parents Dayananda and Kusum Hettiarachchi and to my brother Ganga

Hettiarachchi without whom I would not have made it this far.

Acknowledgements

First and foremost, I would like to thank my advisor, Dr. Volker Briken for giving me the opportunity to grow as a scientist in his lab. Your immense patience, support and guidance throughout my dissertation work taught me how to think like a scientist and how to ask the right questions. Our discussions broaden not only my scientific knowledge, but also my perspective and overall appreciation for science. I would also like to thank my committee members Dr. Peter Swaan, Dr. Dan Stein, Dr. Xiaoping Zhu and Dr. Srinivasan Raghavan for the invaluable insight, time and support you have dedicated to my dissertation over the past five years.

I would like to thank members of the Briken lab who have been with me through the past five years helping me through the hard times. I would like to thank Jessica Miller for showing me the ropes at the beginning and Amro Boshali for sharing your incredible knowledge, skills and sense of humor. A special thanks to Lalitha Srinivasan who has supported me in my scientific research by double checking calculations, troubleshooting and providing incredibly stimulating scientific conversations. Thank you for helping me stay grounded and laughing throughout the past four years. I will miss our coffee runs. To Jeff Quigley, thank you for being such a good person, for your invaluable sense of reasoning, and for taking care of, what seems like, everything in the lab. Long live the "autoclave fairy". Swati thank you for all your support and your candid look on life that helped put things in perspective for me. Sarah Ahlbrand thank you for all your support and help these last few days, I could not have done it without out you! Good luck with your work!

To my best friend, Sarah Naeem, thank you for being such a pillar of strength, confidence and perseverance; you are a constant inspiration for me.

Finally, and most importantly, I would like to thank my family. I am forever grateful to my parents who raised me with precious moral values and unwavering, unconditional love and support which has enabled me to realize my dreams today. I want to thank my father, Dayananda Hettiarachchi, for teaching me by example to strive for excellence and the immense value of consistent hard work. You taught me to never give up and to give nothing but my absolute best in every task, no matter how little or great it may be. I am immeasurably grateful to my mother, Kusum Hettiarachchi, for teaching me the incredible value of kindness, modesty, perseverance and the great strength in elegance and personal character. You are the two single most amazing people I have and will ever meet in my life. I am incredibly lucky to be your daughter. Finally, I would like to thank my brother, Ganga Hettiarachchi, for always <u>always</u> being there to take care of his little sister, and for never saying 'no.' I would not have gotten this far in life and in accomplishing my dreams if it wasn't for the three of you.

TABLE OF CONTENTS

LIST OF TABLES

LIST OF FIGURES

LIST OF ABBREVIATIONS

In alphabetical order

^{177}Lu – 177-Lutetium

α-CD – Alpha cyclodextrin

β-CD - Beta cyclodextrin

γ-CD – Gamma cyclodextrin

ABZ – Albendazole

ADME – Absorption, Distribution, Metabolism, Excretion

ADP – Adenosine diphosphate

AIDS - acquired immune deficiency syndrome

AK – Adenylate kinase

ATP – Adenosine triphosphate

AUC – Area under the curve

AZT – Azidothymidine

BCS – Biopharmaceutical Classification System

CB[n] – Cucurbit[n]uril

CB[5] – Cucurbit[5]uril

CB[6] – Cucurbit[6]uril

CB[7] – Cucurbit[7]uril

CB[10] – Cucurbit[10]uril

CD – Cyclodextrin

CFU – Colony forming units

CHO-R1 – Chinese Hamster Ovary cells

CPI – Critical Path Initiative

CPT – Camptothecin

CYP450 – Cytochrome P450

DDS – Drug delivery system

DMEM - Dulbecco's modified eagle medium

EC_{50} – Effective concentration

EDTA - Ethylenediaminetetraacetic acid

EMB – Ethambutol

ELISA – Enzyme linked immunosorbent assay

EPR – Enhanced permeability and retention

FCS – Fetal calf serum

FDA – Food and Drug Administration

FDC – Food, Drug, and Cosmetic act

FITC - Fluorescein isothiocyanate

FOLR1 – Folate receptor 1

FOLR2 – Folate receptor 2

FOLR3 – Folate receptor 3

GCP – Good clinical practice

HEK293 – Human Embryonic kidney cells

HeLa – Human cervical carcinoma

HepG2 – Heptacellular carcinoma

HIV – Human immunodeficiency virus

HP-α-CD – Hydroxypropyl – alpha - cyclodextrin

HP-β-CD – Hydroxypropyl-beta-cyclodextrin

HSP – Human subject protection

HT-29 – Human colorectal adenocarcinoma

IC_{50} – Inhibitory concentration

IgE – Immunoglobulin E

IgM – Immunoglobulin M

IND – Investigational New Drug

IPI – Inactive pharmaceutical ingredient

i.p – Intraperitoneal

i.v – Intravenous

L1210 – Murine Lymphocytic leukemia cells

L1210FR – Murine lymphocytic leukemia folate receptor overexpressed cells

LD_{50} – Lethal dose

MCF-7 – Mammary gland adenocarcinoma

MEM – Minimum essential media

MFI – Median fluorescence intensity

MTD – Maximum tolerated dose

MTS – 3-(4,5-dimethylthiazol-2-yl)-5-(3-carboxymethyoxyphenyl)-2-(4-sulfophenyl)-2H-tertrazolium

NAPQI – N-acetyl-p-benzoquione imine

NCATS – National Center for Advanced Translational Sciences

NDA – New Drug Application

NFκB - Nuclear factor kappa B

NIH – National Institutes of Health

NSAID – nonsteroidal anti-inflammatory

PBS - Phosphate buffered saline

PEG – Polyethylene glycol

PFA – Paraformaldehyde

PLGA – Polylactic-*co*-glycolic acid

PSMA – Prostate specific membrane antigen

Pt – Platinum

PTX – Paclitaxel

RAW264.7 – Abelson murine leukemia (murine macrophage)

RBC – Red blood cell

RDRD – Rare disease repurposing database

RES – Reticuloendothelial

RIT - Radioimmunotherapy

(SBE)-β-CD – Sulfobutylether-beta-cyclodextrin

siRNA – small interfering RNA

SK-OV-3 – Human ovarian carcinoma

TB - Tuberculosis

THP-1 – Human acute monocytic leukemia

TNF-α – Tumor necrosis factor alpha

VEGF – Vascular endothelial growth factor

V_d – Volume of Distribution

Chapter 1. INTRODUCTION

1.1 The Drug Development Process

For decades, new medicines have increased and improved the quality and extent of life for billions of people across the globe. Just over the past 10 years, the US has seen an almost 40% decrease in deaths due to cardiovascular disease, and significantly increased life expectancy for HIV and cancer patients as a result of novel therapeutic agents[1]. Therefore, the discovery and development of drugs is an integral part of public wellbeing. The quality and safety of these new therapeutic compounds has been of utmost importance since colonial times. Governmental regulation of drug development and marketing first started with the initiation of the Vaccine Act in 1813 followed by the evaluation of imported drugs and agricultural products in 1848[2]. The Food and Drug Administration (FDA), the oldest consumer protection agency, founded in 1906, passed the Pure Food and Drugs Act in 1906 outlawing commercial companies from "adulterating and misbranding" food and drugs. However, there had not been any regulations requiring drugs and foods be tested prior to marketing[3] until 1938. In 1937, an untested compound called Elixir Sulfanilamide killed over 100 people, many of whom were children. Public outrage pushed the government to step in and pass the Food, Drug and Cosmetic (FDC) Act that ensured any future drugs be proven safe before being marketed[2]. This was later enforced in 1962 by the Kefauver-Harris Drug Amendments which detailed the importance of proving efficacy and greater drug safety. Finally, in 1949, the FDA published the first set of guidelines concerning the production and processing of foods and drugs[2].

The FDA has evolved since these early years and is now heavily involved in the assessment of both domestic and imported foods and drugs in order to ensure adequate efficacy and safety. The FDA plays an integral part in each stage of the drug development process. This process begins after the discovery of lead compounds and consists of preclinical testing, clinical trials and finally approval and marketing by the FDA. Each of these steps is governed by specific guidelines that must be fulfilled before approval can be granted[4] (Figure 1). There are three primary categories that are tested for during preclinical and clinical trials. Researchers and industry promoting new drug candidates must firmly establish the compound's adequate efficacy, pharmacology and reasonable safety [4-7]. Efficacy addresses the question of whether a compound can elicit the proposed and necessary response needed for treatment of the specific disease. Pharmacology essentially defines what happens to a compound once it is administered (pharmacokinetics) and also what happens to the organism in response to the test compound (pharmacodynamics). During preclinical and clinical assessment of a candidate compound, it must be established that its benefits significantly outweigh its negative effects[4]. The details of each of these three categories will be discussed later.
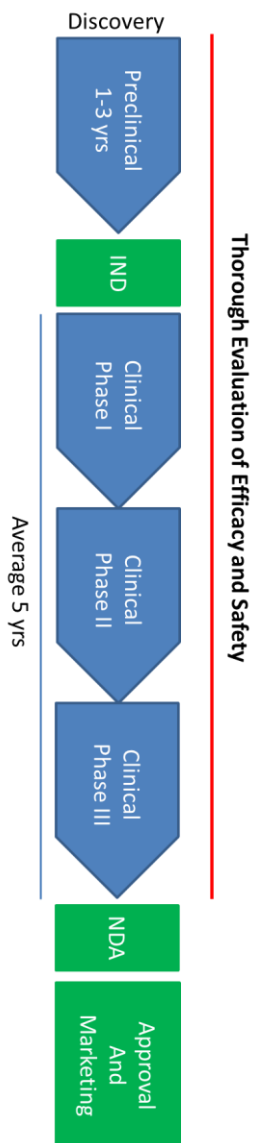
Figure 1: The drug development pipeline in the United States. The drug development process in the U.S involves preclinical testing of candidate drugs using cell based assays and both rodent and non-rodent animal models. This is followed by FDA monitored clinical trials in humans, approval/disqualification, and marketing. Each stage of the pipeline is designed to evaluate three main drug properties: safety, efficacy and pharmacokinetics/dynamics. Figure by Gaya Hettiarachchi

Preclinical testing of drugs involves extensive *in vitro* and *in vivo* analysis of test compounds to firmly determine these three properties. After rigorous testing, in both cell based assays and rodent and non-rodent animal models, an Investigational New Drug (IND) can be filed to receive approval for clinical trials[4]. An IND includes the submission of preclinical data on animal toxicology, efficacy, and pharmacology, manufacturing details including the full chemical composition and formulation of the compound and detailed clinical protocols to minimize unnecessary risk to humans. Once the FDA has reviewed the IND to ensure that adequate safety, efficacy and pharmacokinetics has been established and that clinical trials can be conducted safely, the second stage of the approval process can begin[4, 5].

Clinical trials involve the use of human volunteers to assess the safety, efficacy and pharmacokinetics to determine optimum dosage for a test compound. These trials are often conducted by a medical professional and the length of the trials depends on the specific drug. There are three different clinical trials that must be conducted, Phase I-III, during an approval process[4]. During Phase I, drug testing is conducted at a small scale, between 20-100 volunteers. This is the stage at which toxicity, metabolism and excretion are evaluated. If the candidate compound tests well, it moves into Phase II which comprises of a larger group of volunteers, usually ranging between 100-500 volunteers. During Phase II, efficacy is evaluated along with further studies into compound safety. Finally, Phase III includes the largest scale analysis in clinical trials involving approximately 1000-5000 volunteers. Further evaluation of efficacy and toxicity is conducted at this time and dosage is determined[4]. All clinical trials must be conducted

under good clinical practice (GCPs) guidelines which includes human subject protection (HSP) to ensure the safety of volunteers during these trials[4].

Once the necessary clinical trials are completed, a New Drug Application (NDA) is filed with the FDA clearly stating the findings of all preclinical and clinical trials including compound formulation, dosage regime, and proposed labeling. This information allows for the FDA committee to assess whether the compound is safe and effective in its proposed use, whether the benefits of the drug significantly outweighs its risks, if the labeling is appropriate and complete, and, finally, whether the manufacturing process allows for the maintenance of the compound's quality including strength and purity. The NDA, if approved, allows for marketing and sales of the proposed compound[4].

1.1.1 Drug Development Attrition

Even though the quality of public health relies heavily on the development and commercialization of investigational molecules through the above mentioned process, it is concerning to see that the productivity of the drug development pipeline has significantly decreased[4, 8-10]. For every 10,000 candidate compounds entering the developmental pipeline, only about 250 pass through preclinical trials[10]. Once a compound reaches Phase I clinical trials, it's estimated to have only an 8% chance of being marketed [11, 12]. In clinical trials, attrition rates are upwards of 37% in Phase I, 62% in Phase II and 45% in Phase III[11]. In addition to this, approximately $800 million to $2 billion and over 10 years are invested in developing just one new drug from discovery to marketing [4, 9, 12]. Therefore, this decline in developmental productivity

leads to a significant waste of financial and material resources and also limits the diversity of effective drugs in the market. This decrease in productivity is referred to as drug development attrition[4, 12, 13]. In 2004, the FDA released a statement addressing this issue and, in 2006, they published the Critical Path Initiative (CPI) to help industry battle increasing costs and developmental attrition [11, 14] The CPI addressed several reasons for increasing attritions rates but emphasized the need for new scientific tools to improve compound formulation and testing to study and enhance drug properties.

Though establishing drug safety, high efficacy and pharmacokinetics is increasingly essential during the developmental process, these three properties are also the largest contributors to developmental attrition[4]. High toxicity, seen as adverse effects, in humans, is responsible for about 11% of failing drugs while the lack of efficacy contributes to about 30% of all drugs failing the developmental pipeline[15, 16] (Figure 2). Finally, the most significant factor affecting a candidate compound's success is its bioavailability. Low drug bioavailability contributes to at least 39% of all lead compounds failing the developmental pipeline[15].

Developmental attrition is observed across therapeutic fields, but is more prominent and detrimental in specific diseases such as cancer. Cancer is a disease of the cells that is the leading cause of mortality contributing to about 13% of all deaths worldwide in 2008. Lung, stomach, liver, colon and breast cancers have been shown to have the highest rates of mortality[17]. This high rate of mortality can, in large part, be attributed to the lack of effective drugs. Studies have shown that the success rate for candidate anti-cancer drugs within the drug development pipeline is only about 5%[12]. It should be noted that even marketed anticancer drugs have limited use. This attrition is

primarily due to their low solubilities and high toxicities which will be discussed in detail later[18].

1.1.1.1 Toxicity

Once potential drug bioactivity is established at the discovery stage, the first and foremost study that is conducted is a comprehensive analysis of the compound's toxicity[19, 20]. Toxicity is evaluated at several stages of the drug development pipeline[5, 21]. There are several different forms of toxicity, each of which, if severe enough, can lead to the elimination of a drug from the development pipeline. As stated before, it is essential that the benefits of a test compound greatly out way its risks in order to obtain FDA approval[21]. Oxaliplatin is an example of an anticancer drug that is dose limited by its high toxicity. This drug works by binding to DNA, in turn, forming adducts that prevent DNA synthesis thus inducing cell death. Oxaliplatin is a very potent compound that is effective against a large variety of different types of cancer, however, it is limited by its severe peripheral neuropathy and neurotoxicity[22, 23]. Despite these adverse effects, oxaliplatin is still used at lowered doses in the combination with other anticancer drugs to enhance efficacy[23, 24].

Because the key to alleviating attrition due to toxicity is its efficient prediction before the drug candidate reaches later stages of development, understanding the different forms of toxicity and using the appropriate assays to detect it is essential[19, 25]. The FDA has set guidelines for industry and investigators to help in the proper evaluation of drug toxicity[26]. They recommend testing and providing adequate information on single and multiple dose toxicity that may stem from immunological, biologically activated,

genetic, reproductive and/or developmental toxicities [5, 25-27]. *In vivo* toxicity can be presented as a maximum tolerated dose (MTD), or lethal dose (LD$_{50}$)[20].

Immunological Toxicity

There are five different forms of immunological toxicity; however, the most common are hypersensitivity and immunogenicity to test compounds or their metabolites [26-28]. Drug compounds can bind to and react with proteins that induce the production of antibodies, release cytokines, or induce inflammation[28]. One example is the hypersensitivity to cremophor®EL observed in many patients who are administered this solvent in complex with an insoluble drug [29-31]. Cremophor®EL is a surfactant that was used to solubilize compounds such as the anti-cancer drug paclitaxel (Taxol®). Even though this combination was used for years to treat many types of cancer, the hypersensitivity to cremophor®EL has been shown to include clinical outcomes such as respiratory arrest, cardiac collapse and, in some cases, death [29, 30]. Approximately 41% of all patients receiving Taxol® produced symptoms of severe hypersensitivity. How these adverse reactions are brought about is still unclear, but complement activation by cremophor®EL is thought to be responsible[31].

Immunological toxicity can sometimes be difficult to predict early on in development as a result of individual vulnerabilities in the immune system. However, several assays like ELISAs can be used to detect cytokine release or antibody production. These assays can be run using serum collected from humans and animals following dosing of the test compound. Collected blood samples can also be used to establish white blood cell count and assess any hemolytic effects the candidate may have[28].

Biologically Activated Toxicity

Toxicity resulting from bioactivation is primarily due to the production of toxic by-products during drug metabolism. The liver is the principle organ responsible for drug modification. Metabolism can produce either deactivated, ineffective or potentially toxic metabolites that lead to liver, blood or other organ toxicity. This problem can be somewhat addressed by dose control or medicinal chemistry approaches to substitute sensitive functional groups [32, 33]. One such example is Acetomenaphine, the most widely used drug in the United States. Acetomenaphine has a well-established record of safety and efficacy, however, overdose of this drug can lead to severe liver damage and even liver failure due to the accumulation of the toxic metabolite, NAPQI (N-acetyl-p-benzoquinone imine), in the liver[34, 35].

Biologically activated toxicity in the liver can be predicted through extensive preclinical assays using liver derived microsomes and several isolated CYP450 enzymes. These tools can be used to metabolize drug candidates and check for improper metabolism or toxic by-products by using *in vitro* cell viability or death assays or animal models [36-38].

Genetic Toxicity

Genetic toxicity is defined by the ability of a compound to damage the DNA and/or chromosomes of cells. This damage can then lead to genetic mutations that can, in turn, lead to certain diseases such as cancer or birth defects defined as carcinogenicity[39]. There are several examples of drugs and substances that have been

earmarked to be genetically toxic or carcinogenic. Many anticancer drugs, like tamoxifen and melphalan, are categorized as "Known to be a human carcinogen" by the National Toxicology Program (NIH)'s Twelfth Edition (2011) Report on Carcinogens[40]. Furthermore, cyclosporine A, an immunosuppressant used in organ transplants, is also categorized as "Known to be a human carcinogen."[40]

FDA guidelines require the assessment of both in multiple ways. Some *in vitro* mammalian cell assays include the mammalian lymphoma assay and the Ames test [41-43]. However, following these cell based evaluations, long-term mutogenecity and carcinogenicity studies in animal models must also be conducted to adequately determine the presence or absence of this form of drug toxicity [27, 39, 42, 44, 45].

Reproductive and Developmental Toxicities

Reproductive toxicities refer to damage inflicted on organism fertility, parturition and lactation while developmental toxicity refers to damage to embryo survival, growth, or malformations [27, 46, 47]. One example of a drug that has been shown to cause reproductive toxicity in animals and humans is the broad spectrum antibiotic tetracycline [48].

Reproductive toxicity can be evaluated with histopathological studies conducted using an animal model following repeated dosing of the test compound. Furthermore, these dosed mice can be mated to not only further evaluate the effects of the candidate compound on reproductive organs but also on the development of an embryo and fetus [46, 47, 49]. Damage to embryos with the use of a candidate drug can be assess through the frog embryo teratogenesis assay, for example, which is essentially a 96-hour whole

embryo assay that can measure a compound's ability to induce mortality, malformation, and growth inhibition. Long- term, multiple doses studies may need to be conducted in the *in vivo* preclinical and clinical stages to further assess these types of toxicities [46, 47, 49, 50].

1.1.1.2 Efficacy

Drug efficacy, another factor contributing to the developmental success of a candidate drug, is defined as the maximum response a compound has in its proposed use [4, 19, 51, 52]. Efficacy depends on drug composition or chemistry and testing for it will depend on the drug's purpose or activity[16]. Efficacy has to be established both *in vitro* and *in vivo* in preclinical testing as well as in clinical trials and is usually presented as the effective or inhibitory concentration (EC_{50} or IC_{50}) at which a response halfway between the baseline and maximum responses is observed [19, 51, 52]. These values are calculated from a dose-response curve [4, 16, 52].

Factors leading to developmental attrition.

Low drug efficacy is a growing problem in current day drug development, resulting in approximately 30% of all failed compounds in the FDA approval process and countless more during drug discovery and preclinical trials [5, 12, 15]. Many of these abandoned compounds are shelved while resources are funneled into the synthesis of new candidate drugs. There are several factors that can cause low drug efficacy. One example may be that the drug does not bind to the appropriate receptors. Another is that even if it does bind to the receptor, it may not induce the desired or adequate response at this site [51, 53].

Low drug efficacy is a fast growing problem. Many of these drugs go through preclinical and clinical trials and are shown to be safe for human use, but are not used for actual treatment of diseases due to low efficacy in their proposed purpose[54]. To address this, the FDA and the NIH have turned their attention to repositioning and repurposing many of these abandoned drugs[55]. This idea essentially proposes to take these abandoned, yet safe drugs and find uses for them in the treatment of other common or rare diseases. This concept has been around for some time now, for example zidovudine (better known as AZT), a nucleoside analog reverse-transcriptase inhibitor, was originally developed to treat cancer but was abandoned due to low efficacy. However, this drug was re-investigated during the HIV/AIDs epidemic and became the first drug to be used to treat patients with HIV/AIDs[54]. There are many other drugs like zidovudine that have been repurposed in the past, however, as a result of a significant increase in developmental attrition in recent years, several organizations like the FDA and the NIH, came together to form specialized programs solely for this purpose. One such program is the National Center for Advancing Translational Sciences (NCATS) branch of the NIH[56]. This program has invited researchers to find new uses for 58 compounds released by 8 pharmaceutical companies. All 58 drugs were evaluated through preclinical testing and their safety was established in human clinical trials but were abandoned due to low efficacy in their initially proposed uses[57] Another program set forth by the FDA (Office of Orphan Products Development) focuses on the repurposing of both marketed and abandoned drugs for the treatment of rare diseases; from this program the Rare Disease Repurposing Database (RDRD) was born[58].

1.1.1.3 Pharmacokinetics

Drug pharmacokinetics include several components: absorption (A) of a compound across mucosal surfaces such as the epithelial layer of the GI tract, the systemic distribution (D), liver metabolism (M) and finally the excretion (E) of the compound from the system[15, 59, 60]. The ADME is also referred to as a compound's bioavailability or the rate and extent to which it reaches its necessary site of activity [7, 15, 61, 62]. One of the most significant factors contributing to bioavailability is its aqueous solubility as will be discussed in further detail later [60, 63, 64]. Low bioavailability has become such a predominant problem in drug development that it is specifically addressed in the CPI set forth by the FDA to improve attrition rates. The CPI proposes researchers and industry test their novel compounds is a Phase 0 or eIND stage prior to filing an IND for Phase I clinical trials[11]. These Phase 0 trials would involve using nontherapeutic, microdoses of drug to help weed out compounds with suboptimal pharmacokinetics. During these trials, doses less than $1/100^{th}$ of the therapeutic range would be administered to human volunteers, and extremely sensitive analytical tools would be used to detect pictogram levels of the drug and metabolite concentrations. This testing phase can give a "go/no go" for further clinical study of the candidate compound. However, there are several disadvantages to using this testing step. One such major issue is that at such low doses, many insoluble drugs will readily dissolve and exhibit properties of good absorption. However, when therapeutic doses are used, the low solubility of the drug becomes a major limiting factor[11].

In vivo, drug bioavailability can be measured by administering the candidate drug orally, through a gavage for example, and then collecting blood samples at various time

points. These values can then be plotted as a concentration vs. time curve. The area under the curve (AUC) of this graph is referred to as a drug's overall bioavailability [7, 59, 60, 65]. This value is usually expressed as percent bioavailability of oral administration compared to the i.v administration of the same dose. This method is applied to iv administered drugs as well[66]. Other important factors of bioavailability that should be calculated from these experiments are a drug's volume of distribution (V_d)[67], excretion[68] half-life and clearance[69] rate.

<u>*Absorption*</u>

The absorption of a drug refers to the movement of the compound across mucosal surfaces into the bloodstream. This phenomenon is usually used to define what happens to a drug candidate after oral administration [59, 70, 71]. Orally administered drugs move into the small intestine where they have to be absorbed through the epithelial layer of the GI tract. Absorption is important for the delivery of drugs to therapy targets that are in tissue other than the stomach and GI tract and can only successfully be reached through the blood circulation system. Therefore, after oral administration, inadequate drug absorption can lead to insufficient concentrations of the drug reaching the blood stream for systemic distribution. This directly leads to low bioavailability. Compound absorption across mucosal surfaces can be measured using *in vitro* assays such as the concentration gradient across a monolayer of human epithelial (Caco-2) cell line[72]. *In vivo*, compounds can be fed to animals through an oral gavage and concentrations of the candidate drug can be measured in the blood over the course of time.

Factors leading to developmental attrition.

Drug solubility, dissolution, permeability, the presence or absence of food in the stomach, pH, chemical reactions in the GI tract and the presence of enzymes and bacteria all influence drug absorption [62, 66, 71].

The solubility, dissolution and permeability of drug candidates allows for the organization of drugs into the Biopharmaceutics Classification System (BCS) [60, 70]. The BCS categorizes orally administered drugs into four classes (I-IV). A compound's absorption and classification depends on three molecular properties: solubility, permeability and dissolution [60, 70]. Permeability is defined as a compound's ability to cross mucosal barriers. For classification purposes, a compound is considered highly permeable if its absorption is 90% or more of the administered dose in comparison to an intravenous dose (100%) of the same drug. Dissolution is defined as the rate at which a compound goes into solution. A high dissolution rate is defined by whether 85% of the therapeutic dose dissolves in a volume less than 900 ml within 30 minutes[70]. Compounds with lower dissolution rates have a lower rate of absorption which can sometimes be advantageous towards prolonged efficacy of potent drugs. However, this can also be a limiting factor for drugs with lower efficacy that need to reach the necessary site of activity at high concentrations. Finally, a compound is considered highly soluble if the highest dose strength can be solubilized in 250 ml or less aqueous solution over a pH range of 1-7 [70]. Drug solubility and dissolution can be tested for *in vitro* by using solutions that mimic stomach and gastric fluid[72]. Furthermore, permeability can be assessed *in vitro* by measuring drug transport across a monolayer of the human epithelial cell line, Caco-2[72].

Class I orally administered compounds are both highly soluble and highly permeable; these compounds are readily absorbed and the rate of absorption is usually higher than the rate of elimination[70]. Class I drugs can be formulated into a simple solid oral dose. One example of a class I drug is metoprolol which is a β_1 receptor blocker commonly used to treat heart disease and hypertension[70]. Class II compounds have high permeability and low solubility; the rate of absorption of these compounds is limited by how quickly they are solubilized, or their rate of dissolution. These compounds generally require a solvent or surfactant to improve solubility. An example of a class II drug is naproxen which is a non-steroidal anti-inflammatory drug (NSAID)[70]. Class III molecules have low permeability and high solubility; these drugs have high dissolution rates, however, the drug's bioavailability is limited by its absorption rate. These compounds require permeability enhancers and/or highly localized concentrations in the lumen of the GI tract. One example of a class III drug is cimetidine which inhibits stomach acid production and treats acid reflux binding to histamine H2-receptor[70]. Finally, Class IV compounds have low permeability and low solubility and thus overall low bioavailability. These compounds require solubilizing agent, permeability enhancer and high localized concentrations of the drug at the site of absorption. An example of a class IV drug is Indinavir which is an antiviral drug (protease inhibitor) used to combat HIV infections[70].

Distribution

During systemic distribution the drug will pass in and out of different organs and allow for it to reach its necessary site of activity. Some factors that influence the adequate

systemic distribution and survival of a drug and, thus its bioavailability, are drug solubility, size, and composition[67]. Drug distribution can be measured by excising organs and collecting blood from a treated animal, such as a mouse, and determining the concentration of drug in each organ and blood [7, 67].

Factors leading to developmental attrition.

During a drug's systemic distribution, its solubility, size, and composition will either facilitate or inhibit the uptake and retention of the compound in tissue and organs. Furthermore, drugs can face degradation or inactivation through blood enzymes[67]. Most drugs are in equilibrium between drug molecules that are unbound and bound to blood proteins. This balance depends on the molecular properties of the drug and also dictates how much and how quickly the free drug can reach its necessary site of activity [67, 73]. Drugs also run the risk of being phagocytized and degraded by blood cells such as macrophages that decreases drug bioavailability. Finally, after tissue penetration, it may be necessary for the drug to cross cell membranes in order to reach intracellular sites of activity which provides yet another obstacle against drug bioavailability. Finally, molecular properties can also dictate which tissue or organs these compounds accumulate in. Many compounds tend to accumulate in the liver or kidneys. One example is cisplatin which is a potent anticancer drug that favorably accumulates in the kidney, leading to severe hepatic toxicities[74].

Metabolism

Drug metabolism is the process by which compounds are prepared for excretion. Metabolism primarily occurs in the liver and is usually conducted through the system of

CYP450 enzymes. There are two forms of drug metabolism in the body, first-pass and second-pass metabolism. First-pass metabolism occurs in the liver and is responsible for the majority of drug metabolism[75]. As stated before, microsomes extracted from human livers or purified CYP450 enzymes can be used, *in vitro*, to predict the extent of metabolism a candidate drug will go through[7].

Factors leading to developmental attrition.

Metabolism is a major contributing factor influencing bioavailability because the rate and extent to which the drug is metabolized, plus the metabolites formed, affect the quantity and amount of time the active drug circulates in the blood system[32]. A second consequence of drug metabolism is the formation of harmful metabolites that can result in liver damage and other adverse effects *in vivo* as discussed before[75]. However, some investigators have used metabolism to their advantage when formulating a compound by using a prodrug system[76]. When the prodrug passes through the liver, the metabolism of the compound produces an active form of the drug. This byproduct can then enter systemic distribution as an active compound.

After orally administered compounds are absorbed through the GI tract, they are directed into the liver through the hepatic portal vein for modification in preparation for excretion. Liver metabolism can break down a candidate drug into inactive components or toxic metabolites in preparation for excretion. The polarity of the compound influences the extent to which it will be degraded in the liver[32]. If a compound is polar and soluble enough in aqueous solution, it can be eliminated from the body with minimal modifications through the urine. However, if a compound is non-polar it will need to be modified by the CYP450 in order to prepare the compounds for coupling with a

solubilizing agent[32]. Drug compounds must survive unmodified through the liver's metabolic system in order to reach the blood full efficacy intact. Extensive metabolism leads to low drug bioavailability[75].

With i.v administered drugs, metabolism can occur as a result of enzymes and proteins present in the blood that promote the clearing of these test compounds from the system[32].

Excretion

Finally, the drug will be cleared from the blood by kidney filtration and excreted through the urine. Drugs passing through the kidneys undergo glomerular filtration, active tubular secretion and passive tubular reabsorption. Glomerular filtration is the first step of renal excretion and is the process during which free drug enters the renal tubule. Filtration occurs in the glomerulus of the kidney[77]. If a drug is highly bound to plasma proteins, this will be a slow process. Another process drugs undergo is active tubular secretion which happens in the proximal tubule of the kidney. Weak acids and bases usually undergo active tubular secretion. Drugs may also be passively reabsorbed in the blood stream from the tubular lumen. The extent of reabsorption depends on the drugs lipophilic properties, urine pH, and chelating agents[77].

Excretion and clearance rate are usually determined by quantifying the amount of drug present in urine and bile over a period of time[7]. It can also be determined by quantifying the rate at which the concentration of drug in the blood decreases [7, 77].

Factors leading to developmental attrition.

Excretion becomes a contributing factor towards low drug bioavailability when the candidate compound is eliminated from the body too quickly through the liver or kidney filtration, thus, reducing the amount of time it has to circulate the blood system and limiting its access to the target site[77]. Furthermore, inadequate or inefficient excretion can lead to high drug concentrations that can result in toxicity.

1.1.2 Summary

The drug developmental pipeline is essential for the wellbeing of public. This pipeline encompasses all stages after the discovery of a drug candidate and involves preclinical and clinical trials with final FDA approval and marketing. Preclinical and clinical trials focus on three main properties of a candidate drug: its toxicity, efficacy and pharmacology.

A few essential types of toxicity that should be tested for prior to FDA approval are immunotoxicity, hypersensitivity, genetic toxicity and reproductive and developmental toxicity[25]. *In vivo* toxicity can be presented as an MTD value or LD_{50} value. Key organs that should be assessed are the liver and kidneys as these are organs where drugs are metabolized and tend to have extended periods of higher concentrations of the drugs. Drug efficacy should be evaluated *in vitro* and *in vivo* using dose response experiments and is typically presented as an EC_{50} or IC_{50} value. Finally, the pharmacology of a candidate drug is of utmost importance [51, 52]. Research should be conducted using rodent and non-rodent model to determine the bioavailability of the

candidate. Metabolic rate and characteristics of any metabolites should also be recorded along with the clearance rate[69], and distribution properties[67].

The compilation of all this data in the preclinical setting allows for the successfully filing of an IND and helps predict the drug's success in clinical trials, and also helps determine protocols and dosing for clinical trials[26]. Addressing these topics in human trials allows for the adjustment of doses and the assessment of the overall feasibility of marketing the drug.

Even though the drug development pipeline from preclinical through clinical evaluation of a candidate's toxicity, efficacy, and pharmacology is essential to public wellbeing, the productivity of this pipeline has significantly decreased (citation). Toxicity, efficacy and pharmacology evaluation along the way can uncover many suboptimal properties of a candidate drug which can lead to its elimination from the drug development pipeline. This will result in a significant waste of time and resources and ultimately lead to decreased diversity of drugs in the market. Two of the highest contributing factors that can lead to drug developmental attrition are low bioavailability as a result of low drug solubility[78] and dose limiting toxicity[25].

1.2 Solubilizing Excipients and Drug Delivery Systems

For many years, researchers and industry have struggled to find an adequate solution to growing drug development attrition. Solubilizing agents and, in recent years, drug delivery systems (DDS) have emerged and continue to grow exponentially as a promising solution [79-81]. Solubilizing excipients can aid in the development and approval of drugs because they can enhance the solubility of drugs, thereby, allowing for

the formulation of therapeutically efficacious doses. In addition to increasing drug solubility, DDSs have the unique ability to enhance stability, reduce the toxicity, and improve the pharmacological properties of problem drugs [60, 78]. Additionally, DDSs have the unique abilities to allow for controlled release and target the delivery of drugs[82]. This is especially important in cancer treatment where the majority of anti-cancer drugs are toxic to healthy tissue resulting in severe adverse side effects[83]. Tumor specific properties like the over-expression of folate and biotin receptors can be used to target drugs to these cancerous cells specifically by using folate[84] or biotin[85] functionalized drug delivery molecules. Furthermore, DDSs could allow for the co-delivery of two or more drugs allowing for efficient combination therapy [81, 86].

Drug delivery systems have also opened the door to the evolution of novel therapies that exclude chemical molecules such as siRNA for cancer treatment[87]. Without drug delivery systems, siRNA was subject to fast degradation in human serum, limited distribution and cellular uptake. Furthermore, free siRNA was known to cause severe immune responses, off-target toxicity effects, depletion of certain blood cells and organ toxicity in liver, spleen, and kidney. As a result, *in vivo*, siRNA proved very difficult to use until DDSs were used to appease these harsh side effects and improve stability and uptake [83, 87].

Due to these numerous advantages, it can be thought that by coupling problem drugs to DDSs or solubilizing excipients, thus improving their bioavailability, toxicity and/or efficacy, these new formulations can re-enter the FDA approval process and successfully be marketed [88]. This would, in turn, reduce attrition rates, costs and waste of valuable resources and increase the diversity and availability of therapeutic

compounds to the public[89]. In fact, the CPI set forth by the FDA suggests doing just this by emphasizing the development of new technologies, like nanotechnology, to address increasing attritions rates[11].

It is essential that an efficient excipient or DDS be highly soluble in aqueous solution, highly biocompatible and be eliminated from the body efficiently so as to not cause toxic accumulation[90]. The binding affinity between the excipient or DDS and the drug must be strong enough to allow for binding and retention of the guest but also weak enough to allow for the unloading of the drug when required. This release of the drug may be triggered by different stimuli including pH, and competitive displacement compounds that offset the equilibrium between bound and unbound guest molecules[90]. They should also have a certain amount of selectivity towards specific drugs. This would naturally entail that no one DDS will be able to bind to and improve the molecular properties of all drugs, thus, there is a need for a large diversity of DDSs[89, 90].

There are many different kinds of excipients and DDSs currently being studied, some of which are approved by the FDA and marketed across therapeutic fields [89, 90]. Below is a summary of some of the most widely studied. Furthermore, a new family of macromolecules, the cucurbit[n]urils (CB[n]), will be discussed.

1.2.1 Polymer-Based Drug Delivery Systems

Polyethylene Glycol (PEG)

A polymer is a compound that is comprised of repeating structural units. Specific kinds of polymers, particularly ones that are water-soluble and generally inert, can be utilized for drug delivery purposes. Polymer therapeutics includes polymer-drug

conjugates, polymer-protein conjugates, and polymeric nanoparticles[91]. Conjugation of polymers to drugs or other carrier molecules can serve as drug delivery resulting in enhanced drug solubility, increased systemic circulation, protection from enzymes, reduced immunogenicity, passive targeting of drugs to tumors and controlled release of drugs based on the structural specificity of the polymer chains that dictate their degradation[92]. There are many different kinds of polymeric units that can be used as drug delivery systems, one of the most commonly used is polyethylene glycol (PEG). Consisting of repeating ethylene oxide subunits, the unique properties of these polymers rely on the length of their chains. PEG is water soluble, and FDA approved and currently used in a large variety of foods, cosmetics and pharmaceuticals[92].

Currently there are PEGs ranging from 300-10,000,000 g/mol available commercially. Ideally, chain lengths of upwards of 2000 g/mol leads to increased solubility, *in vivo* stability and systemic circulation [91, 93, 94]. As a drug delivery system, PEG can be bound to hydrophobic or hydrophilic compounds in order to solubilize and prolong the systemic circulation of drugs. These polymers accomplish this by protecting drug compounds from being cleared through the reticuloendothelial system (RES), which can severely limit the systemic circulation of a drug. The RES is a clearance system that is part of the immune system and is comprised of phagocytic cells, primarily monocytes and macrophages, that localize in the lymph nodes and spleen[91]. PEG chains limit the uptake of drug compounds by phagocytic cells like macrophages in the blood and also slow the degradation of drug compounds by enzymes by preventing their binding. This, in turn, increases the systemic circulation of drug compounds,

allowing for higher drug concentrations in the blood and more time for these drugs to reach their necessary site of activity[91].

PEGylated compounds can also passively target pharmaceutical agents to tumors during cancer treatment. This is called the enhanced permeability and retention (EPR) effect [95-97]. When tumors develop, rapidly growing cells are in need of large quantities of nutrients and oxygen quickly. As a result, tumor vasculature develops rapidly and, in turn, abnormally. The EPR effect takes advantage of this irregular tumor vasculature[97]. The phenomenon states that compounds of certain size and chemical properties can favorably accumulate in tumors as opposed to healthy tissue because they can enter and accumulate in the tumor vasculature [96, 98, 99]. This entrapment allows for drugs to be retained in the tumor for extended periods of time at higher concentrations. This is a method that is currently being studied as a drug targeting mechanism to alleviate high toxicity[100]. Furthermore, increased circulation time and selective distribution of PEG-drug particles may allow for improved drug pharmacokinetics and, in turn, bioavailability [98, 100].

There are, however, several disadvantages to the use of PEG chains as DDSs. Specific chains of PEG have been shown to be somewhat difficult to formulate and purify, and, therefore, can be fairly expensive to use. Furthermore, these polymer arms have been found to be difficult to conjugate to drugs without changing drug bioactivity, and are not compatible with all compounds[92]. Therefore, PEG is primarily used as attachments to nanoparticles like liposomes for drug delivery. Secondly, though the longer the chain length of these polymers, the better the solubility and circulation time, extensive polymerization can lead to self-association and nanoparticle aggregation

leading to inefficient drug loading[100]. Finally, recent studies have shown that repeat dosing of PEGylated compounds can elicit an immune response through complement activation, hence, leading to hypersensitivity [101, 102]. PEG, also does not degrade readily, which enhances the systemic circulation of a drug, but can also decrease the activity of said drug because of the lack of release of the drug [100]. When PEG does degrade, it is broken down into ethylene glycol units which are categorized as "Known to be a human carcinogen"[40]. PEG and the EPR effect will be further discussed in Project 2 section.

PEG is used in several marketed laxatives such as MiraLAX®. Another example of a PEGylated compound is Genexol-PM® [103] which is currently in clinical trials. Genexol-PM® is a PEGylated micelle formulation of the anticancer drug PTX.

1.2.2 Lipid-Based Drug Delivery Systems

Liposomes

Liposomes were first discovered in 1961 by Alec D. Bangham and were initially used to study cell membranes before its utility as a DDS was discovered. Nearly 2,000 papers and more than a 150 reviews were published in 2003 alone on the subject of liposomology[104]. These nanoparticles are composed of a lipid or phospholipid bilayer membrane surrounding an aqueous center (Figure 2). There are two types of liposomes: multilamellar, which are vesicles formed of multiple bilayers, and unilamellar, which are containers composed of only one lipid bilayer. Small unilamellar vesicles are usually within the size range of 100 nm while large unilamellar vesicles are in the range of 200-800 nm. Multilamellar vesicles are within the size range of 500-5000 nm[104].

Liposomes have the ability to delivery both hydrophilic and lipid soluble drugs and have the unique ability to fuse to cellular lipid membranes and degrade into highly biocompatible components. These nanoparticles can be formulated into different forms of administration such as oral or intravenous. Another advantage to the liposomes is that the phospholipid bilayer of liposomes can be easily modified to customize the molecules to varying sizes. They have also been shown to induce the EPR effect at specific sizes. Liposomes can also protect their cargo from degradation [104, 105].

Liposomes have several disadvantages that limit their use[106]. One of the primary downfalls of the liposome is its rapid clearance from the body through the RES. The high clearance rate of liposomes has been somewhat circumvented with the use of PEG arms bound to the surfaces of liposomes, in turn, protecting the liposomes from phagocytosis and protein degradation [105, 107]. These new long-circulating liposomes are now marketed as STEALTH® liposomes [88, 107, 108]. However, these new liposomes have their own limitations, such as the difficulty with which the vehicles are modified with PEG arms and the fact that it can limit the adhesion of targeting ligands. These PEG molecules have also shown higher levels of hypersensitive reactions as explained before. In addition, while the protection of liposomes from the RES clearance system improves circulation time, this lack of uptake up by cells is observed in tumor cells as well, thereby, limiting the efficacy of drugs encapsulated in these liposomes [88].
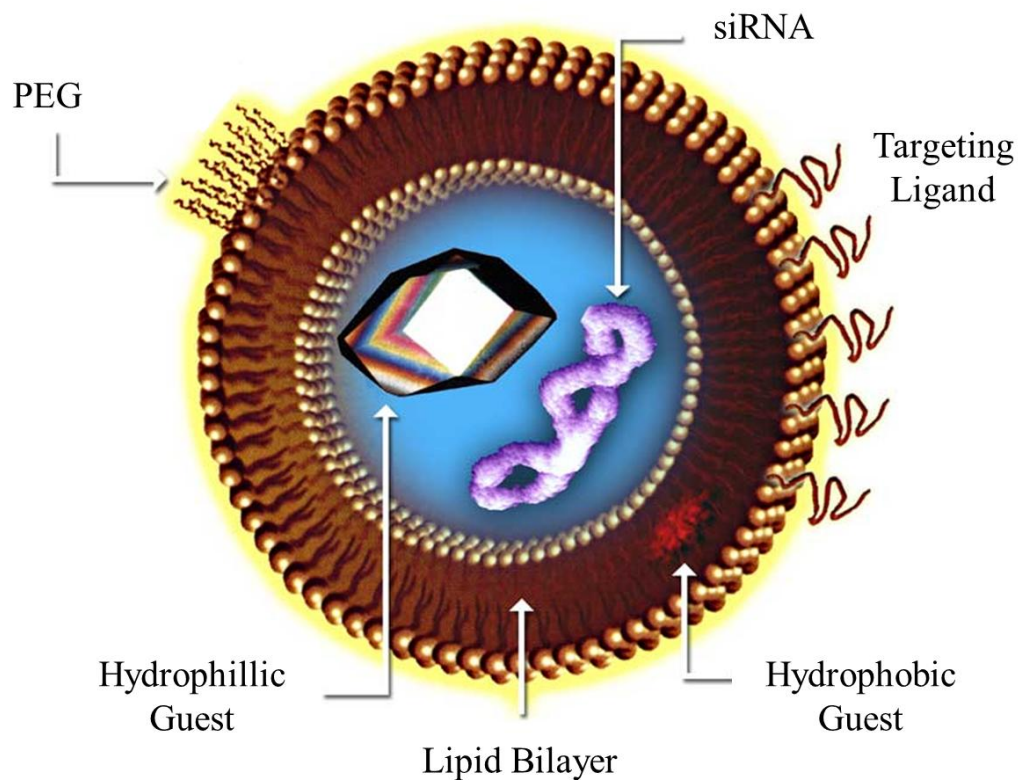
Figure 2: Liposomes are composed of a lipid or phospholipid bilayer membrane surrounding an aqueous center. Hydrophilic compounds can be loaded in its aqueous cavity while hydrophobic compounds with high binding affinities can be loaded into the lipid bilayer. Liposomes can also be functionalized with PEG or targeting ligands. Adapted from[109].

Methods to circumvent this problem involve using stimuli induced disconnection of PEG chains from liposomes. One such trigger would be the lower pH observed in tumor tissue. Liposomes have also been known to have high production costs, low solubility, leakage of encapsulated drugs and possibly elicit an immune reaction [107, 110, 111]. Another limitation of the liposome is its drug encapsulation efficiency. This is a problem primarily with hydrophobic drugs like paclitaxel (PTX) which have very low affinity to the lipid bilayers of liposomes. Liposomes can only be used to delivery drugs that can be efficiently encapsulated within the nanoparticle with strong binding affinities so as to limit the amount of lipid being administered. Administering high concentrations of lipids can lead to toxicity and unpredictable pharmacokinetics[112].

Liposomes have been coupled with a large variety of drugs, primarily anticancer compounds, some of which are currently approved and marketed. One such approved complex is the drug now marketed as Doxil® [88, 113]. This formulation is composed of the anticancer drug doxorubicin encapsulated in STEALTH® liposomes[108]. Encapsulation with PEGylated liposomes have both enhanced the solubility and reduced the side effects of this drug. This complex is currently being used to treat ovarian cancer. Liposomes have also served as carriers for other insulin[114], cytokines like recombinant TNF-α[115], antimicrobial agents[116], and siRNA[117]. In addition to parenteral delivery, liposomes can be used for oral delivery as demonstrated by preliminary studies conducted with insulin[114]. They can also be used for aerosolized delivery as shown by the delivery of rifampicin to alveolar macrophages, showing promise in enhanced Tuberculosis treatment[116]. Liposomes can also be targeted using different ligands such

as folate[118, 119], and transferrin[120] whose receptors are overexpressed on tumor cells and monoclonal antibodies[121].

1.2.3 Macromolecular Excipients

Cyclodextrins (CDs)

Cyclodextrins (CDs) are one of the most extensively studied and widely utilized solubilizing excipients. The earliest reference to these molecules was in 1891 and by 1953, the first patent for drug formulations emerged[122]. CDs are cyclic oligosaccharides composed of 6-8 dextrose units joined through 1-4 bonds. There are three naturally occurring CDs: α, β and γ (Figure 3). The essential difference between each is the number of glucose subunits that composes each [123, 124]. These glucose subunits come together to form a hollow conical structure that allows for the encapsulation of different drugs in their cavities. CDs have hydrophilic exteriors and hydrophobic interiors that allow for the encapsulation of neutral or anionic guest molecules [122, 125]. The varying number of glucose subunits allows for different sized cavities; α-CD is a hexamer with a cavity diameter of 4.7-5.3Å; β-CD is a heptamer with a cavity size of 6.0-6.5Å and finally the γ-CD is composed of eight glucose subunits and has a cavity size range of 7.5-8.3Å (Figure 4). One of the greatest advantages of the CD family is their high solubility: 16 mM (β-CD), 149 mM (α-CD) and 178 mM (γ-CD). The loading of a drug into the cavity of a CD molecule is determined through many different factors. One obvious factor is whether regions of a particular drug can physically fit in the CD cavity. Structural and molecular properties, such as charge and hydrophobic and ionic regions, of the drug are also important[125]. CDs are more prone to bind to neutral

and anionic drug compounds and have been shown to bind at an affinity of approximately $1 \times 10^5 \text{ M}^{-1}$.

CD structure and solubility allows for these vehicles to encapsulate and hide hydrophobic drugs or hydrophobic regions of drugs from water molecules, thus allowing for the CDs to increase the solubilities of these compounds [125]. It should be noted, however, that solubilizing excipients like the CDs may not increase the solubility of the free drug, but will, instead, maintain the drug in aqueous solution by establishing a rapid equilibrium between the highly soluble complex (drug + CD) and poorly soluble free drug. Therefore, the total amount of drug present in solution, hence its solubility, refers to the sum of both bound and unbound drug.
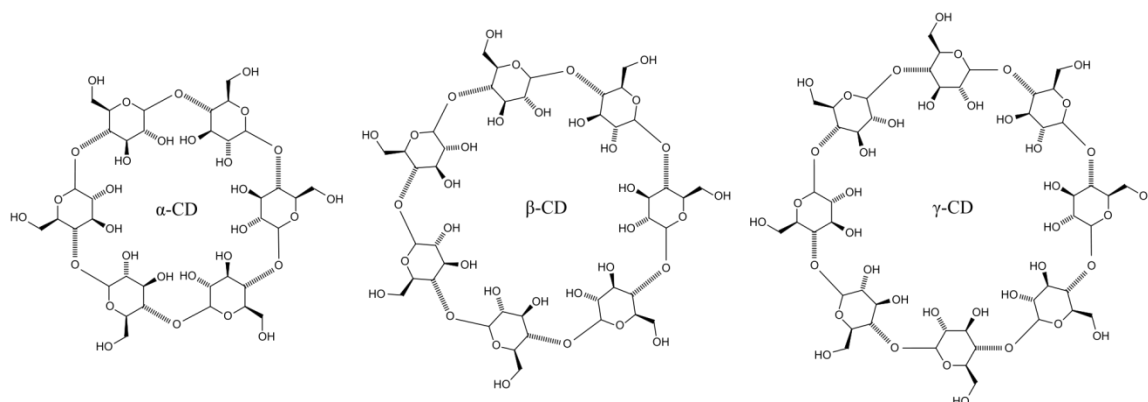
Figure 3: The CD family: α-CD, β-CD, and γ-CD. α-CD is a hexamer with a cavity diameter of 4.7-5.3Â; β-CD is a heptamer with a cavity size of 6.0-6.5Â and finally the γ-CD is composed of eight glucose subunits and has a cavity size range of 7.5-8.3Â. Figure from[126].

It may be necessary for a drug to cross cellular and mucosal membranes in order to reach its necessary site of activity as stated earlier in this thesis. However, it is also accepted that CDs do not diffuse through cell or mucosal membranes. As a result, in order for the increase in drug solubility to lead to an increase in bioavailability and efficacy, it is obvious that the drug must be released from the CDs. The constant forming and breaking of bonds between CDs and drugs dictates that the drug can be released from the CDs and remain free when this equilibrium is changed. One factor that influences the equilibrium between bound and unbound drug is the binding affinity of the CD to the drug. If the binding affinity is high, then the CD and drug will be bound together tightly and result in decreased concentrations of free drug and thus decreased bioavailability. Another factor influencing the equilibrium is the ratio of CD:drug. This means that if there is a significantly higher concentration of CD than is needed to solubilize a specific amount of drug (an excess of CDs), there will be a decreased concentration of free drug at any given time. Therefore, during the process of drug formulation with excipients like the CDs, it is essential to consider drug binding affinities and appropriate CD:drug ratios in order to optimize the adequate release of the drug so that it may reach its necessary site of activity. Other possible factors that can influence the equilibrium and promote the release of the drug from the CDs are: 1) drug-protein binding that can cause a decrease in free drug concentration thereby shifting the equilibrium to release more drug from the CDs, 2) competitive displacement by an endogenous or exogenous compound that has higher affinity to the CD that can essentially kick the drug out and finally 3) drug uptake into tissue that are not accessible or conducive to complex or free CD uptake[125]. Furthermore, it is thought that, in the case of orally administered drugs, the empty CDs

can bind to and extract lipids from intestinal cell membranes thus changing membrane fluidics and membrane transport of free drug into the cells. This is thought to contribute to increased absorption of the drug across the mucosal surface and into systemic circulation.

Until recently, CDs have been tested primarily for oral administration of insoluble drugs[127]. The parent CD compounds have not been approved for use with i.v administered drugs in the US because of the severe nephrotoxicity observed with all three CDs [128, 129]. This toxicity primarily arises from the high affinity the CDs have for cholesterol and phospholipids[128]. When administered parenterally, CDs have been shown to extract erythrocytes and other blood cells of cholesterol leading to cell lysis and toxicity. This extraction of cholesterol not only leads to blood cell lysis but also has been shown to form crystals in the kidney and lead to severe renal toxicity[128]. Furthermore, studies have shown that this toxicity is not isolated to blood cells; CDs can extract phospholipids and proteins from other types of cells leading to cell death. The LD_{50} for i.v administration in rats has been established at 1g/kg for α-CD and 0.79 g/kg for β-CD[129]. An LD_{50} of 3.75g/kg has been established in rats for γ-CD, however, some reversibility of this toxicity was also observed [128, 129].

As a result of these limitations in i.v administration, several different CD derivatives have been synthesized; the two most well-known are hydroxypropyl-β-CDs (HP-β-CD)[130] and sulfobutyl ether-β-CD ((SBE)-β-CD)[131] now known as Captisol®. HP-β-CD has been shown to improve drug solubility, stability and overall bioavailability of guest compounds[132]. This derivative has a significantly improved safety profile than that of β-CD, however, this improvement comes at a cost; with the

higher degree of hydorxypropyl substitution, the CD's ability to bind to drugs is decreased[133]. Parenteral administration of HP-β-CD has been tested in both animals and humans. Minor reversible histological changes in the kidney were observed at doses ranging from 100-400 mg/kg in addition to some damage to red blood cells. However, these effects were not readily reflected in humans[130]. Two year toxicology studies in humans did not show signs of carcinogenicity. HP-β-CD has also been used to orally delivery drugs, however, like the parent compounds, very limited amounts of CD reach the blood stream[134]. It is believed that the drug is released in the GI tract and it is then absorbed across the mucosal membrane without the CDs[130]. One approved and marketed drug that is formulated in HP-β-CD is itraconazole (antifungal)[135]. Furthermore, this CD derivative is currently in clinical trials for the treatment of Neimann-Pick Type C Disease which, without treatment, is a terminal disease affecting children by inhibiting the body's ability to process cholesterol. Thus HP-β-CD has been pioneered to harvest excess cholesterol, in turn, improving patient survival[136].

(SBE)-β-CD or Captisol® is a very successful CD derivative that has shown high solubility and no interactions with cell membrane cholesterol or phospholipids. Parental studies done in mice up to 10 g/kg have shown no signs of toxicity. Similarly, human studies have shown no adverse effects. There are several Captisol® formulated drugs that are currently FDA approved and marketed including Nexterone (life threatening heart rhythm disorders), VFend® (antifungal), Geodon™(antipsychotic), Cerenia™ (motion sickness), Abilify® (antipsychotic), and Kyprolis™ (multiple myeloma)[131].

Cucurbit[n]urils (CB[n])

The cucurbit[n]uril (CB[n]) family of macromolecules was first isolated by Behrend *et al* in 1905 through the condensation reaction of glycoluril and formaldehyde under acidic conditions[137]. These particles were fully characterized later by Mock *et al* in 1981. CBs are composed of repeating glycolurils that form a cylindrical structure much like the CD family[138]. The parent compounds of the CB[n] family include five compounds, CB[5], [6], [7], [8], and [10], that vary in cavity size based on the number of glycoluril units each consists of (Figure 4). The CB[n] exteriors are hydrophilic and negatively charged at the portals and the interior cavity is predominantly hydrophobic[138]. Like the CDs, molecular properties of the guest, like charge and size, determine binding to CB[n] molecules[137]. Because of the negatively charged glycoluril groups at the portals of these containers and the hydrophobic interior, they favor the binding of positively charged particles with regions of hydrophobicity [139]. This family of nanoparticles is unique in their high binding affinity and specificity towards guest molecules. Because CB[n]s attract cationic and neutral molecules, they serve as a counterpart to the CD family that binds neutral or anionic guest molecules[138, 139]. It should also be noted that CB[n]s bind significantly more tightly ($K_a > 10^5$ M^{-1}) to its guest molecules than CDs do to theirs ($K_a < 10^5$ M^{-1}) allowing for longer host-guest complexation, stabilization, and the need for significantly lower concentrations of excipient to solubilize equal amounts of drug[138]. For example, it was shown that >6 times higher concentrations of β-CD than CB[7] is need to solubilize the same amount of albendazole (ABZ)[140-142].

Cyclic Cucurbit[n]urils
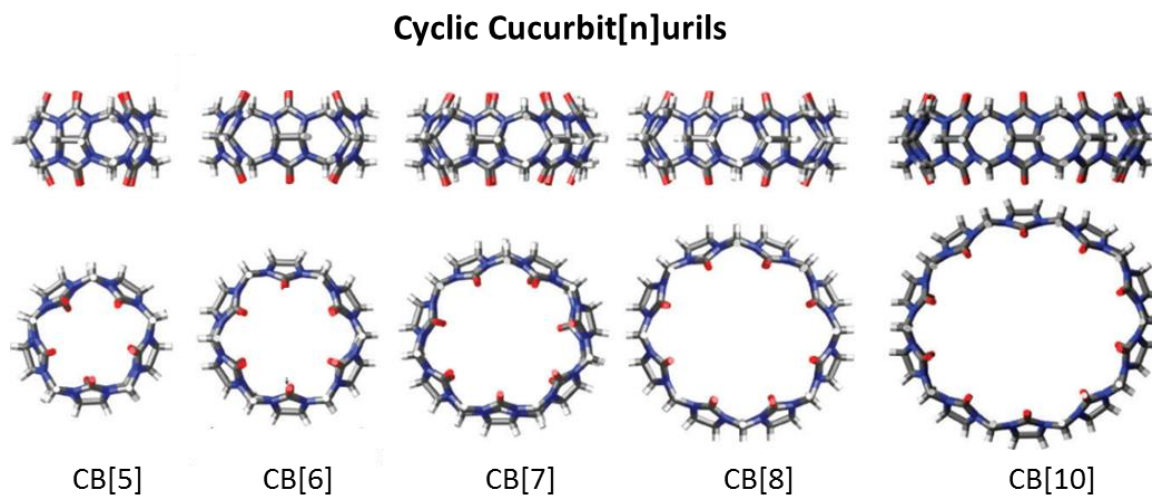
CB[5]   CB[6]   CB[7]   CB[8]   CB[10]

Figure 4: The Cucurbit[n]uril Family: CB[5], CB[6], CB[7], CB[8] and CB[10]. Cavity sizes range from 4.4 Â(CB[5]), 5.8 Â(CB[6]), 7.3 Â(CB[7]), 8.8 Â (CB[8]), and 10.7-12.6 Â (CB[10]). Adapted from [138].

Aside from these advantages, there are several other properties that suggest the CB[n] family would be good solubilizing excipients. CB[5] and [7] are the most soluble of the family at 20-30 mM which is comparable to β-CD (16 mM) Though the parent CB[n] compounds are not as soluble as the parent CD compounds, CB[n]s have relatively weak basic portals which are protonated under acidic conditions, thus increasing the compounds' relative solubilities under acidic conditions such as that found in the stomach and small intestine[138, 139]. Even with somewhat limited solubility, members of this family have shown promising results in increasing the solubility and stability (both chemical and enzymatic) of certain drugs[143, 144]. Like with the CD family, it is thought that there is an equilibrium between CB[n] bound and unbound drug and, as a result the drug release mechanisms are thought to be similar.

The CB[n] family (4.4-12.6 Å) exceeds CDs (4.7-8.3 Å) in the range of cavity sizes which allows for larger drugs to bind to CB[n]s. CB[n] toxicity has been tested both *in vitro* and *in vivo* with promising results. *In vitro* testing in Chinese Hamster Ovary (CHO-K1) cells, human kidney (HepG2), and human kidney (HEK293) cell lines showed high cell survival up to 1 mM of CB[7] up to 48 hrs[141, 145]. An *in vivo* study using a single i.v dose of CB[7] up to 300 mg/kg established the MTD of CB[7] at 250 mg/kg. Mice recovered in weight within 5-8 days possibly suggesting reversible toxicity [141]. Uptake of CB[7] through phagocytosis has been demonstrated through fluorescence microscopy.

Consequently, several studies have been conducted using CB[n]s in the past with oxaliplatin (anticancer)[141, 146], ABZ (anthelminthic/anticancer)[142]**,** camptothecin

(CPT; anticancer)[147], cisplatin (anticancer)[148], and several anesthetics (procaine, tetracaine dibucaine etc.)[149]. However, none of these compounds have advanced to clinical trials or marketing yet. These studies do show great potential towards the use of CB[n]s for solubilizing and stabilizing purposes and, in fact, they seem to be great counterparts to the CD family of macromolecules.

There are several factors that may limit the use of CB[n]s. One is the rigid circular structure of these compounds. Though their cavity sizes are larger than the CD family, their structure still limits the size of drug that can be bound to the CB[n]s. However, the most significant factor that may limit their use is their low solubility. CB[5] and CB[7] are the most soluble, however, CB[5] has been shown to be too small to encapsulate many drugs. CB[7] is, as a result, the most studied, but at a solubility of only 20-30 mM, the enhancement of drug solubility with this compound is limited[139].

1.3 Summary and Significance

Drug delivery systems provide many advantages in the pharmaceutical industry by being able to significantly increasing drug solubility, stability, enhancing systemic circulation, decreasing toxicity and providing the option to target drug to specific cells. Furthermore, solubilizing excipients like the CDs can significantly improve the solubility of many drugs. These advantages allow for problem drugs to be pushed through both the developmental and approval processes thus reducing attrition rates. There are many different kinds of excipients and DDSs currently being studied, the most prominent of which are PEG chains, liposomes and CDs. A fairly new family of macromolecules currently being studied for solubilizing purposes is the cucurbit[n]urils.

This dissertation work evaluates three new CB[n]-type molecular compounds, Motor1, Motor2 and a biotin functionalized-CB[7], developed during a five-year collaboration with Dr. Lyle Isaacs (University of Maryland, Department of Chemistry)[145, 150, 151]. With so many different types of successful excipients and DDSs being studied, one might ask why this work is significant. The answer lies in the fact that no one host molecule can bind to, solubilize and deliver all drug molecules. Therefore, a diversity of host molecules is necessary to encapsulate the large variety of problem drugs. It is essential to continually expand the tool box of drug delivery systems. Table 1 presents some compelling data collected by the Isaacs lab that strongly supports the need for a larger variety of excipients and delivery molecules and that these novel CB[n] derivatives hold great potential to succeed.

DRUG	INTRINSIC SOLUBILITY	MOTOR 1 Max = 100 mM		MOTOR 2 Max = 14 mM		HP-β-CD Max = 100 mM	
		Host	Drug	Host	Drug	Host	Drug
Paclitaxel (anti-cancer)	0.004	5	0.6	10	-	10	-
PBS-1086 (anti-cancer)	-	10	7.5	8	6.1	20	-
Melphalan (anti-cancer)	0.01	10	16.9	11.2	16.9	10	5.6
Tamoxifen (anti-cancer)	0.01	12	0.21	10	1.18	10	0.42
Albendazole (anthelmintic/anti-cancer)	0.03	10	1.86	10	4.48	10	0.2
Camptothecin (anti-cancer)	0.02	10	0.91	10	11.6	10	0.1
Tolfenamic Acid (NSAID)	0.15	10	0.41	10	5.6	10	0.11
Indiometacin (NSAID)	0.12	10	0.33	10	6.7	10	0.33
Amiodarone (anti-arrhythmic)	0.015	10	0.75	10	5.1	10	0.1
Clopidogrel (anti-platelet)	0.004	10	1.07	14	-	100	-
Estradiol (hormone)	0.03	10	3.75	10	9.2	10	2.1
Cinnarizine (anti-histamine)	0.013	15	4	10	0.55	10	0.3

Table 1: Comparative study of drug solubilities with Motor1, Motor2 and HP-β-CD clearly revealed the need for a large toolbox of excipients and DDSs to accommodate the large diversity of drugs available. Many drugs like PBS-1086 and PTX show significant solubility enhancement with only Motor1, whereas CPT and estradiol showed the greatest increase in solubility with Motor2. The drugs presented here showed limited increases in solubility with HP-β-CD. Work done by Ben Zhang and Dr. Lyle Isaacs. (unpublished)

The following information will be presented as two main projects. One will focus on using Motor1 and 2 to increase the solublities of several insoluble drugs. There are several advantages to Motor1 and 2 that support their use in this field. Not only do they have very high intrinsic solubilities (105 mM and 14 mM respectively) but they also have great structural flexibility due to their acyclic formation allowing for the encapsulation of larger variety of different sized drugs.

The second section of this thesis will focus on alleviating drug toxicity by using ligand targeted CB[n] and CB[n]-type compounds. Targeted drug delivery can be used to alleviate anticancer drug toxicity by delivering these toxic drugs specifically to tumors by way of passive targeting or tumor specific ligands[90]. This will result in tumor specific cytotoxicity, leaving healthy cells unharmed and leading to decreased drug side effects. Here we will introduce a biotin targeted CB[7] compound that was tested for tumor specificity[151].

Dr. Isaacs' lab has evaluated the molecular properties of these three CB[n]-type including their intrinsic solubilities and drug solubilizing capabilities. My work has evaluated the biological significance of these increased solubilities and targeted drug delivery both *in vitro* and *in vivo* in cancer therapy background.

Project 1: Enhancing Drug Solubility using Novel CB[n]-type Compounds.

Chapter 2. PROJECT 1 INTRODUCTION

2.1 Drug Solubility

Solubility is defined as the maximum amount of solute (eg: NaCL) that can dissolve in a given amount of solvent (eg: water) thus reaching a state of equilibrium between dissolution and precipitation of the solute[63]. A compound is soluble in a solvent when there are attractive molecular forces between the solute and solvent molecules making the reaction energetically favorable. For example, when NaCl dissolves in water, the positive Na^+ ions are attracted to the somewhat negatively charged oxygens in H_2O, while the negatively charge Cl^- ions are attracted to the positively charged hydrogen atoms of water. Furthermore, the polarity of the solute and solvent also determines solubility, if a compound is highly polar (hydrophilic) it will most like dissolve readily in water which is also polar. However a non-polar (lipophilic) compound (eg: oil) will not dissolve in a polar substance like water due to forces like the hydrophobic effect. Solubility is usually defined at standard temperature (25^0C) and pH (7). Changing these parameters will increase or decrease the solubility of a compound. Solubility is expressed as a concentration (Molarity, g/L, etc) and usually refers to aqueous solubility unless specifically stated. The FDA defines a compound as highly soluble if the highest therapeutic dose necessary is soluble in 250 mL or less of aqueous solution over a pH range of 1-7.

Low drug solubility is the major cause of drugs failing within the developmental pipeline due to low bioavailability[60, 64]. Approximately 70% of all orally administered drugs entering the pipeline have high permeability but are solely limited by their solubilities (Class II) (Figure 10)[1]. This fraction of the population is higher than that of

drugs in the pipeline limited solely by low permeability (Class III; <10%) or by low solubility plus low permeability (Class IV; 20%). This majority is reflected in marketed drugs with 30% of these drugs being limited solely by their solubilities[1]. Orally administered drugs are not the only compounds that suffer from low drug solubility. In fact, studies have shown that over 40% of all drug candidates, through all forms of administration, are failing the developmental process due to low solubility[60, 64, 78]. Low drug solubility directly affects the absorption of a drug across mucosal membranes in the orally administered compounds. It will lead to low or variable absorption of the compound into the blood stream, thus resulting in a limited amount of drug reaching systemic distribution. The end product of low drug solubility is low unpredictable bioavailability[64]. The solubility of a compound is also a fundamental factor in its formulation at clinically relevant dosages for i.v administration[60]. All of these factors can lead to the elimination and abandonment of the candidate drug during the developmental process thus leading to increased attrition rates[60, 64, 78].

There are several different approaches to overcome low drug solubility[78]. Medicinal chemistry can help restructure candidate compounds early in the discovery and preclinical stages of development. However, in some cases, structural adjustments are not an option because it can compromise the potency of the drug. Therefore, other approaches to increase drug solubility are necessary. There are many different ways to improve the solubility of a drug. Some of these include adjusting pH, using salt solutions, or solid dispersions. Other methods include using excipients such as surfactants like cremophor®EL and CDs or DDSs like liposomes as mentioned before[60, 78]. Despite this large diversity of solubilizing strategies, each method has its advantages and

disadvantages that actually promote the need for such a large spectrum of methods. However, as stated before, no one host molecule can bind to and solubilize all drugs (Table1). As a result, there is a constant demand for a larger diversity of solubilizing agents. Therefore, here, we introduce two new CB[n]-type molecular compounds to add to the toolbox of solubilizing strategies [150]. This study will provide a proof-of-principle for the use of Motor1 and 2 for drug delivery using four different anticancer drugs: PBS-1086, PTX, CPT and ABZ.

2.3 Drugs with Low Solubility

PBS-1086

PBS-1086 is an un-marketed anticancer drug still in the preliminary developmental stages[152]. The mechanism of action for this compound is through the inhibition of both canonical and non-canonical NFκB pathways[152]. Both or one of these pathways is upregulated and constantly turned "on" in many types of cancer[153]. This is because the NFκB pathways are responsible for initiating DNA transcription, cell proliferation and survival which are favored in cancer growth and progression. PBS-1086 is coined as a pan-Rel inhibitor because it can block the activity of all five members of the NFκB family of proteins that have the Rel homology domains responsible for DNA binding and dimerization. Blocking all five proteins down-stream of both pathways essentially inhibits the translocation of these proteins into the nucleus and, thus, the binding and initiation of DNA transcription[152]. PBS-1086 has shown promising results in the treatment of aggressive, usually terminal cancers such as head and neck cancers, however, it is severely limited by its very low, undetectable, solubility. Various studies

were conducted with other excipients without success, therefore, initial studies with this new compound were conducted using a mixture of DMSO and cremophor®EL. However, due to the toxicity issues associated with these solvents, an alternative was needed[152]. As a result, through a recent collaboration with relMD Inc. (Balitmore, MD) and Profectus Biosciences Inc. (Baltimore, MD) we were able to encapsulate the drug in Motor1 to significantly increase its solubility safely and thereby improve its therapeutic index. The fact that Motor1 can safely and significantly increase the solubility of PBS-1086 when other excipients could not is of great importance because it is an ideal example of how necessary it is to have Motor1 as an approved excipient. This is because drugs, like PBS-1086, that are affective against aggressive cancers, like head and neck cancers, are rare and, therefore, essential to public health. Without Motor1, further study and the possibility of approval or marketing of PBS-1086 may be limited.

Paclitaxel (PTX)

As previously discussed, PTX is a well-known, currently marketed anticancer drug that stabilizes microtubules essentially halting cellular replication[154]. This drug had been administered i.v using cremophor®EL, until recently, due to its very low solubility **(0.03 mg/ml)**. Marketed under the name Taxol®, this formulation was used to treat a variety of different cancers, however, the severe side effects associated with this formulation was a dose limiting factor. Extensive research revealed that the majority of adverse effects observed with Taxol® administration was, in fact, due to cremophor®EL and not PTX[31]. Cremophor®EL causes severe hypersensitivity, nephrotoxicity, and neurotoxicity[29, 30]. As a result of these severe side effects, Taxol® was typically administered at a concentration of 175 mg/m^2 over a period of 3 hrs[155]. Furthermore,

special packaging was necessary for storage and administration because cremophor®EL was found to leach plastic into the drug solution[31]. As a result of these limitations, a replacement for cremophor®EL is actively sought after, especially because this solvent is not only used in the administration of anticancer drugs, but also for the administration of drugs like cyclosporine A and several anesthetics. In fact, patients who have received liver transplants using cremophor®EL have exhibited cardiac toxicity. Therefore, replacing this solvent with an improved alternative would impact the administration of drugs across therapeutic fields[31].

A new albumin formulation of this PTX, Abraxane®, is currently approved (2005) and marketed[156]. Clinical studies conducted with a dosing every 3 weeks using Abraxane® showed that with the elimination of cremophor®EL, PTX could be administered at an increased dose (260 mg/m^2) over a shorter time period (30 mins) with decreased side effects in comparison to a dosing of 175 mg/m^2 of Taxol® over 3hrs [156-158]. However, this new formulation still has its own drawbacks such as, neutropenia (abnormally low number of neutrophils), sensory neuropathy (loose of sensation), alopecia (baldness), and hypersensitivity[156]. Furthermore, both reproductive and developmental toxicities were observed in rats. This formulation also comes with the remote risk of transmitting viral diseases due to the human albumin used to solubilize PTX[156]. Though it is a significant improvement from Taxol®, it is clear that there still are limitations to this new formulation of PTX and plenty of room for improvement. As a result, there is still a great deal of interest in PTX. For example, Genexol-PM®, a PEGylated micelle formulation of PTX, is currently in clinical trials[103]. This formulation is thought to not only increase drug solubility but also improve PTX

pharmacokinetics by inducing the EPR effect. In our study, PTX will serve as a tool for establishing a proof-of-principle towards the use of novel CB[n]-type compounds for drug delivery.

Camptothecin (CPT)

CPT is an anticancer drug that works by blocking topoisomerase I, effectively halting DNA synthesis[159]. Though CPT has been shown to have good activity at lower concentrations, formulating this compound to doses with clinical efficacy has been difficult due to its low solubility (4 μg/ml)[160]. This low solubility has led to unreliable treatment and unpredictable adverse effects in humans. Furthermore, CPT is also limited by is *in vivo* instability. This compound is quickly hydrolyzed into an inactive, yet more soluble compound that has prolonged circulation time[160, 161]. As a result of these limitations, CPT research was abandoned early on and two new analogs, topotecan and irinotecan, were synthesized and marketed. Though these two new compounds have potent activity and good solubility, they also have dose-limiting toxicity which limits their clinical use. Several recent studies have tried to pull CPT back into clinical use, one such compound is currently in clinical trials. CRLX101 is a nanoparticle that is composed of CD and PEG repeating units that can bind to, solubilize and stabilize CPT[162, 163]. CPT is conjugated to the PEG units, thus preventing the hydrolysis of the drug and increasing its solubility by 3 orders of magnitude. This compound was also shown to increase drug circulation *in vivo* as a result of the PEG arms[163]. This compound has been moved into Phase II clinical trials. CPT has been successfully coupled with CB[7] and CB[8] with improved drug solubility and stability, therefore, CPT will serve as another proof-or-principle towards the use of CB[n]-type compounds for drug delivery.

Albendazole (ABZ)

ABZ, the final drug that will be used in conjugation with Motor1, is a safe and approved orally administered anthelmintic drug that has been used for close to 30 years now. ABZ's mechanism of action is very similar to that of PTX[164]. It can bind to and inhibit microtubule depolymerization leading to cell death. This drug was also shown to be a potent inhibitor of vascular endothelial growth factor (VEGF) which is upregulated in many tumors[165]. Due to these mechanisms of action, researchers recently became interested in the application of this drug in cancer treatment. A pilot study to determine MTD value was conducted in patients with colorectal and other forms of cancer. This study showed some decline in tumor biomarker levels in plasma with oral administration of ABZ[166]. The optimal dose was determined to be 1200 mg, twice daily on a 21-day cycle. Furthermore, rats with peritoneal human HT-29 tumors dosed i.p with ABZ at 150 mg/kg on a once weekly schedule showed significant reduction of tumor volume. Finally, ABZ has been demonstrated to have potent activity against PTX resistant cells [164]. However, this drug has limited use due to its low solubility and rapid metabolism; it cannot be formulated at clinically relevant doses for i.v administration[165]. Due to the great potential ABZ has an anticancer drug in addition to its already well-established safety profile, many researchers have sought to improve its solubility by using DDSs. One such study used HP-β-CD which showed the ability to increase ABZ solubility up to 1.2 mg/ml using 400 mM HP-β-CD[140]. Though this study showed promising results, one must remember the negative side effects associated with this derivative of the CD family. Furthermore, it has been shown that the CB[n] can bind to and solubilize ABZ more efficiently than the CD family with a lower concentration of the DDS. CB[6,7,8]

has been shown to increase the solubility of ABZ by 2000-fold without the addition of other solvents[142]. Therefore, here we will discuss the use of Motor1 conjugated ABZ in the treatment of tumors.

2.4 Motor1 and 2

Below we will discuss the conjugation of these four drugs and others with Motor1 and 2 and present both chemical (Isaacs) and biological (Hettiarachchi) assessment of these compounds. Both these compounds are acyclic and, as a result, are extremely flexible in binding to various sized guest molecules. It is composed of the same essential backbone as the parent CB[n] compounds and has negatively charged exteriors and a hydrophobic interior[150, 167], therefore, it has high affinity to both neutral and positively charged guest molecules with hydrophobic regions. The positive charges on the guest can induce ion-dipole interactions with the negatively charged portals on Motor1 and hydrophobic interactions are formed between the cavities of both compounds with respective regions on guests. Furthermore, the two terminal aromatic groups on both Motor1 and 2 are thought to interact with aromatic regions on guest molecules through π-π interactions. It is thought that like the CDs and the CB[n]s, Motor1 and 2 maintain an equilibrium between bound and unbound drug, thus the factors that influence the release of the drug are as stated before. Both these compounds were found to have low self-association, thus reducing the probability of host aggregation. Motor1 and 2 are currently patented[167].

Motor1 is highly soluble up to 105 mM in phosphate buffer (20 mM) due to the four sulfonate groups attached at either end of the molecule (Figure 5). Phase solubility studies conducted by the Isaacs group have shown tremendous increases in drug

solubility upon binding to Motor1 even, and especially, in comparison to HP-β-CD (Table1). For example, PTX conjugated with Motor1 results in a 2750-fold increase (Figure 6A; 0.004 mM to 11 mM) in the drug's solubility. Similarly, the complexation of Motor1 with ABZ increases its solubility by 226-fold (Figure 6B; 0.03 mM to 6.78 mM) and complexation of Motor1 with clopidogrel (anticoagulant) results in a 1220-fold increase in solubility (Figure 6C; 0.004 mM to 4.88 mM)[150].

Motor1 was shown to most significantly enhance the solubility of paclitaxel which was surprising (Figure 6A). This is because paclitaxel is a neutral drug and also the largest the Isaacs group had tested. These results demonstrated Motor1's great structural flexibility and it ability to bind to neutral, aromatic compounds through π-π interactions and the hydrophobic effect. Furthermore, it is thought that Motor1 forms hydrogen bonds with paclitaxel instead of ion-dipole interactions. These results are significant because they demonstrate the great diversity of pharmaceutical compounds Motor1 can possibly encapsulate. It should also be noted that the phase solubility diagram of paclitaxel showed linear regions at lower concentrations of Motor1 and curved upwards at higher concentrations. This kind of phase solubility diagram is called an A_p-type plot and suggests a near 1:1 binding ratio of Motor1:paclitaxel for the linear regions and the presence of higher order complexes such as two Motor1 molecules to one paclitaxel molecule at higher concentrations of Motor1[150].

A

R = CH₂CH₂CH₂SO₃Na

B

Figure 5: Motor1 is an acyclic member of the CB[n] family with four glycouril units in its backbone and four sulfonate groups at either end which make it highly soluble (105 mM) in aqueous solution. Linear chemical Structure (A) and folded x-ray crystal structure (B). Work done by Da Ma and Dr. Lyle Isaacs[150]

Figure 6: Motor1 significantly increases the solubility of several drugs like PTX (A; ~2750-fold increase), ABZ (B; ~226-fold increase), and clopidogrel (C; ~1220-fold increase). Work done by Da Ma and Dr. Lyle Isaacs[150].

Motor2 has large aromatic groups attached at the ends of a chain of 6 glycouril units (Figure 7). This results in a lower intrinsic solubility at 14 mM in phosphate buffer (20 mM) but it also allows guest molecules to bind more easily and tightly to Motor2. This results in the need for lower concentrations of host molecules to significantly increase the solubility of guest molecules. CPT coupled with Motor2 results in a 580-fold increase in the drug's solubility (Figure 8A; 0.02 mM to 11.6 mM) whereas an increase in drug solubility was barely detectable upon coupling with HP-β-CD (Table1). Furthermore, this increase in drug solubility was accomplished with only 10 mM of Motor2 while Motor1 conjugations necessitate a concentration upwards of 50 mM. ABZ conjugated to Motor2 results in a 149-fold increase in the drug's solubility (Figure 8B; 0.03 mM to 4.48 mM) and finally tamoxifen bound to Motor2 results in a 118-fold increase in drug solubility (Figure 8C; 0.01 to 1.18 mM).

Motor2 binds to CPT at an ideal 1:1 ratio between host and drug as seen in the linear region of the phase solubility curve (Figure 8A), however, with several other drugs, a plateau was seen at higher concentrations of Motor2. This is known as an A_N-type plot and suggests Motor2 self-association at higher concentrations. As stated before, Motor2 may have lower solubility, however, it also binds to many drug compounds, like CPT, with very high affinity, thus potentially inhibiting the drug's release. This does not, however, render Motor2 useless. It may be possible to use Motor2 for targeted delivery of drugs that requires the encapsulation of the drug within the carrier until the system reaches the necessary binding site. This will be discussed further later on in this thesis. In taking advantage of its high affinity to drugs, Motor2 is currently being studied by Dr. Matthias Eikermann (Massachusetts General Hospital and Harvard medical School,

Boston, MA) for the purpose of harvesting of neuromuscular blocking agents *in vivo* to reverse their effects[168]. Motor2 binds very strongly (3.4×10^9 M^{-1}) to the neuromuscular blocking agent rocuronium. By binding to rocuronium in blood, Motor2 depletes the concentration of the drug at the neuromuscular junctions, thus reversing the anesthetic effects. Once bound, Motor2-rocuronium is cleared from the body. Sugammadex, a derivative of γ-CD, has been marketed in Europe for this same purpose but it has not been approved for use in the US because of its potential to cause severe allergic reactions and hemorrhagic side effects. Sugammadex also only binds to rocuronium with an affinity of 1.05×10^7 M^{-1}. Motor2 The advantages Motor2 has over Sugammadex allows for the faster and safer reversal of rocuronium, thus making it an attractive alternative to Sugammadex[168].

A

R = CH$_2$CH$_2$CH$_2$SO$_3$Na

B
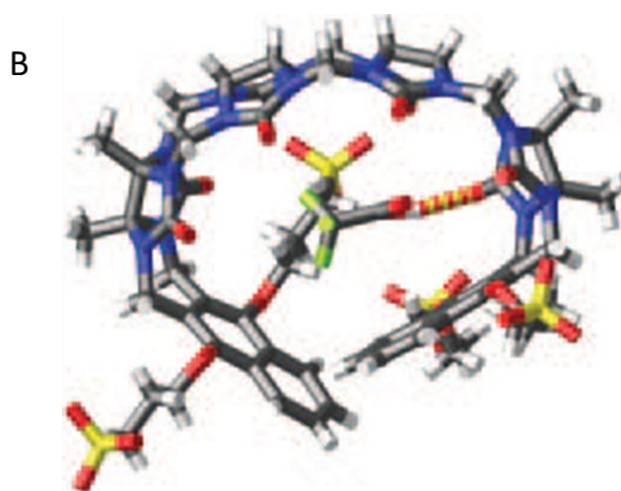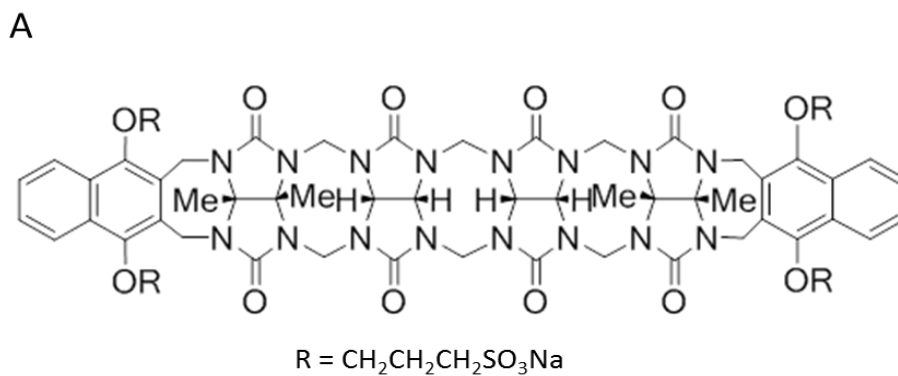
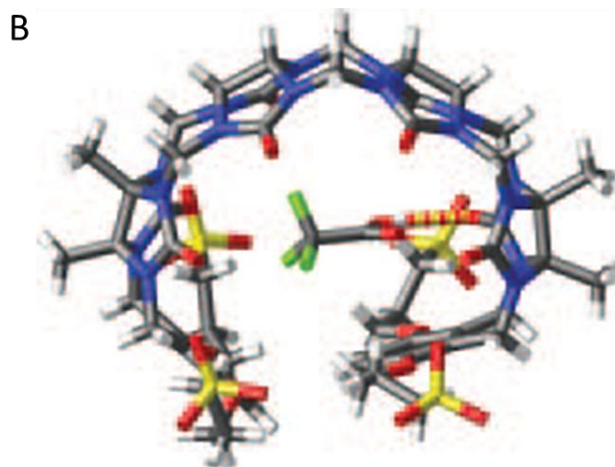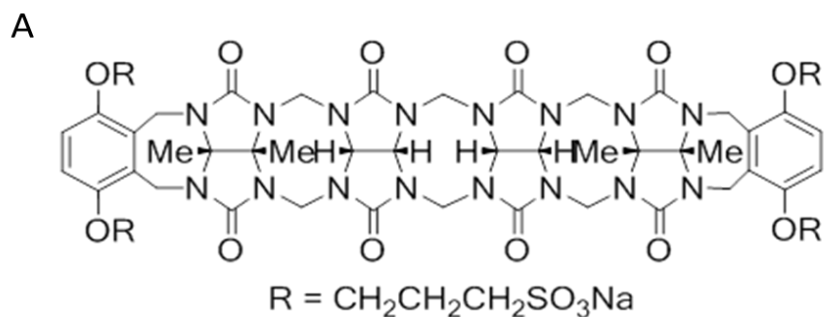**Figure 7:** Motor2 is an acyclic member of the CB[n] family with six glycouril units in its backbone and four sulfonate groups in addition to large aromatic groups at the ends [150]. Linear chemical Structure (A) and folded crystallography structure (B). Work done by Da Ma and Dr. Lyle Isaacs[150].
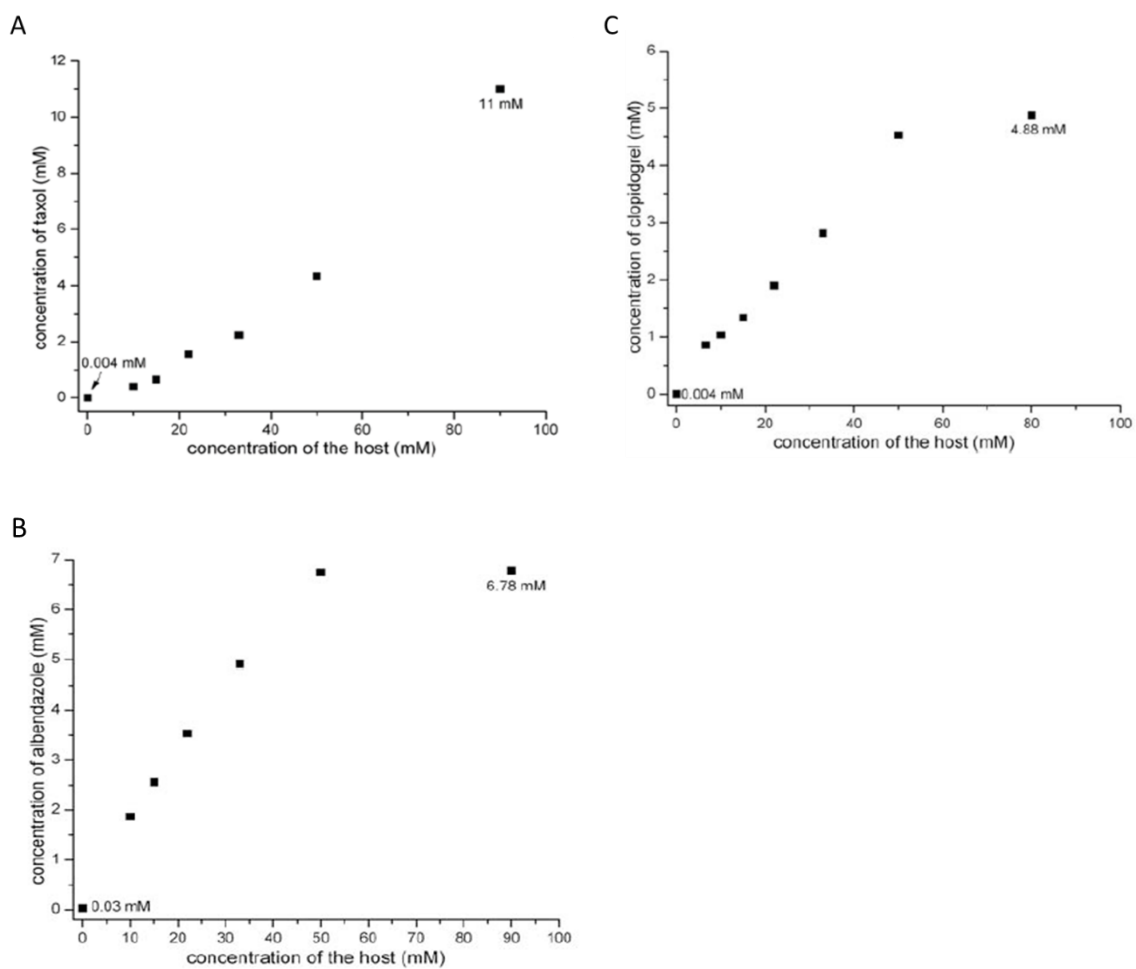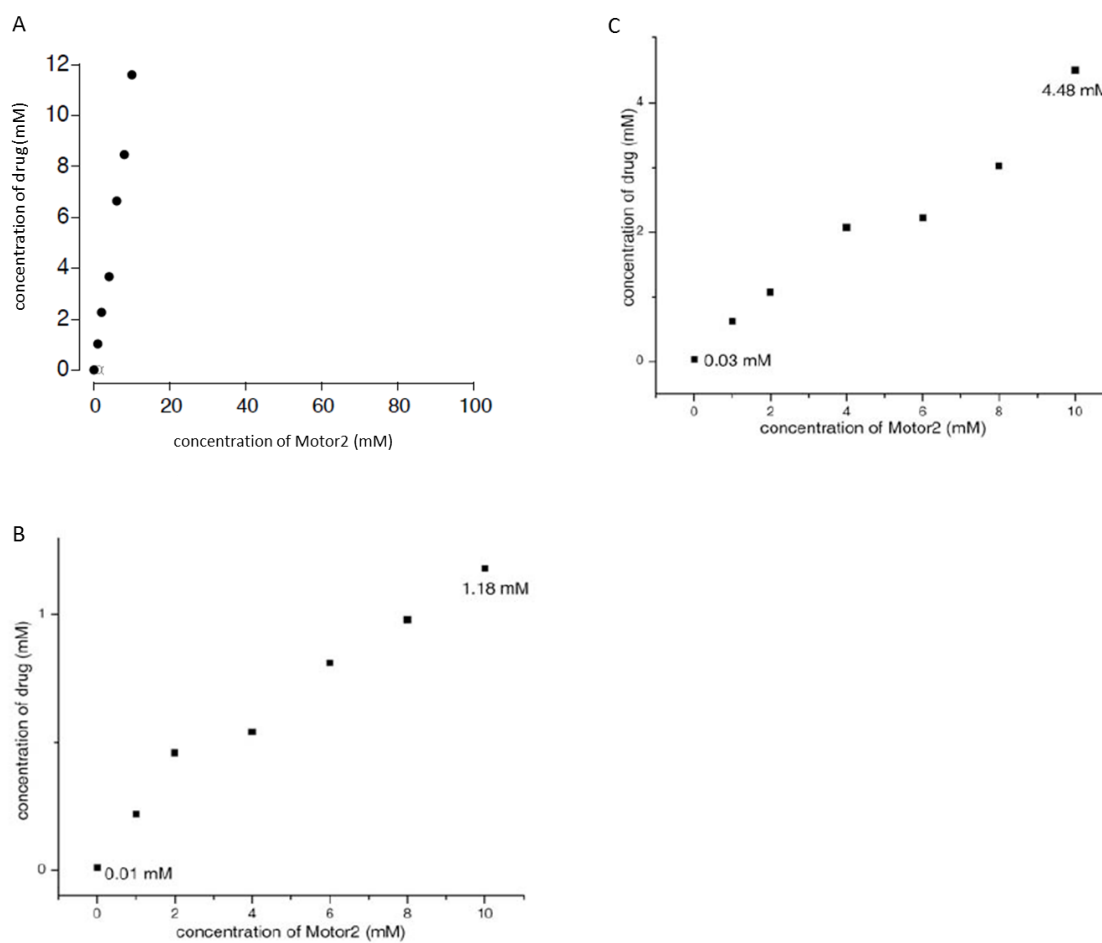
Figure 8: Motor2 significantly increases the solubility of several drugs such as CPT (A; ~580-fold increase), ABZ (B; ~149-fold increase), tamoxifen (C; ~118-fold increase). Work done by Da Ma and Dr. Lyle Isaacs[150].

2.5 Hypothesis

Though the molecular properties of Motor2 are discussed, all biological data presented here will be using Motor1. This is primarily because Motor1 provided with the highest solubility and ideal binding affinities towards multiple drugs that would allow for their *in vivo* release.

The above data provides encouraging proof that CB[n]-type molecular compounds can be used to improve the solubility of drugs that are failing the drug development pipeline for this reason. By doing so, they will not only improve attrition rates, but also enhance public health by providing a larger diversity of drugs in the market across therapeutic fields. Based on these molecular properties in addition to the success of other CB[n] compounds and their close counterparts, the CDs, I hypothesized that Motor1 can be used as an excipient to increase the solubility of many candidate and marketed drugs, thereby, improving their bioavailability and the easy with which these pharmaceutical agents are formulated for clinical use.

Chapter 3. PROJECT 1 MATERIALS AND METHODS

3.1 Materials

PTX was purchased from LLC Laboratories. CPT and ABZ were purchased from VWR. PBS-1086 was a gift from Dr. Timothy Fouts (Profectus Biosciences Inc., Baltimore, MD). Hoechst33342 was obtained from Sigma-Aldrich. Prolong Gold Antifade Agent, AlexaFluor-555 Phalloidin and Trypsin/EDTA were purchased from Invitrogen. CellTiter 96 AQueous Kit® (MTS) was purchased from Promega and the Toxilight® BioAssay Kit (AK) from Lonza. Cell Death Detection ELISA® was purchased from Roche®. BD Matrigel™ was purchased from BD Biosciences. Analytical instruments used in this study included Spectramax M5e (Molecular Devices), Bio-TEK Synergy HT plate reader, Leica SP5 X Confocal, and BD FACSCanto II.

3.2 Methods

Cell and Bacterial Culture.

HEK293 cells (Human Embryonic Kidney, ATCC #CRL-1573) were grown in DMEM (GIBCO media Invitrogen) with 10% heat inactivated fetal calf serum (FCS, Hyclone), and 1% Penicillin/Streptomycin (Invitrogen). HepG2 (Heptacellular carcinoma, Human, ATCC #HB-8065), HeLa (Human cervical carcinoma cells, kindly provided by Dr. David Mosser) and MCF-7 (Mammary Gland Adenocarcinoma, ATCC #HTB-22) cells were grown in MEM media (ATCC #30-2003) with 10% FCS and 1% Penicillin/Streptomycin. THP-1 (Blood Monocytes, ATCC #TIB-202) cells were grown in RPMI media (ATCC #30-2001) with 10% FCS and 1% Penicillin/Streptomycin. SKOV-3 (Ovarian

Adenocarcinoma, ATCC #HTB-77) cells were grown in McCoy's (ATCC #30-2007) with 10% FCS and 1% Penicillin/Streptomycin.

Blood samples (50 mL) were collected from three healthy volunteers (University of Maryland IRB protocol #06-0218). *M. smegmatis* was cultured as described in Velmurugan *et al* [169].

Animal Studies

Maximum tolerated dose (MTD) studies were performed at the University of Maryland, Greenbaum Cancer Center Translation Laboratories, Baltimore, MD under the supervision of Dr. Rena Lapidus (IACUC protocol #0405001). A total of 30 Female Swiss Webster mice were obtained from University of Maryland, Baltimore.

Tumor studies were conducted at the University of Maryland, College Park, MD. NCrNU-F mice were purchased from Taconic (protocol# R-09-35).

3.2.1 *In vitro* and *in vivo* assessment of Motor1 biocompatibility.

Cell Viability and Cytotoxicity Assays

HEK293 cells (2.5×10^6), HepG2 cells (4×10^5) and THP-1 cells (2.5×10^6) were seeded in a 96 well plate (Corning) at 200 µL/well. After the cells were allowed to adhere for 24 hrs, they were treated with 0.010, 0.1, 1 and 10 mM of Motor1 over a 48 hr period. Six technical replicates were used for the untreated samples while four technical replicates were used for all treatment samples including the distilled water treatment conducted before the cells were assayed. Cells were assayed using the MTS and AK assay according to vendor instruction. The AK assay was conducted by aliquoting 20 µL of supernatant

from each sample into a separate black well plate (Corning) after the 48 hr treatment period. These samples were run prior to using the MTS assay. The plates were read using the Spectramax M5e (Molecular Devices) and Bio-TEK Synergy HT plate reader. Data was collected in the form of units of absorbance and luminescence and normalized to percent cell viability (MTS) and percent cell death (AK) with the use of equations (**1**) and (**2**):

% Cell Viability = $(Abs_{sample}/Average\ Abs_{UT}) \times 100$ **(1)**

% Cell Death = $(RLU_{samples}/Average\ RLU_{distilled\ water}) \times 100$ **(2)**

Hemolysis Assay

Red blood cells (RBCs) were collected from 3 healthy donors and purified by centrifugation of whole blood at 1,200g for 15min. RBCs were then incubated with varying concentrations of Motor1 for 3 hours at a 1:10 dilution. Concentrations of Motor1 used were 0.01, 0.1, 1 and 1 mM. Hemolysis was evaluated by measuring absorbance at 540 nm. Percent hemolysis was normalized using equation (**3**).

% Hemolysis = $(Abs_{sample}/Average\ Abs_{distilled\ water}) \times 100$ **(3)**

In vivo *Toxicology*

Thirty female Swiss Webster mice were used for this MTD study. Five different concentrations of Motor1: 154.1 mg/kg, 308.2 mg/kg, 616 mg/kg, 924.6 mg/kg and 1230 mg/kg were used including a PBS control group. Each concentration and the control group included 5 mice/group. Mice were dosed at 10 ml/kg according to their weights

once every 4 days for 8 days and were then monitored for 2 weeks after administering the last dose. Mice were dosed by tail vein intravenous injection.

3.2.2 Evaluation of drug efficacy upon loading into Motor1

In Vitro *Bioactivity and EC$_{50}$ Studies.*

PTX

 HeLa cells (1×10^4), MCF-7 (2×10^4) and SK-OV-3 cells (2×10^4) were seeded in three well slides (Electron Microscope Science) and allowed to adhere overnight. Cells were then treated with different concentrations of PTX complexed to Motor1 (5 mM) for 24 hr, and then fixed and stained with AlexaFluor 555-Phalloidin and Hoechst33342 according to the vendor instructions. Control groups included untreated cells, staurosporine, and treatment with Motor1. Cells were then incubated with Prolong Agent® overnight at 4°C and analyzed using the Leica SP5 X Confocal microscope. Quantification was performed on three replicate wells for two independent experiments by counting a total of 500 cells per well and determining the fraction of fragmented nuclei.

For EC$_{50}$ studies using 1×10^4 HeLa and 2×10^4 SK-OV-3 cells were seeded in triplicates in 96 well plates, incubated with Motor1-PTX at various concentrations for 24 hrs. The Cell Death ELISA® was then performed. Prism Graph 5.0 best-fit, non-linear analysis was performed to calculate EC$_{50}$ values.

PTX, PBS-1086, CPT and ABZ

Comparative bioactivity studies were conducted using HeLa cells seeded at 1×10^4 cells in triplicates in 96 well plates. Drugs were stirred overnight at maximum solubilities in 5

mM of Motor1 and HP-β-CD solutions. Dilutions were made from these stock solutions (1, 0.5, 0.1, 0.05, 0.01, 0.005, 0.001, 0.0005, and 0 mM of Motor1 and HP-β-CD). Cells were incubated for 24 hrs with these solutions and the Cell Death Detection ELISA® was performed.

 In vivo *Tumor Treatment*

Sixty-five female NUDE mice were injected subcutaneously under the neck with 1×10^7 cells/100 μl of HeLa cells (DMEM/BD Matrigel™). Tumors were allowed to grow until a volume of 150-200 mm^3 prior to the start of treatment.

Drug solutions were made with Motor1 at the following concentrations:

PTX (55.6 mg/kg) + Motor1 (924.6 mg/kg)

PBS-1086 (134.16 mg/kg) + Motor1 (894.8 mg/kg)

CPT (5.22 mg/kg) + Motor1 (184.9 mg/kg)

ABZ (17.8 mg/kg) + Motor1 (924.6 mg/kg)

Mice were injected 3 times, each 4 days apart i.v. through the tail vein. Mice were dosed by weight (10 mL/kg). Two days after the last dose, mice were dosed again every day for four days. One week after the last dose of this schedule, mice were dosed a third time three times, one/day, by weight, i.p. Tumor volume, mouse weight and survival were monitored throughout treatment and for 1 week after the final dose. Experimental endpoints were: 1500 mm^3 in tumor volume or a 20% drop in weight.

3.2.3 Statistical Analysis.

Experimental data were presented as means ±SD except where otherwise stated. The results were analyzed using two-tailed Student's unpaired t-test with Graph Pad Prism Graph 5.0 software

Chapter 4. PROJECT 1 RESULTS AND DISCUSSION

4.1 *In vitro* and *in vivo* assessment of Motor1 biocompatibility.

4.1.1 Motor1 is well tolerated *in vitro* in human erythrocytes and monocytic, kidney and liver cell lines

The human kidney cell line (HEK293) treated with concentrations of Motor1 at 0.01, 0.1, 1, and 10 mM resulted in an average of 92%, 96%, 89% and 79% cell viability in the MTS assay (Figure 9A). Distilled water treated samples were at an average of 0.2% cell viability. The AK release assay (Figure 9B) showed an average of 2%, 1%, 1% and -2% AK release in 0.01, 0.1, 1 and 10 mM of Motor1. The AK assay revealed an average 3% AK release in untreated samples.

In the MTS (Figure 9C) assay, the human liver cells (HepG2) treated with 0.01, 0.1, 1 and 10 mM of Motor1 resulted in an average of 104%, 100%, 102%, and 82% cell viability. Distilled water was at an average of 1% cell viability. The AK assay (Figure 9D) conducted using the HepG2 cell line showed an average of 55% 56% 50% and 17% AK release after treatment with increasing concentrations of Motor1 (0.01, 0.1, 1, and 10 mM respectively). Untreated samples revealed an average of 59% AK release.

Human monocytes (THP-1 cell line) treated with Motor1 (0.01, 0.1, 1, and 10 mM) showed an average of 98%, 142%, 145% and 112% cell viability in the MTS assay (Figure 9E). The distilled water treated samples resulted in an average of 0% cell viability. The AK assay (Figure 9F) showed an average of 17%, 5%, 4% and 2% AK release after Motor1 treatment (0.01, 0.1, 1, and 10 mM respectively). The untreated samples resulted in an average 20% AK release.

Finally, the hemolysis assay conducted using primary human red blood cells (Figure 9F) showed 4%, release of hemoglobin from erythrocytes treated with 0.01, 0.1, 1, and 10 mM Motor1 respectively. The untreated samples showed an average 3% release of hemoglobin.

MTS (Figure 10A) and AK assays (Figure 10B) conducted on HepG2 cell line using HP-β-CD (1, 5, and 10 mM) resulted in an average of 104%, 88% and 121% cell viability and 13%, 11% and 11% AK release respectively. Treatment with cremophor®EL (8.75 and 17.5 mM) showed an average 18% cell viability at both doses and an average 47% and 56% AK release respectively.

4.1.2 Motor1 was well tolerated *in vivo* in female Swiss Webster Mice.

Mice dosed with 154.1, 308.2, 616, 924.6, and 1230 mg/kg of Motor1 via bolus tail vein injection three times over 8 days and monitored for an additional two weeks showed a steady increase in weight from day 0 (Figure 11). No signs of sickness were visually observed.
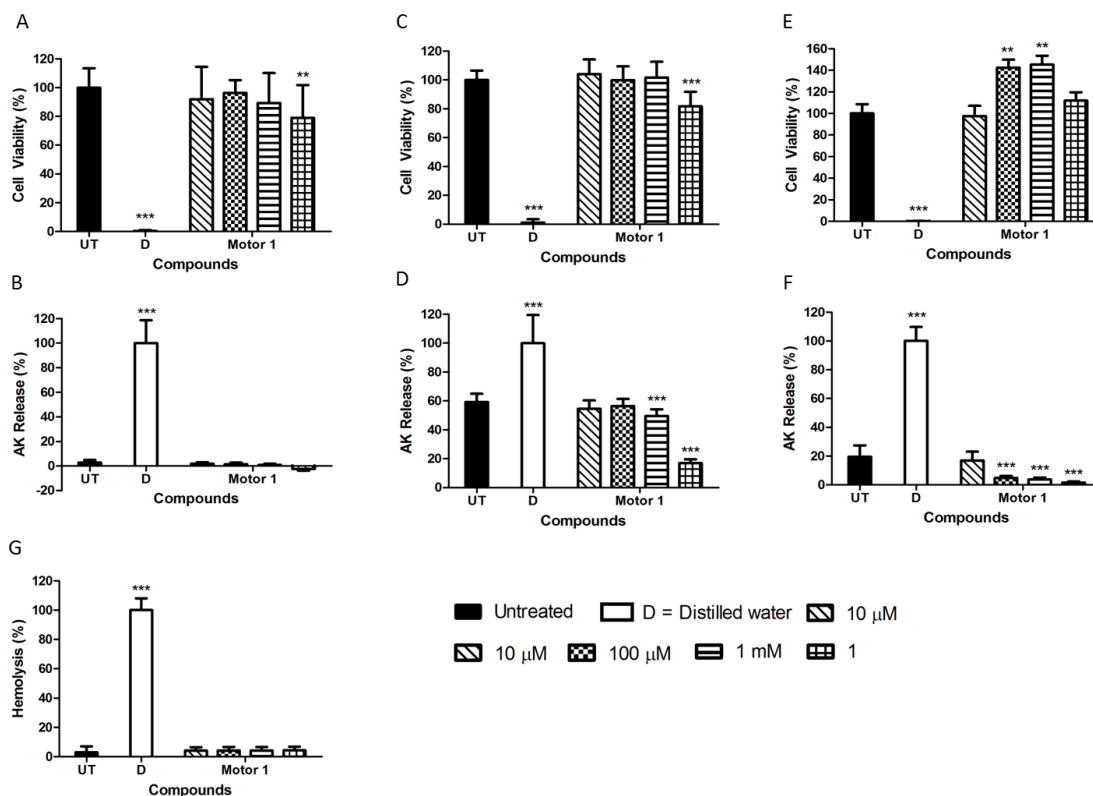
Figure 9: Motor1 is non-toxic in human kidney, liver and monocyte cell lines and human erythrocytes. Plots of cell viability (MTS assay; A C, E) and cell death (AK release assay; B, D, F) obtained for Motor1 (0.01 mM, 0.1 mM, 1 mM, 10 mM) after 48 hr incubation with three cell lines: HEK293 cells (A, B), HepG2 cells (C, D) and THP-1 cells (E, F). Data presented in A-F are the average values from triplicate experiments and the corresponding standard deviation values. Hemolysis assay (G) conducted using purified human red blood cells diluted in phosphate buffered saline and then incubated with Motor1 for 3 hr. Data represents the average and standard deviation values from three replicate experiments with four donors. For all panels, unpaired t-test analysis was used (*P=0.01–0.05; **P=0.001–0.01; ***P < 0.001). Work done by Gaya Hettiarachchi and Volker Briken[150].
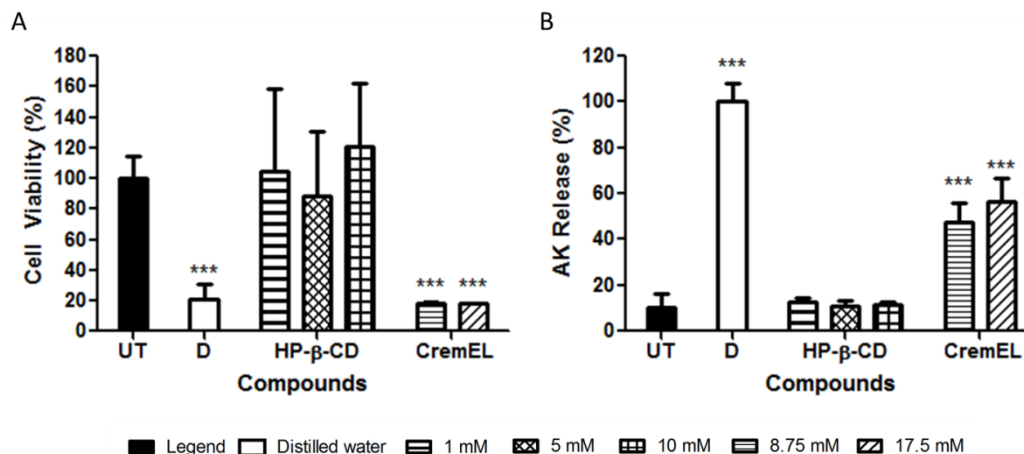
Figure 10: HP-β-CD is non-toxic in human liver cells up to a concentration of 10 mM while cremophor®EL is toxic at both 8.75 and 17.5 mM. Cell viability (A) and cell death (B) obtained for HP-β-CD (1 mM, 5 mM, and 10 mM) and cremophor®EL (8.75 mM and 17.5 mM) after 48 hr incubation with HepG2 cells. Data is representative of three replicate experiments. Unpaired t-test analysis was used (*P=0.01–0.05; **P=0.001–0.01; ***P < 0.001). Work done by Gaya Hettiarachchi and Volker Briken[150].
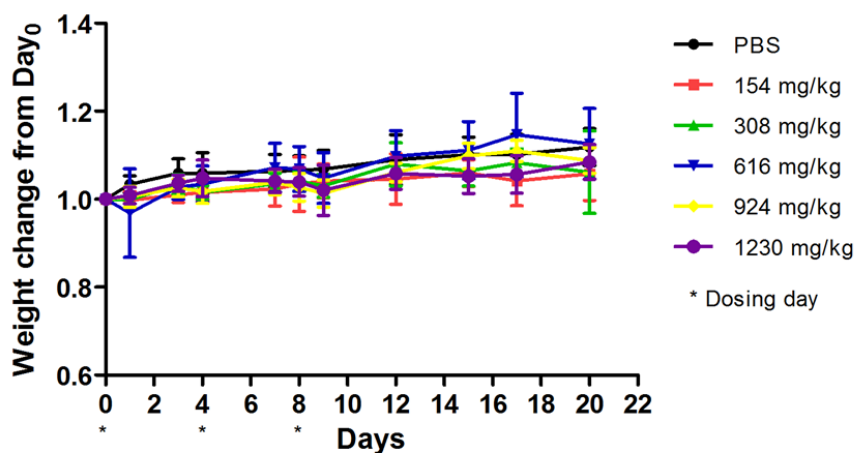
Figure 11: Motor1 is highly biocompatibility *in vivo*. Female Swiss Webster mice (n=5 per group) were dosed via the tail vein on days 0, 4 and 8 (* = dosing day) with PBS or different concentrations of Motor1. The normalized average change in weight per group is indicated. Error bars represent standard error of the mean. Work done by Gaya Hettiarachchi and Volker Briken[150].

4.1.3 Discussion

For the *in vitro* toxicology work, two complementary cellular assays were used: MTS (CellTiter96 AQueous Kit®) assay which measures cellular metabolism, and the AK (ToxilightBioAssay Kit®) assay which measures cell death via the release of the cytosolic enzyme AK into the supernatant. In the cell viability assay, the MTS reagent is internalized and hydrolyzed by metabolically active cells into a colorimetric compound which can then be measured by a spectrophotometer. Therefore, the amount of colorimetric compound that is synthesized is directly proportional to the amount of metabolically active cells present in the sample and, thus, serves as a quantification of cell viability[170]. The AK assay quantifies the release of AK from cells with damaged membranes. AK is a cytosolic enzyme that converts ADP to ATP providing an energy source for the cell. When cells undergo necrosis, the cell membrane ruptures releasing cytosolic proteins, like AK, into the sample supernatant. In the AK assay, ADP is converted to ATP by this released AK. ATP then converts luciferin to light by using luciferase as a catalyst. This luminescence assay, therefore, provides a quantification of the release of AK from necrotic cells. Therefore, the AK assay provides a quantification of cell death[171].

There are some drawbacks to these assays. In the MTS assay, the production of false positives may be likely. If cells are in the process of dying, they may become highly metabolically active giving false positives. However, the following experiments were done over a matter of days, therefore, the likelihood that dying cells remain metabolically active over the lengthy incubation periods is unlikely. A drawback of the AK assay is that this assay is dependent on the amount of AK in the cytosol of the particular cell. The

concentrations of AK can differ from cell type to cell type thus resulting in varied results. We see this in effect in Figure 9D where the untreated HepG2 cells showed almost 60% cell death. This experiment was repeated several times and with other cell lines. This phenomenon was only observed with the HepG2 cell line.

Both assays were used to assess the biocompatibility of Motor1 (Figure 9) in three different cell lines: human kidney (HEK293), liver (HepG2), and monocytic (THP-1) cell lines. Two of these cell lines, the HEK293 and HepG2 cells, are commonly used in drug toxicity studies because the kidney and liver are organs where substantial amounts of drugs accumulate for metabolism and clearance by the body. This makes these key locations at which toxicity could occur. The THP-1 cell line was used to investigate any detrimental effects of Motor1 towards immune cells upon intravenous injection. For similar reasons, the hemolysis assay (Figure 9F) was used to determine whether Motor1 induces red blood cell lysis following intravenous injections. This was an important assay to conduct because as previously stated, the CB[n] family's closest relative, the CDs, leads to hemolysis by extracting red blood cell membranes of cholesterol[124].

These initial toxicology work suggests that Motor1 surpasses some of the most commonly used DDSs such as CDs and cremophor®EL. Motor1 resulted in high cell viability and low cell death up to a concentration of 10 mM in HEK293, HepG2, and THP-1 cell lines (Figure 9A-F). Furthermore, the hemolysis assay showed that Motor1 is non-toxic to red blood cells (Figure 9G) up to a concentration of 10 mM. A comparative toxicity study using HP-β-CD and cremophor®EL in HepG2 cells was also conducted (Figure 10). These compounds were incubated for 24 hrs with HepG2 cells at

concentrations up to 10 mM (HP-β-CD) and 17.5 mM (cremophor®EL). These experiments revealed no significant decrease in cell viability or increase in cell death (Figure 10A and B) upon incubation with HP-β-CD. These results are comparable to those collected in Motor1 testing. In contrast, cremophor®EL was found to be highly toxic at concentrations of 8.75 and 17.5 mM. The MTD study using Female Swiss Webster mice and Motor1 up to a concentration of 1230 mg/kg/dose revealed no decrease in body weight from day 0 or deviation from the rate of weight gain observed in the PBS control group (Figure 11). We were not able to establish an MTD value using this dosing schedule due to limitations with Motor1 solubility.

CD toxicity is well established; this family, including its derivatives, are been known to cause toxicity in erythrocytes by extracting red blood cell membranes of cholesterol. The *in vitro* hemolytic activity of this family (at 1 mM) is as follows: β-CD > α-CD > HP-β-CD > γ-CD >> HP-γ-CD ≥ HP-α-CD in erythrocytes [124, 128]. In this regard, Motor1 was demonstrated to be superior up to a concentration of 10 mM. CD toxicology *in vivo* has been well established as well. The most toxic side effect observed is the family's hemolytic activity, however, severe kidney damage after *in vivo* parental administration of CDs in rats and dogs has also been observed[129]. This damage is thought to be a result of cholesterol/CDs complexes depositing in the kidney and forming crystals. Concentrations ranging from 100-400 mg/kg of HP-β-CD showed minor reversible histological changes in the kidneys and erythrocyte damage in animal models. However, it should be noted that this phenomenon is not observed in humans[124, 130]. HP-β-CD is, however, limited to 400 mg/kg (i.v) due to the emergence of reproductive and developmental toxicities. (SBE)-β-CD was shown to be generally non-toxic in

animals and humans, however, it is limited to approximately 5 g/kg (i.v) due to reproductive and developmental toxicities[128]. For comparative purposes, a rigorous (ex: daily i.v dosing), long term, *in vivo* testing of Motor1 at varied dosing schedules will need to be conducted to determine an MTD value for this compound.

Motor1 also surpassed cremophor®EL in safety. The toxicity of cremophor®EL is also very well established both *in vitro*, *in vivo* and in human clinical trials. Approximately, 30 mL/m^2 of cremophor®EL can be administered in humans with some safety over a 3 hr infusion[31]. The primary adverse reaction associated with this formulation is severe hypersensitivity which is thought to be brought on by complement activation. Other severe adverse effects include neurotoxicity and liver damage[29, 31]. *In vitro* assays have established complement activation in several tumor cell lines with only 2 µg/mL of cremophor®EL which is readily available in clinical dosing[30]. Furthermore, *in vivo* studies conducted in dogs showed significant histamine release leading to hypersensitivity[29]. This histamine release is observed and connected to cardiac toxicity in other *in vivo* models[30].

Within the limits of this study, Motor1 showed to be an attractive alternative to currently used technologies, like CD derivatives or surfactants such as cremophor®EL. If *in vivo* efficacy of multiple Motor1-drug complexes can successfully be established, further toxicity studies will need to be conducted to firmly establish the biocompatibility of this compound in hopes of filing an IND with the FDA and move Motor1 into clinical trials. As introduced before, there are different forms of toxicity that the FDA requires testing for during preclinical screening for excipients, like Motor1. There are different toxicity assessments for short term, intermediate and long term use of an excipient.

Before clinical trials can be started, adequate information on an excipient's acute and repeat dose toxicities, genetic toxicity, immunogenicity, reproductive and developmental toxicity must be collected[20, 26]. Assessing these types of toxicities utilizes both *in vitro* and *in vivo* assays and most of these *in vivo* studies will need to be done in one rodent model, usually in rats, and one non-rodent model. Many of these studies should be conducted in the future before an IND for Motor1 can be submitted to the FDA[5, 26].

Acute toxicity refers to toxicity after single high dose[27]. This assessment is recommended for short term, intermediate and long term use of Motor1. A repeat dose study can also be conducted using escalating doses instead of a single dose study. Repeat dose studies are, however, required for intermediate and long-term usage of Motor1. These studies should have a duration of 1-3 months for intermediate usage and 6-9 months for long-term usage of Motor1. These studies must conclude with histopathology work to evaluate any toxicities to vital organs such as the liver, kidneys, spleen etc.[27]. These studies should also try and establish an MTD value for Motor1 if possible. Repeat dose evaluation of both Motor1 and 2 in rats is already underway in a collaboration with Dr. Matthias Eikermann at Massachusetts General Hospital and Harvard Medical School, Boston, MA[168].

The Ames test and assays like it are important *in vitro* studies to conduct to assess any potent mutagenic properties Motor1 might exhibit[20, 41, 43]. However, this assay has been known to give false positive and negative results. In addition, the Ames study utilizes salmonella which is not an ideal model for study of eukaryotic cells. Therefore, genetic toxicity studies should also be evaluated in mammalian cell assays like the mouse lymphoma assay, and in *in vivo* mouse studies by using, for example, the Muta® mouse

model or the micronucleus assay[41, 42, 44, 45]. Both of these methods are accepted and well utilized evaluations of compound genetic toxicity. If these results are positive, further testing will be required to assess whether the compound can be carcinogenic upon administration[43]. Carcinogenicity evaluation usually involves a two year study using two different rodent species[26, 39].

The most relevant studies in immunological toxicity to focus on for Motor1 would be hypersensitivity and immunogenicity. Testing for these could be to monitored using ELISAs to detect and quantify the expression of specific cytokines like TNF-α, Interferon γ or antibodies such as IgE or IgM[27, 28]. These assays can be conducted using cell lines and animal models. Blood samples can be collected from rodent and non-rodent models that had been administered with increasing concentrations of Motor1. These samples can then be purified and the presence of cytokines and/or antibodies can be quantified[20, 28]. It is generally recommended to do immunotoxicity evaluation as part of a repeat dose study as well as a single dose study.

Reproductive and development studies are not required by the FDA prior to the start of clinical trials as long as pregnant women are not enlisted in the trials. However, this assessment is required prior to Phase III trials and if child-bearing women will be part of the study[47]. Reproductive and developmental studies are long term assays that usually involve repeat dosing followed by histological evaluation of reproductive organs, sperm count, etc. Furthermore, repeatedly dosed mice need to be mated and the growth and development of the embryo and fetus needs to be recorded[47]. These studies will most likely not be conducted with Motor1 until absolutely necessary.

In addition to these studies, the FDA also has guidelines in evaluating toxicity to vital functions and organs such as cardiovascular function[27]. One *in vitro* assay that can study the effect of Motor1 on cardiovascular function is the hERG assay[20]. This assay assesses whether a compound can block the potassium ion channel that contributes to the electrical activity needed to beat the heart and keep regular rhythm. Intravenous administration of Motor1 requires the evaluation of hemolytic properties and plasma concentrations of creatinine levels at clinically relevant doses to evaluate potential muscle damage[20]. Though hemolytic properties of Motor1 have been assessed in the scope of this current study, higher concentrations will need to be evaluated to assess injection site specific toxicities.

The majority of this future work should be conducted in the rat model before translation into non-rodent models, however, this work is much farther down the developmental pipeline in pursuit of FDA approval. A few studies that could be addressed in the near future are the genetic and immune toxicity evaluations.

4.2 As a result of increased solubility, an increase in drug efficacy was observed upon loading into Motor1

4.2.1 An increase in the efficacy of PTX is observed due to increased solubility once coupled with Motor1

Human cervical cancer cells (HeLa) were incubated with a saturated solution of PTX (2 μM; Figure 12D) or with a solution containing PTX (0.6 mM; Figure 12E) solubilized with Motor1 (5 mM). Controls included untreated cells (Figure 20A), staurosporine treated (Figure 12B) and Motor1 alone (5 mM; Figure 12C). Cell death was

detected by morphological changes, which were highlighted by staining the actin skeleton, and nuclear fragmentation. Quantification of the percentage of cells with fragmented nuclei demonstrated that after 24 hrs less than 5% of PTX-treated cells showed fragmented nuclei, whereas close to 90% of cells treated with Motor1–PTX had fragmented nuclei (Figure 12F). Dose–response experiments using HeLa and SK-OV-3 cells incubated with Motor1-PTX (Figure 12G, and H) revealed EC_{50} values of 0.7 µM and 0.8 µM respectively.

The Cell Death Detection ELISA® was conducted using HeLa cells treated with Motor1 (5 mM), Motor1-PTX (0.6 mM), cremophor®EL (17.5 mM) and cremophor®EL-PTX (0.6 mM). Untreated cells resulted in an average 19% cell death while Motor1, Motor1-PTX, cremophor®EL, and cremophor®EL-PTX resulted in an average 21%, 69%, 61%, and 73% cell death (Figure 13).

4.2.2 Anticancer drugs, PTX, PBS-1086, CPT and ABZ, bound to Motor1 showed significantly higher efficacy in HeLa cells than when these drugs were complexed with HP-β-CD.

Dose response studies using Motor1 and HP-β-CD encapsulating PTX, PBS-1086, CPT and ABZ were conducted over a 24 hrs period in HeLa cells. An average of 76%, 66%, 68% and 91% cell death was observed for PTX (Figure 14A), PBS-1086 (Figure 14B), CPT (Figure 14C) and ABZ (Figure 14D) respectively at the highest concentrations of Motor1 (1 mM; red line) used. An average 52%, 24%, 29% and 43% cell death was observed for PTX (Figure 14A), PBS-1086 (Figure 14B), CPT (Figure

14C) and ABZ (Figure 14D) respectively at the highest concentrations of HP-β-CD (1 mM; blue line) used.
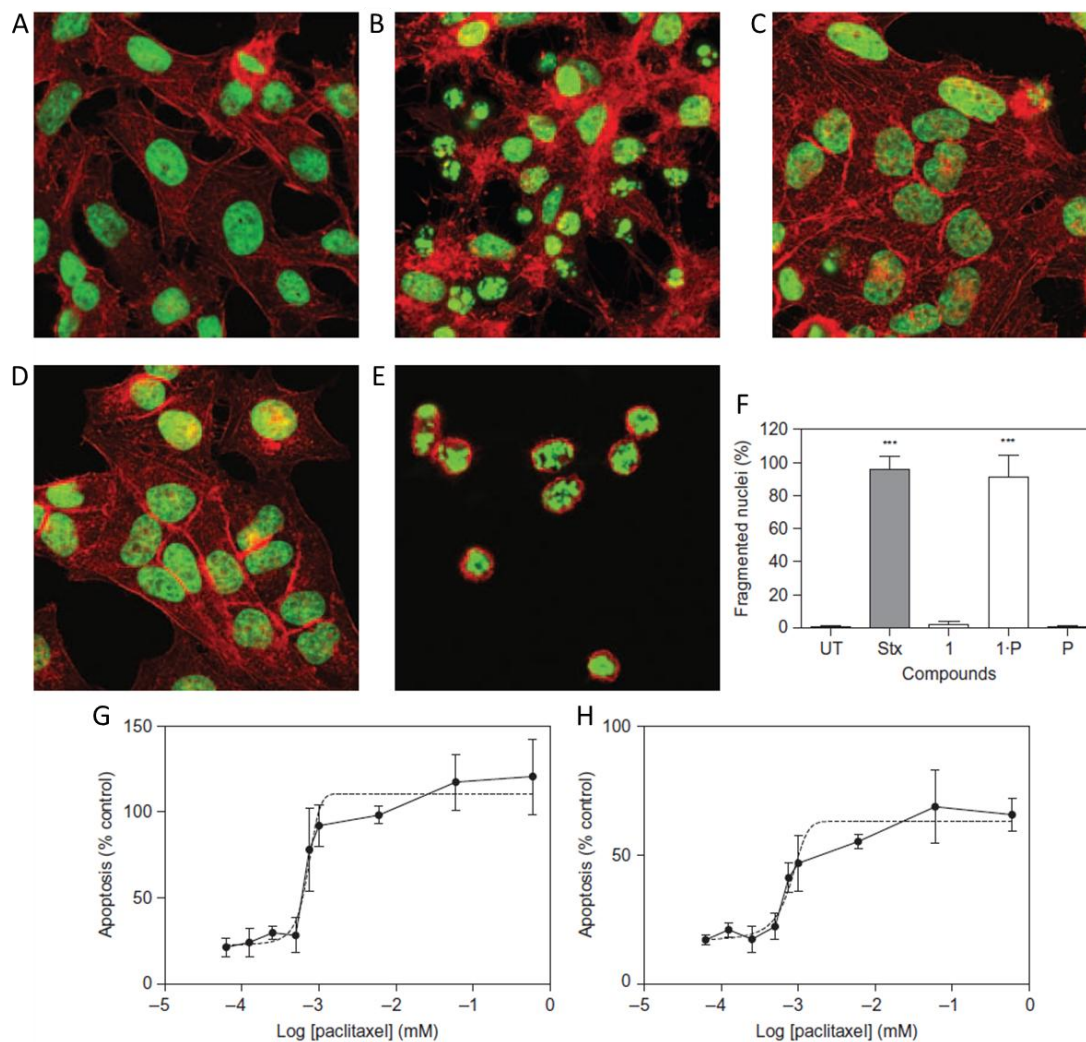
Figure 12: Cell death induction assays performed on HeLa cells indicated an increase in PTX efficacy as a result of increased drug solubility upon loading into Motor1. HeLa cells were incubated for 24 h with cell culture medium alone (A), staurosporine (1 μM) (B), Motor1 (5 mM) (C), PTX (2 μM) (D), a solution containing Motor1 (5 mM) and PTX (0.6 mM) (E). Nuclei are stained in green and actin in red. Percent of cells (F) with fragmented nuclei in A-E. Scale bar for all panels, 25 mm. EC_{50} determination for Motor1–PTX on HeLa (G) and SK-OV-3 (H) cancer cells. Cells were incubated with solutions containing Motor1 (5 mM) and the indicated concentrations of PTX for 24 hrs. The average and standard deviation of cell apoptosis induction was

determined for six replicates and normalized to the amount of apoptosis detected in cells killed with the apoptosis inducer staurosporine (1 µM). The best-fit, nonlinear regression curve is indicated by the broken line. Unpaired t-test analysis was used (*P=0.01–0.05; **P=0.001–0.01; ***P < 0.001). Work done by Gaya Hettiarachchi and Volker Briken[150].
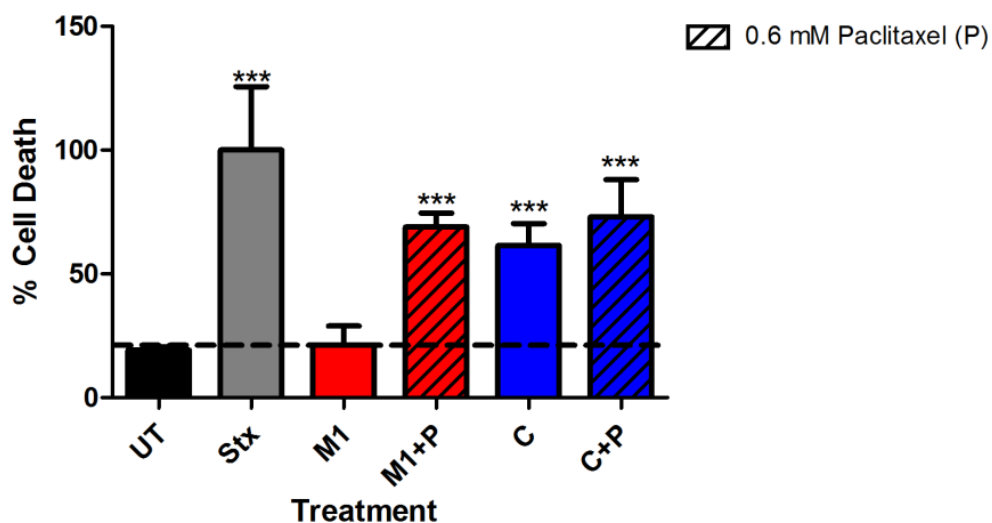
Figure 13: Motor1-PTX (M1+P) cytotoxicity in HeLa cells was as a result of PTX bioactivity whereas cytotoxicity observed in the cremophor®EL-PTX (C+P) is indiscernible from cremophor®EL alone toxicity. Roche® Cell Death ELISA® was conducted on HeLa cells after 24 hrs of continuous incubation with the compounds with the compounds. Conditions: UT = untreated (black), Stx = staurosporine (1 μM) (gray); M1 = 5 mM (red); M1+P: M**1** = 5 mM, P = 0.6 mM (red pattern); C = cremophor®EL (17.5 mM)(blue); C+P: C = 17.5 mM, P = 0.6 mM (blue patterned). This is an average of two separate experiments. The unpaired t-test analysis was used (*P = 0.01–0.05; **P = 0.001–0.01; ***P < 0.001). Work was done by Gaya Hettiarachchi and Volker Briken[150].
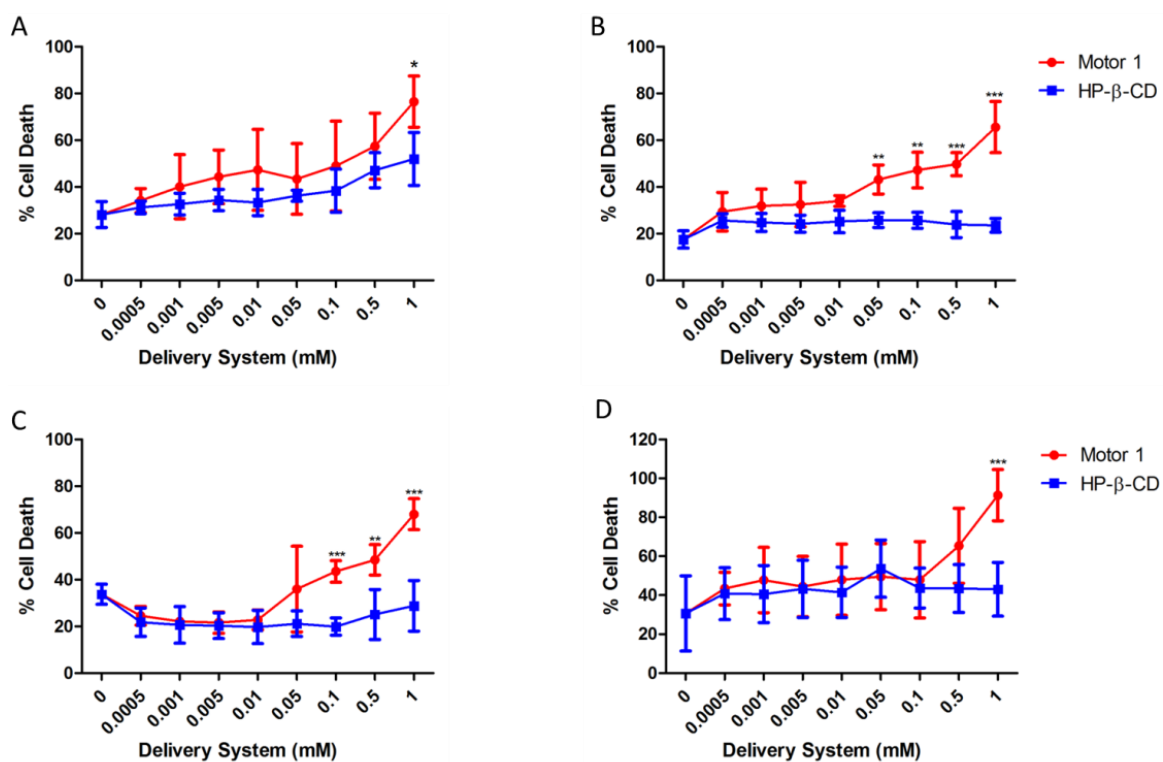
Figure 14: Cell Death ELISAs® performed on human cervical cancer cells using PTX, PBS-1086, CPT and ABZ conjugated to Motor1 or HP-β-CD indicated enhanced cytotoxicity with Motor1. HeLa cells were incubated for 24 hrs with PTX (A), PBS-1086 (B), CPT (C), ABZ (D) conjugated to Motor1 (red) or HP-β-CD (blue). The average and standard deviation of cell apoptosis induction was determined for four replicates and normalized to the amount of apoptosis detected in cells killed with the apoptosis inducer staurosporine (1 μM). This is representative of two repeat experiments. Unpaired t-test analysis was used (*P=0.01–0.05; **P=0.001–0.01; ***P < 0.001). Statistical analysis was done in comparison of Motor1 to HP-β-CD at each concentration. Work done by Gaya Hettiarachchi and Volker Briken(unpublished).

4.2.3 *In vivo* treatment using Motor1-PTX, Motor1-PBS-1086, Motor1-CPT and Motor1-ABZ against HeLa cell tumors showed promising efficacy in Motor1-PTX and Motor1-PBS-1086 treated mice.

Mice were given subcutaneous injections of HeLa cells under the neck skin and tumors were allowed to grow to approximately 150-200 mm^3. Treatment was conducted using three different administration methods. PBS and Motor1 alone treatments are indicated in black and green lines respectively in all figures.

Administration Method 1: 3 i.v doses, each one 4 days apart – last dosing on day 9.

On the last day of treatment (day 9), tumor volumes showed an average of 1110($\pm$170), 1300($\pm$220), 845($\pm$230), 740($\pm$174), 933($\pm$242), and 951($\pm$219) mm^3 for PBS (Figure 15), Motor1 (Figure 15), PTX (Figure 15A), PBS-1086 (Figure 15B), CPT (Figure 15C), and ABZ (Figure 15D) conjugated to Motor1 respectively. Mouse weights were an average of 1.06 ($\pm$0.05), 1.07 ($\pm$0.07), 1.03 ($\pm$0.06), 1.04 ($\pm$0.06), 1.07 ($\pm$0.06), and 1.08 ($\pm$0.07) for PBS (Figure 16), Motor1 (Figure 16), PTX (Figure 16A), PBS-1086 (Figure 16B), CPT (Figure 16C), and ABZ (Figure 16D) conjugated to Motor1 respectively. At this point, mouse survival rates were 100% for all treatments (Figure 17A-D).

Administration Method 2: 4 i.v doses, once daily – first dosing day 11, last dosing day 14

At the end of 11 days, mouse survival (Figure 17) stood as such for each of the treatments: 90% survival for PBS, 40% survival for Motor1, 100% survival for all other treatments. Mouse change in weight (Figure 16) from day 0 was an average of 1.06

(±0.05) 1.08 (±0.07), 1.05 (±0.06), 1.03 (±0.07), 1.06 (±0.05), and 1.09 (±0.08) for PBS, Motor1, Motor1-PTX, Motor1-PBS-1086, Motor1-CPT, Motor1-ABZ on day 11 and tumor volumes were 1159 (±225), 1203(±55), 849(±196), 820(±208), 863(±192), and 1054(±212) mm^3 respectively (Figure 15). Further treatment continued with an altered dosing regimen, starting on day 11.

At the end of this dosing schedule (day 14), tumor volumes were as such: 1472, 768(±107), 799(±111), 839(±348), and 999(±241) mm^3 for PBS (Figure 16), Motor1-PTX (Figure 15A), Motor1-PBS-1086 (Figure 15B), Motor1-CPT (Figure 15C), and Motor1-ABZ (Figure 15D). Mouse weights had changed an average of 1.08, 1.03(±0.06), 1.02 (±0.06), 1.00(±0.07), 1.04(±0.06) from day 0 for PBS (Figure 16), Motor1-PTX (Figure 16A), Motor1-PBS-1086 (Figure 16B), Motor1-CPT (Figure 16C), and Motor1-ABZ (Figure 16D). Mouse survival at day 14 was 10% (PBS; Figure 17), 0% (Motor1; Figure 17), 90% (Motor1-PTX; Figure 17A), 90% (Motor1-PBS-1086; Figure 17B), 100% (Motor1-CPT; Figure 17C), and 60% (Motor1-ABZ; Figure 17D) survival.

Administration Method 3: 4 i.p. doses, once daily – first dosing day21, last dosing day 24

At the start of this treatment on day 21, average tumor volumes (Figure 15), changes in weight (Figure 16), and percent survival (Figure 17) were as follows for Motor1-PTX, Motor1-PBS-1086, Motor1-CPT, and Motor1-ABZ: 998(±230), 1098(±131), 1133(±109), and 1245(±173) mm^3; 0.99(±0.05), 1.01(±0.02), 0.99(±0.04), and 1.04(±0.04); 50%, 50%, 30% and 50% survival.

On the last dosing day, tumor volumes (Figure 15) were at an average of 982(±101), 1038(±142), 1190(±21), and 1231 (±125) mm^3 for Motor1-PTX, Motor1-

PBS-1086, Motor1-CPT, and Motor1-ABZ respectively. Weight change (Figure 16) and percent survival (Figure 17) was: 0.92(±0.02), 0.98(±0.02), 0.99(±0.02), and 0.99(±0.02); 50%, 50%, 30% and 30% survival in Motor1-PTX, Motor1-PBS-1086, Motor1-CPT, and Motor1-ABZ respectively.

On day 30, all mice were sacrificed.
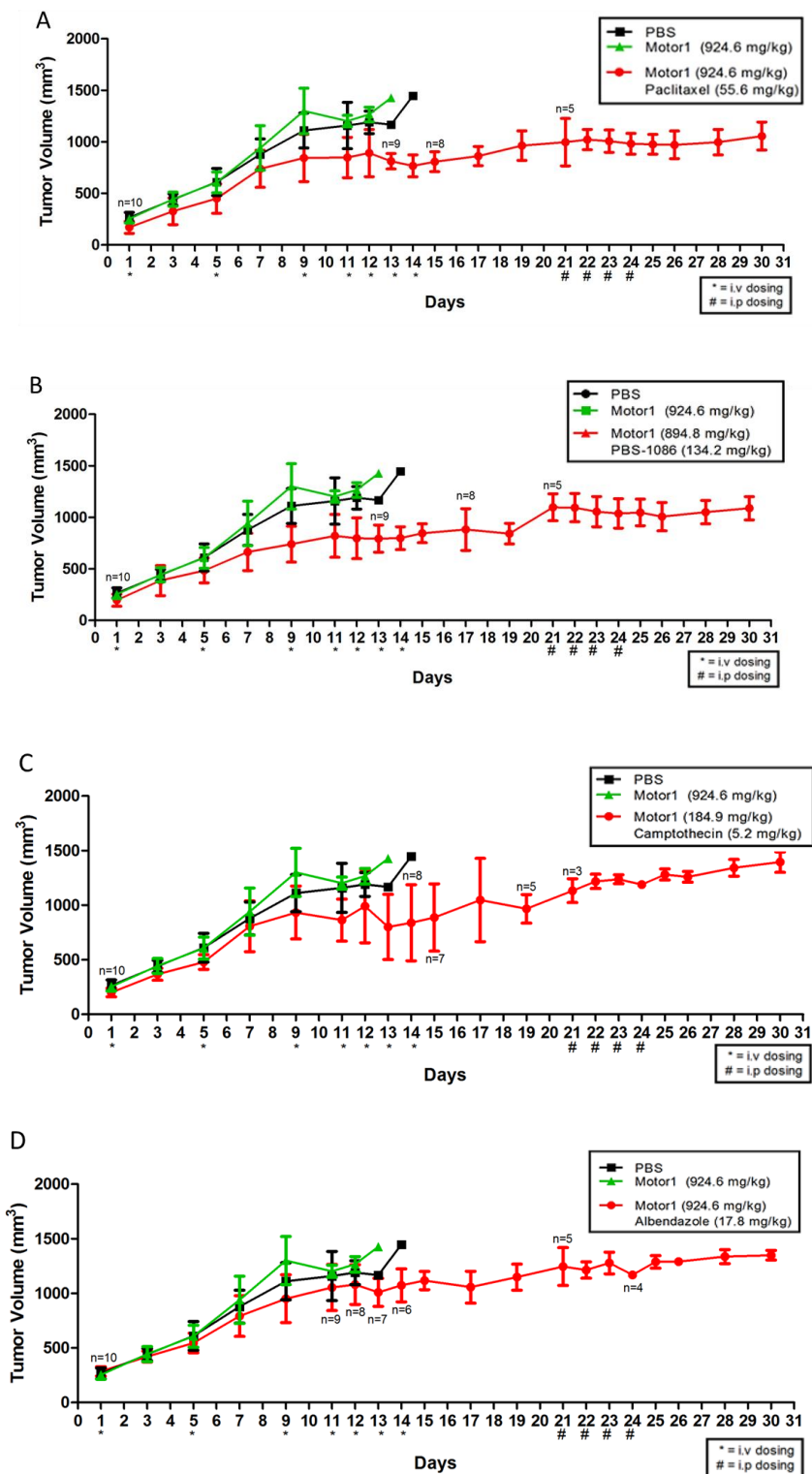
Figure 15: Motor1-PTX (A) and Motor1-PBS-1086 (B) treatments showed significant stabilization of HeLa cell tumors in NUDE mice compared to PBS,

Motor1, Motor1-CPT (C) and Motor1-ABZ (D). 60 female NUDE mice were injected subcutaneously with 1×10^7 cells/100 μL of HeLa cells. Tumors were allowed to grow to approximately 150-200 mm^3 prior to using three methods of treatment. First dosing schedule: tail vein i.v dosing three times, once every four days. Second dosing schedule: tail vein i.v dosing four times, once every day. Third dosing schedule: i.p dosing four times, once every day. All mice were sacrificed on day 30. Treatments were PBS (black), Motor1 (green), Motor1-PTX (A; red), Motor1-PBS-1086 (B; red), Motor1-CPT (C; red), Motor1-ABZ (D; red). Starting n= 10 mice, changes in 'n' value for treatment group indicated; *= i.v dosing; #=i.p dosing. Work done by Gaya Hettiarachchi(unpublished).
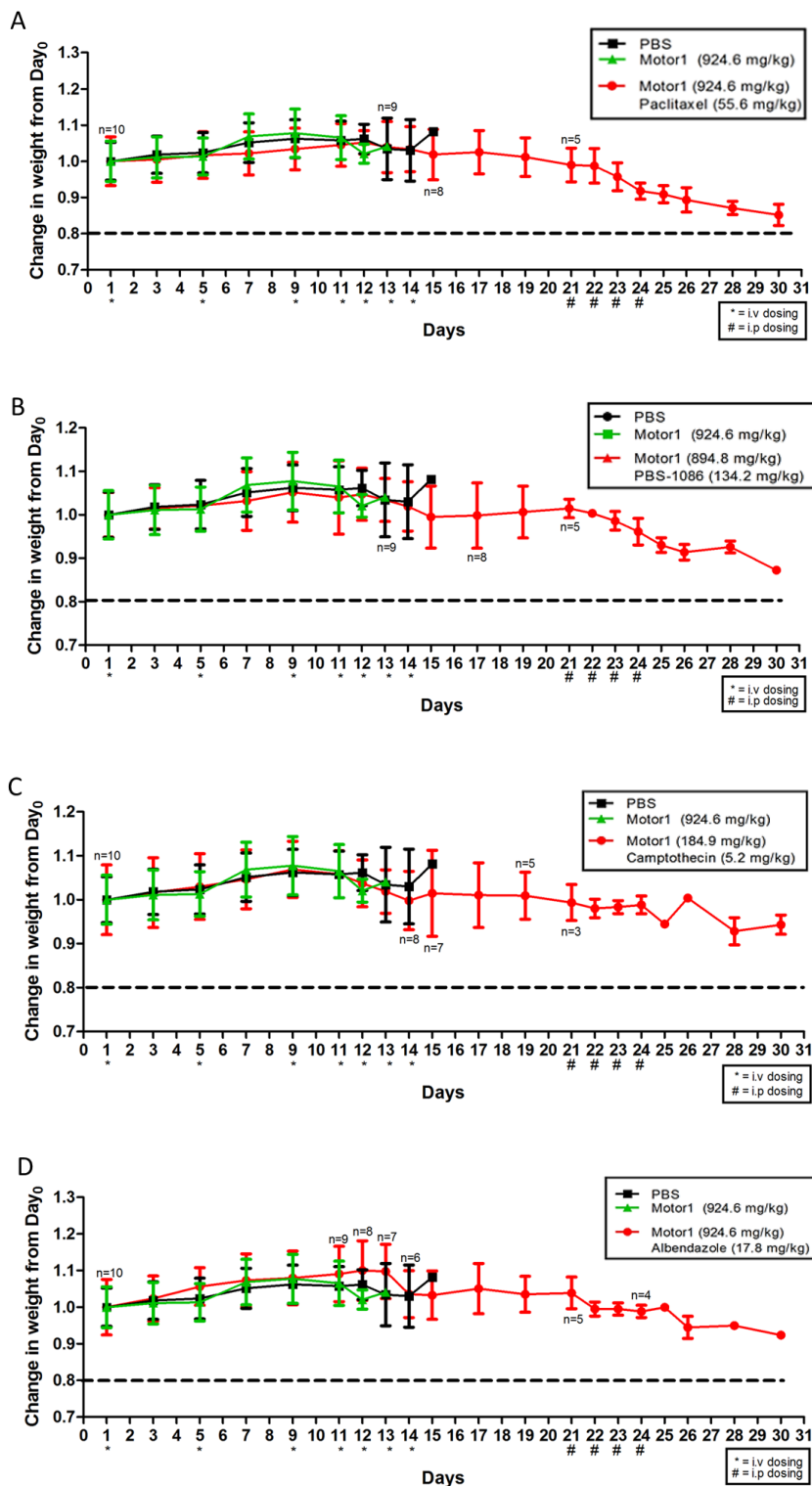
Figure 16: Mice in all treatment groups maintained healthy weights until day 21 when tumor sizes were 1000 mm^3 or more and i.p dosing was started. 60 female

NUDE mice were injected subcutaneously with 1×10^7 cells/100 µL HeLa cells. Tumors were allowed to grow to approximately 150-200 mm^3 prior to using three methods of treatment. First dosing schedule: tail vein i.v dosing three times, once every four days. Second dosing schedule: tail vein i.v dosing four times, once every day. Third dosing schedule: i.p dosing four times, once every day. Treatments were PBS (black), Motor1 (green), Motor1-PTX (A; red), Motor1-PBS-1086 (B; red), Motor1-CPT (C; red), Motor1-ABZ (D; red). All mice were sacrificed on day 30. Starting n = 10 mice, changes in 'n' value for drug treatment group indicated; *= i.v dosing; #=i.p dosing. Work done by Gaya Hettiarachchi (unpublished).
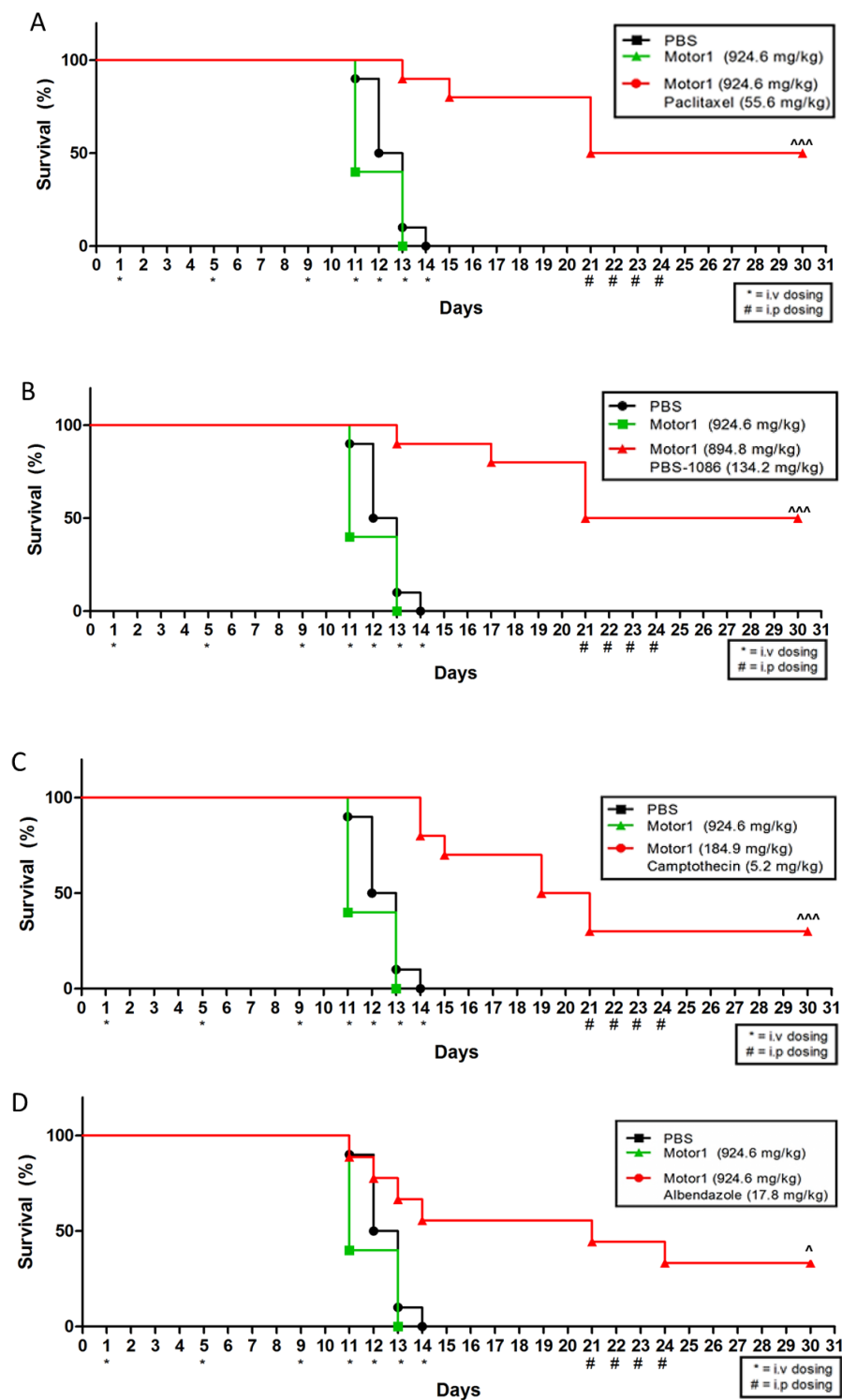
Figure 17: All treatments with Motor1, especially with PTX and PBS-1086 extended mouse survival in comparison to PBS and Motor1 treatments. 60 female NUDE mice

were injected subcutaneously with 1×10^7 cells/100 µL. Tumors were allowed to grow to approximately 150-200 mm^3 prior to using three methods of treatment. First dosing schedule: tail vein i.v dosing three times, once every four days. Second dosing schedule: tail vein i.v dosing four times, once every day. Third dosing schedule: i.p dosing four times, once every day. All mice were sacrificed on day 30. Treatments were PBS (black), Motor1 (green), Motor1-PTX (A; red), Motor1-PBS-1086, Motor1-CPT (C; red), Motor1-ABZ (D; red). Starting n= 10 mice, changes in n value for drug treatment group indicated. The logrank statistical analysis was conducted. * = i.v dosing; # = i.p dosing; ^P = 0.01–0.05; ^^P = 0.001–0.01; ^^^P < 0.001. Work done by Gaya Hettiarachchi and Volker Briken (unpublished).

4.2.4 Discussion

      Treatment of human cervical (HeLa) and ovarian (SKOV-3) cancer cell lines with Motor1-PTX showed that the increased concentrations of PTX being delivered to the cells as a result of Motor1 encapsulation enabled for more efficient killing of both types of cancer cells (Figure 12). This study also demonstrated that binding of PTX inside Motor1 does not interfere with the bioactivity of the drug. The quantification of fragmented nuclei post treatment clearly showed a significant difference in Motor1-PTX vs. PTX alone. 5 mM of Motor1 was able to solubilize 0.6 mM of PTX; this resulted in significantly higher levels of cytotoxicity when compared to the maximum solubility of PTX (0.002 mM) (Figure 12F). The EC_{50} values (Figure 12G and H) established in this study were comparable to those of Taxol® (1.7 μM[172]) indicating equal, if not slightly improved efficacy. However, the difference lies in the fact that cytotoxicity in Taxol® can, in large part, be attributed to cremophor®EL and not only PTX as demonstrated in cell death studies using HeLa cells (Figure 13). These cytotoxicity studies clearly indicated that the cell death observed by Motor1-PTX was as a result of drug bioactivity while Taxol® activity may have been primarily due to cremophor®EL.

      In vitro comparative bioactivity studies with four different anticancer drugs (Figure 14A-D) encapsulated in Motor1 and HP-β-CD were conducted to confirm whether increases in drug solubility using these DDSs can, in fact, result in increased bioactivity in other drugs. These studies also provided information on whether the encapsulation of these drugs in Motor1 can in any way inhibit their bioactivities. Studies were conducted with: PTX, PBS-1086, CPT and ABZ.

PTX is soluble up to 0.6 mM in 5 mM of Motor1, whereas no detectable increases in solubility were observed when PTX was coupled with 10 mM of HP-β-CD (Table 1). It is clear that Motor1 can significantly increase the solubility of this drug while HP-β-CD cannot. This increase in solubility was somewhat translated into increased PTX bioactivity in HeLa cells using Motor1 vs. HP-β-CD showing an average of 76% cell death vs. 52% cell death respectively (Figure 14A). More striking differences were seen in the comparative treatment of PBS-1086, CPT and ABZ with Motor1 vs. HP-β-CD.

Motor1 was able to increase the solubility of PBS-1086 from undetectable levels to 7.5 mM in 10 mM Motor1. Encapsulation of PBS-1086 in 20 mM HP-β-CD did not provide any detectable increases to drug solubility (Table 1). These results were clearly reflected in the comparative bioactivity study conducted using HeLa cells. PBS-1086 encapsulated with 1 mM of Motor1 showed an average of 66% cell death while encapsulation of the drug with 1 mM HP-β-CD showed only approximately an average of 24% cell death which was not an improvement from the cytotoxicity of PBS-1086 treatment alone (Figure 14B). Out of all four bioactivity studies conduct, this was the most striking.

Motor1 at a concentration of 10 mM can solubilize approximately 0.91 mM of CPT while 10 mM of HP-β-CD can only solubilize 0.1 mM CPT (Table1). This, almost 10-fold, difference in solubility is reflected in the bioactivity study where 68% cell death was observed in the most concentrated Motor1-CPT treatment than with the most concentrated dosing of CPT-HP-β-CD (29% cell death) (Figure 14C).

ABZ is soluble up to 1.86 mM in 10 mM of Motor1 and 0.2 mM in 10 mM of HP-β-CD (Table 1). This difference was again translated into drug bioactivity in the cell

death ELISA® with a 91% cell death in Motor1-ABZ (1 mM) while only 43% cell death was observed with ABZ-HP-β-CD (1 mM) (Figure 14D).

These comparative bioactivity studies showed that Motor1 can, in fact, solubilize drugs that HP-β-CD cannot and this ability to deliver higher concentrations of the drug leads to more efficient killing of HeLa cells *in vitro*. This data supports that Motor1 is an excellent counterpart to HP-β-CD when solubilizing and delivering anticancer drugs PTX, PBS-1086, CPT and ABZ. Further study will also need to be conducted in order to understand how Motor1 will compare to other forms of delivery such as liposomes, dendrimers and other forms of the CD family such as β-CD or Captisol®.

As promising as these results may be, they do not, of course, mean that Motor1 can increase the bioactivity of a drug *in vivo*. *In vivo* treatment introduces a multitude of variables, such as pH, blood proteins and enzymes, macrophages, etc., that can affect the activity of the drug, its release from Motor1, biodistribution, and other factors that determine the rate and extent to which the drug will reach its necessary site of activity[67, 69, 73]. Therefore, extensive *in vivo* studies will need to be conducted before conclusions can be made. Here, I conducted a small scale tumor treatment study to begin to evaluate the practicality of using Motor1 as a drug delivery system.

This very initial pilot study of *in vivo* tumor treatment using drug conjugated Motor1 was an opportunity to discover the optimal dosing schedule and administration method for the each of the drugs used with Motor1: PTX, PBS-1086, CPT, and ABZ. Therefore, several different dosing schedules and administration methods (both i.v dosing and i.p) were used. This study was also conducted with the purpose of selecting the most effective treatments to conduct more thorough studies using the ideal dosage schedule

and comparative bioactivity using other delivery systems such as HP-β-CD or Captisol® for example. The study was conducted using 60 female NUDE mice that were injected subcutaneously with HeLa cells. Tumors were allowed to develop to a volume of approximately 100-250 mm^3, after which time treatment of these tumors commenced using PBS, Motor1 alone (924.6 mg/kg), PTX(55.6 mg/kg)-Motor1, PBS-1086(134.2 mg/kg)-Motor1, CPT(5.2 mg/kg)-Motor1 and ABZ(17.8 mg/kg)-Motor1. Each dosing group consisted of 10 mice (Figure 15-17).

Administration Method 1: 3 i.v doses each 4 days apart.

In the first dosing schedule, mice were dosed through the tail vein, by weight (10ml/kg) 3 times, each one four days apart. Upon monitoring tumor volume and body weight, this dosing regimen did not yield any decrease in body weight. On the last day of treatment (day 9) with Motor1-PTX (845 ±230 mm^3; Figure 15A) and Motor1-PBS-1086 (740±174 mm^3; Figure 15B) seemed to indicate some slowing in tumor growth rate in comparison to the tumor growth of mice treated with Motor1-CPT (933±242 mm^3; Figure 15C), Motor1-ABZ treated (951±219 mm^3; Figure 15D), Motor1 (1300±220 mm^3; Figure 15; green) and PBS (1110±170 mm^3; Figure 15; black). During this treatment schedule, more striking differences were not observed for two possible reasons: 1) HeLa cells make for very aggressive tumors[173, 174], which means that 2) an equally aggressive treatment regimen is required with these specific formulations to see greater drug efficacy.

Administration Method 2: 4 i.v doses, once daily dose.

Therefore, two days after the last dosing of the first administration method, the mice were dosed through i.v for four days consecutively with the same treatment samples at 10 ml/kg. At the end of this dosing schedule (day 14) a stabilization of tumor volume where no significant increase or decrease of tumor volume was observed in the treated mice (Figure 15). No significant weight loose was observed on this dosing schedule, however, it should also be noted that there was a stabilization of weight change during this treatment schedule (Figure 16). Mouse survival (Figure 17) at this point decreased significantly for those treated with PBS (10% survival) and Motor1 (0% survival). The tumors in these mice grew to 1500 mm^3, at which point they were sacrificed. Therefore, even though a decrease in tumor volume may not have occurred, the treatments significantly extended the life span of these mice. Though this dosing regimen yielded more promising results in the Motor1-PTX and Motor1-PBS-1086 treatments, continued i.v. dosing was not possible, due to difficulty in injecting as a result of extensive scar tissue. Mice were allowed to recover for a week. During this time, tumors started to grow in volume (Figure 15).

Administration Method 3: 4 i.p doses, once daily dose.

In order to continue dosing and to check Motor1-drug efficacy, we decided to continue to dose the mice by weight with the same treatments on a daily schedule using i.p administration. This method is extensively used in pilot *in vivo* studies to establish dosing schedules and determine MTD values for treatments in cancer research[175]. This is in large part due to the fact that extended daily dosing can be conducted easily and

effectively because i.p administration in the animal model has been shown to closely mimic the bioavailability of i.v administered drugs. Tumor volumes were stabilized during this treatment, but some initial decrease in mouse weight was observed. This was thought to be a result of aggressive dosing and the presence of large aggressive tumors for an extended period of time. Mouse survival was at 50% for Motor1-PTX and Motor1-PBS-1086 and 30% for both Motor1-CPT and Motor1-ABZ. This showed significant survival rates in mice treatment with Motor1-PTX and Motor1-PBS-1086 as opposed to Motor1-CPT and Motor1-ABZ.

At the conclusion of this study, we found that Motor1-PTX and Motor1-PBS-1086 demonstrated the greatest anti-tumor activity as shown by stabilization of tumor volumes and high survival rates. We also determined i.p dosing would be an effective alternate dosing method for future studies. Based on these studies and understandings, important future studies that will need to be conducted to further validate the use Motor1 as an adequate solubilizing excipient. The first and foremost would be to adjust the dosing regimen and administration method. I.p dosing may be used as a daily dosing method, until either no measurable tumors are present or severe adverse effects set on. A second study that will need to be conducted is to test the effectiveness of these new drug formulations against a variety of different tumors. It should be noted that an aggressive dosing regimen can lead to excessive weight loss and sickness directly as a result of the treatment. Therefore, a more adequate solution to this dilemma may be to use an alternative less aggressive tumor model. The doses and dosing schedule will need to be revised accordingly. Using the optimal concentrations, form of administration and dosing

schedule are key in the success of these initial proof-of-principle *in vivo* studies and in elucidating the appropriate uses for Motor1.

A second important study to include alongside these treatment studies is the evaluation of Motor1-drug pharmacokinetics or bioavailability through i.v and i.p dosing to both elucidate properties of the delivery complex as a whole and also to confirm that both dosing methods can present with equal bioavailability. This kind of experiment can be conducted by dosing mice or rats with Motor1-drug through i.v and i.p and collecting blood samples after 5 mins, 10 mins, 30 mins, 60 mins, 3 hrs, and onwards up to at least 24 hrs. Blood will need to be collected through cardiac puncture (terminal procedure). From collected blood, Motor1, drug and Motor1-drug samples can be purified through HPLC methods (will be done by the Isaacs lab) and the concentrations of each can be determined in an attempt to understand its pharmacokinetics. Some of this work has already been initiated by Dr. Eikermann in rats.

Though this initial tumor treatment study needs to be repeated under optimal conditions, it still provides some encouraging results towards the use of Motor1 as a DDS. Importantly, these results indicate that encapsulation in Motor1 does not inhibit the drug's activity and the drug is, in fact, released from the delivery molecule. Further evaluation of Motor1-drug efficacy and pharmacokinetics will help determine dosage and dosing schedules for non-rodent studies and clinical trials in the future.

Project 2: Targeted Drug Delivery by Cucurbit[n]urils

Chapter 5. PROJECT 2 INTRODUCTION

The three leading causes of attrition in the drug development pipeline are low drug efficacy (30%), high drug toxicity (11%) and low drug bioavailability (39%)[12]. One way to alleviate developmental attrition is to improve drug solubility using drug delivery systems as discussed before. However, there is another way, especially in cancer therapy, to reduce attrition rates. Chemotherapy involves the use of severely cytotoxic compounds that primarily target the replication and growth of cells to reduce or halt tumor growth. However, these drugs not only kill cancerous cells but also lead to severe side effects as a result of killing healthy cells[84, 91]. The targeted delivery of drugs specifically to diseased tissue can not only ensure that the drug gets to the necessary site of activity efficiently, in turn, improving bioavailability but also significantly reduce drug toxicity. Drugs that are specifically delivered to tumors would theoretically exhibit selective toxicity primarily limited to cancerous cells leaving normal cells healthy[84, 90]. This would, in turn, significantly reduce the severe side effects associated with chemotherapy. Not only are there numerous candidate anti-cancer drugs in the pipeline that are dose or development limited by their high toxicities, there are also an extensive amount of approved and marketed chemotherapy drugs that are not as effective as they could be in tumor treatment because of their dose limiting toxicities[23]. Targeted delivery could allow for the safe increased dosage regiments rendering many anti-cancer drugs more effective.

In cancer therapy, there are two main forms of targeting: passive and active (Figure 18). Both these forms of targeting necessitate the use of drug delivery systems like liposomes, CDs, or polymers.
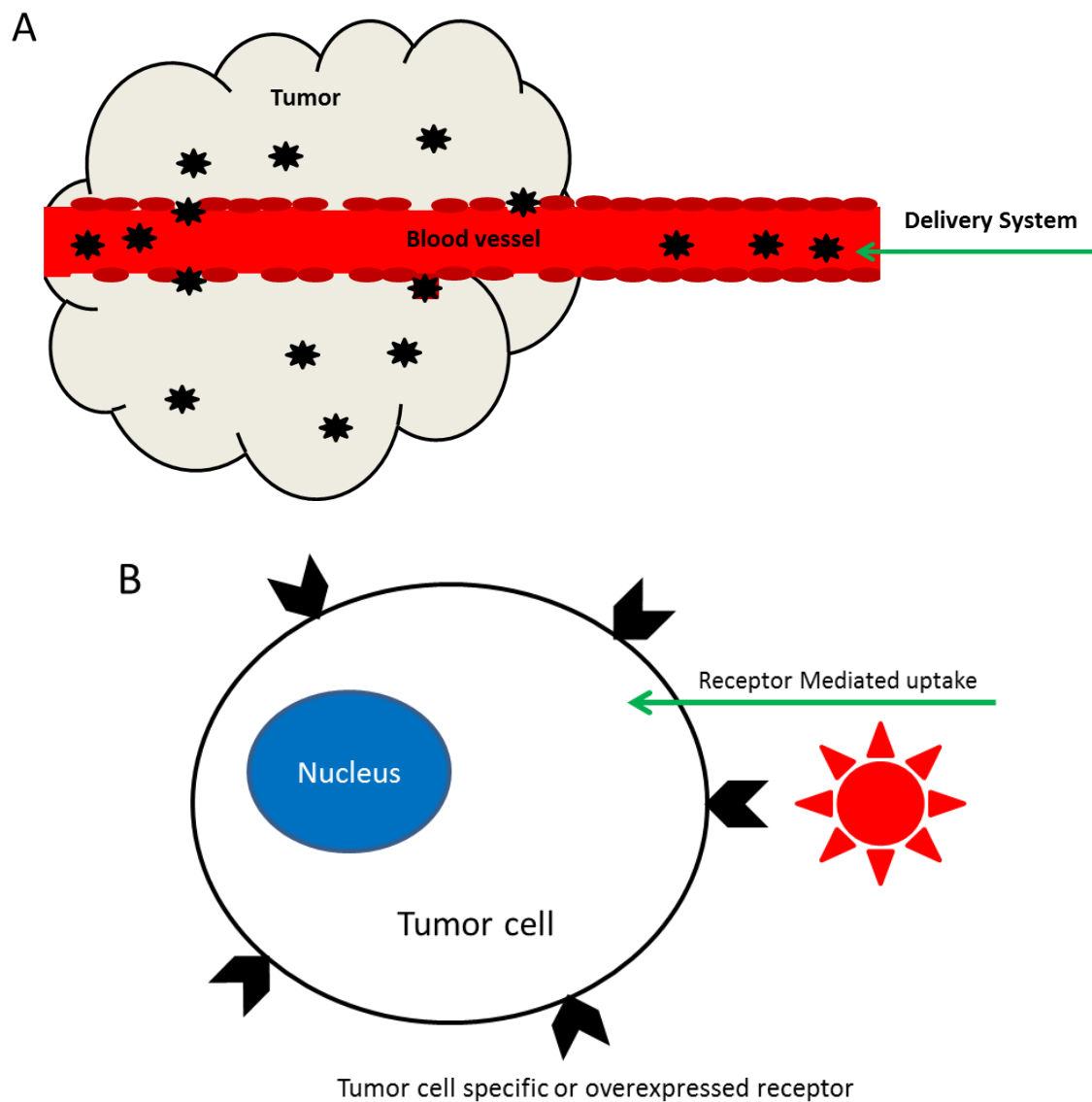
Figure 18: Passive targeting and active targeting of anticancer drugs to tumors. Passive targeting involves the filtering of compounds into irregular tumor vasculature based on their molecular properties. Active targeting entails the use of a tumor receptor-specific ligand. Figure by Gaya Hettiarachchi

5.1 Passive Targeting

Passive targeting refers to the Enhanced Permeation and Retention (EPR) effect. The EPR effect is a well-known phenomenon that was first discovered and characterized by Hiroshi Maeda in 1986[94, 95]. When tumors form, their rapid growth results in the formation of irregular vasculature (Figure 18); this defective network of blood vessels enhances permeability into the tumor thus increasing the flow of nutrients and oxygen necessary for the rapid growth of the tumor [95]. EPR effect is defined by the fact that molecules of certain size and lipid composition are favored to enter and accumulate in this irregular vasculature[96, 98]. For example, macromolecules in the range of 10-500 nm in size leak out of blood vessels and accumulate in tumor tissue[99, 176]. The EPR effect is a great advantage in chemotherapy because it not only allows for the selective delivery of anticancer drugs to tumors and therefore, selective cytotoxicity in cancer cells, but the EPR effect also enables these compounds to become trapped and accumulate within the tumor due to its defective drainage system[94]. In fact, some studies have shown that 24hrs to several days following i.v administration, macromolecules were at 10-200 times concentrations than normal tissue[95]. This retention of anticancer drugs allows for the drugs to be maintained at high concentrations within the tumor over an extended period of time resulting in increased drug efficacy.

One important discovery that has helped researchers take advantage of the EPR effect is PEG[92, 177]. These polymers, depending on the number of chains used and their length, not only increases the systemic circulation of a compound, but also favors the EPR effect[178]. As a result, because most drugs do not naturally exhibit the properties needed to induce the EPR effect, they must either be directed conjugated to

PEG chains or drug delivery systems such as PEGylated liposomes must be used[102]. PEGylating drugs themselves without changing the efficacy or toxicity of the drug is very difficult, therefore, anticancer compounds, either in the developmental pipeline or those already marketed, are more often encapsulated in PEGylated DDS. One example of this is Doxil® which is now FDA approved and marketed. Doxil® is the trade name for the anticancer drug doxorubicin encapsulated in PEGylated liposomes known as STEALTH® liposomes[113, 179, 180]. Studies have shown that STEALTH® liposomes not only have improved pharmacokinetics as a result of extended systemic circulation, but more importantly, they exhibit reduced side effects as a result of selective drug toxicity[180] (60, 61). Another example is Genexol-PM®[103] which uses PEGylated micelles (currently in clinical trials).

Though there are many advantages towards the use of the EPR effect, it is not without its problems. Even though the irregular vasculature of a tumor allows for increased macromolecule permeability, it also results in inadequate heterogeneous distribution of the drug throughout the tumor. Furthermore, individual tumors and certain tumor types vary in the extent of vasculature and permeability leading to variable results in treatment[95]. It was also discovered that the EPR effect is more prominent in smaller tumors (0.5-1cm) *in vivo* as opposed to larger tumors (1-2cm) which seems to be, in part, due to irregular vasculature. In an effort to circumvent these issues, Maeda *et al* have recently attempted to intensify the EPR effect in tumors where treatment had failed. One method they used was to increase blood pressure while another was to introduce nitric oxide releasing agents to expand the vasculature[95]. Both these methods have their disadvantages. Studies have also shown that PEG can elicit PEG-specific IgM production

which, in turn, activates complement *in vivo* after repeated dosings[101, 102, 181]. This leads to rapid blood clearance and significantly decreased bioavailability of the drug. PEGylated particles have also shown slower uptake by tumor cells in comparison to non-PEGylated macromolecules which leads to increase systemic circulation time but also leads to decreased drug efficacy over time. This problem is known as the PEG dilemma. One way to address this problem could be to use linkages that could be cleaved by proteases one the cargo reaches tumor cells[182].

5.2 Active Targeting

An alternative to passive targeting is active targeting (Figure 18) which entails the use of ligands that are specific to receptors that are uniquely expressed or overexpressed on tumor cell surfaces. There are several examples of these targeting ligands that can be used such as monoclonal antibodies, prostate specific membrane antigen (PSMA), folate and biotin.

PSMA is a type 2 integral membrane glycoprotein that is the single most tissue specific unsecreted surface antigen established to date[183]. The exact function of PSMA is still unknown, but it is found on all prostate cancers and its expression is significantly increased in higher grade prostate cancers, metastatic diseases and has also been found in the neovasculature of nonprostate tumor malignancies[183]. All these properties make it an ideal targeted for tumor specific delivery of therapeutics[184]. PSMA is generally targeted by using anti-PSMA monoclonal antibodies; one that is currently approved for human research is J591[183].

Several therapeutics conjugated to J591 are currently in clinical trials. Radioimmunotherapy (RIT) is a technique used for cancer therapy that involves the targeted delivery of a radionuclide, such as 177-Lutetium (^{177}Lu), linked to a monoclonal antibody. One that is showing success in Phase II clinical trials is ^{177}Lu-J591[183]. Furthermore, this antibody can be used to specifically deliver anticancer drugs such as Maytansinoid 1, a potent microtubule- depolymerizing compound. This compound is also currently in Phase II trials[185]. PSMA-targeted nanoparticles include dendrimers, liposomes, and micelles all of which have shown successful preclinical delivery to and killing of cancerous cells[74, 186]. Polymer encapsulated drugs have also been targeted with PSMA. In these instances, several studies have also been conducted using anti-PSMA aptamers, such as A10 RNA, as targeting ligands instead of antibodies. One successful example of this comes from Dr. Omid Farokhad's lab (Harvard Medical School, Boston MA), who has created two systems using polymer nanoparticles and A10 RNA targeting mechanism to deliver the anticancer drug docetaxel (BIND-014; in clinical trials) and combination of cisplatin and doxorubicin which has demonstrated great preclinical success[74, 187, 188].

Two other extensively studied cancer specific target are the folate and biotin receptors. These receptors are found on all cell surfaces but are significantly overexpressed in many cancers such as breast and ovarian cancers. Folate and biotin are essential components in DNA synthesis, repair, methylation and overall cell growth. They are especially important during rapid cell division and growth which alludes to the overexpression of these receptors on the surface of cancer cells[84]. There are three folate receptors, alpha (FOLR1), beta (FOLR2), and gamma (FOLR3) which bind to folate at a

high affinity (10^{-9} M^{-1}). FOLR1 and 3 are particularly overexpressed in breast, uterine and ovarian cancers, however, FOLR1 is also overexpressed in lung, kidney and placenta cells. There are several examples of folate targeted nanoparticles in preclinical studies including dendrimers, liposomes and carbon nanotubes with anticancer drugs like doxorubicin, CPT, and methotrexate[84, 189, 190].

Finally, biotin is not synthesized by human and mammalian cells but, instead, must be acquired through exogenous sources such as food and intestinal floral[191]. Biotin, like folate, is an essential nutrient necessary for DNA synthesis, cell replication and growth. Therefore, like folate, the receptor for biotin is expressed on all normal cells but is significantly overexpressed on cancer cells. Targeting with biotin is a quickly growing field of interested in drug delivery; this molecule is used in conjugation with several nanoparticles such as dendrimers, liposomes and polymer based nanoparticles and is also studied through direct conjugation of the nutrient to anticancer therapeutics[192-194]. One example of this is biotin conjugated to the taxoid SB-T-1214[194].

5.3 Biotin-CB[7]

In this section of my thesis, I will discuss the use of a novel biotin functionalized CB[7] compound, created in Dr. Isaacs' lab. This molecule will serve as a proof-of-principle towards the use of CB[n]-type compounds for targeted delivery of drugs. CB[7] is probably the most extensively studied parent molecule from the CB[n] family due to its high intrinsic solubility (20 mM) and large cavity size. This new biotin-CB[7] compound has a solubility of approximately 1 mM, therefore, it may not lend much towards increasing the solubility of a drug (Figure 20). However, the unique property of this compound lies in its ability to target cells overexpressing the biotin receptor[151].

Therefore, this host molecule can be used to actively target fairly soluble anti-cancer drugs to tumors thus significantly minimize any adverse side effects administering the drug alone may produce.

For this study, the potent drug, oxaliplatin, was used to test the functionality of biotin-targeted CB[7]. Oxaliplatin is a first and second line form of therapy for many aggressive cancers. It works by binding to DNA and forming adducts thus halting DNA synthesis. However, as widely used as it is, oxaliplatin is dose limited by somewhat poor pharmacokinetics and severe side effects such as neurotoxicity and hypersensitivity[22, 195]. Therefore, though this drug is essentially effective in combination therapy, there is significant room for improvement through targeted delivery. Furthermore, oxaliplatin has been successfully conjugated with CB[7] before [146, 196].

5.4 Hypothesis

Based on the promising studies in biotin targeted drug delivery conducted by other researches and the inherent properties of the biotin-CB[7] compound, I hypothesize that functionalized CB[n] and CB[n]-type particles, like biotin-CB[7] can be used to specifically localize and/or increase the uptake of anticancer agents by tumor cells thereby improving the pharmacokinetics and efficacy of compatible pharmaceutical agents.
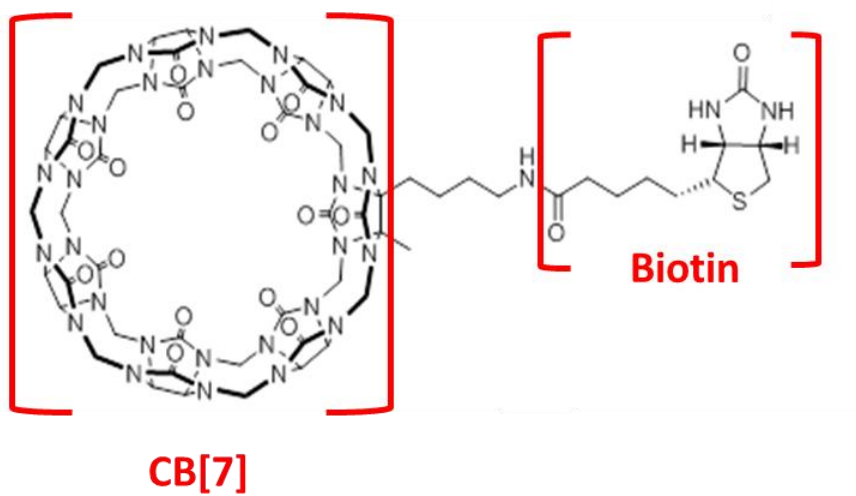
Figure 19: Biotin targeted CB[7] is soluble up to 1 mM[151]. Work by Liping Cao and Dr. Lyle Isaacs.

Chapter 6. PROJECT 2 METHODS AND MATERIALS

6.1 Materials

Oxaliplatin was purchased from Selleck Chemicals LLC. Hoechst33342 was obtained from Sigma-Aldrich. Dextran-Alexa647, Prolong Gold Antifade Agent, and Trypsin/EDTA were purchased from Invitrogen. FITC was purchased from…CellTiter 96 AQueous Kit® was purchased from Promega and the Toxilight® BioAssay Kit from Lonza. Cell Death Detection ELSA was purchased from Roche®. Analytical instruments used in this study included Spectramax M5e (Molecular Devices), Bio-TEK Synergy HT plate reader, Leica SP5 X Confocal, and BD FACSCanto II.

Cell and Bacterial Culture.

RAW264.7 cells (Mouse leukemic monocyte macrophage, ATCC #TIB-71) and HEK 293 cells (Human Embryonic Kidney, ATCC #CRL-1573) were grown in DMEM (GIBCO media Invitrogen) with 10% heat inactivated fetal calf serum (FCS, Hyclone), and 1% Penicillin/Streptomycin (Invitrogen). HepG2 (Heptacellular carcinoma, Human, ATCC #HB-8065), L1210/FR cells (murine lymphocytic leukemia cells, kindly provided by Dr. Iwao Oijma, State University of New York at Stony Brook, Stony Brook, NY) were grown in RPMI media (ATCC #30-2001) with 10% FCS and 1% Penicillin/Streptomycin.

6.2 Methods

6.2.1 *In vitro* assessment of CB[7] biocompatibility.

HEK293 cells (2.5×10^6 cells/mL), HepG2 cells (4×10^5 cells/mL) and RAW264.7 cells (8×10^4 cells/mL) were seeded in a 96 well plate (Corning) at 200 μl/well. After the cells were allowed to adhere for 24 hrs, they were treated with increasing concentrations of CB[7] (0.01, 0.1 and 1 mM) for 48 hrs. Cells were assayed using the MTS and AK assay according to vendor instruction. The AK assay was conducted by aliquoting 20 μl of supernatant from each sample into a separate black well plate (Corning) after the 48 hr treatment period. These samples were run prior to using the MTS assay. The plates were read using the Bio-TEK Synergy HT plate reader. Data was collected in the form of units of absorbance and luminescence and normalized to percent cell viability (MTS) and percent cell death (AK) with the use of equations (**1**) and (**2**).

6.2.2 Determination of the uptake and localization of CB[7] and biotin-CB[7] compounds in mammalian cells.

CB[7]-Alexa 555 uptake and localization

RAW264.7 cells were seeded in a 24 well plate (Corning) at 5×10^5 cells/mL. All samples were done in technical quadruplets and then combined to form doublets per sample. Controls included untreated cells and cells treated with Alexa555 alone. The CB[7]-Alexa555 complex was incubated with cells at the respective concentrations for 20 min and then collected for analysis. Cells were collected and fixed with 4% PFA before analysis by flow cytometry. For the time course assay, CB[7]-Alexa555 was again incubated with cells for 20 min at a concentration of 32 mM after which time the cells

were washed and incubated for 15, 20, 120 min with fresh medium (DMEM, and 10% FCS) before analysis by flow cytometry.

For the intracellular localization study, RAW264.7 cells were seeded at 10^4 cells/200 µL in 3-well glass slides (Electron Microscopy Sciences). Controls included cells stained with Hoechst33342 staining alone, Dextran-647 alone and CB[7]-Dextran-647 alone. Dextran-647 was incubated with cells overnight at a concentration of 125 µg/mL. The CB[7]-FITC complex was incubated with cells for 20 min. at a concentration of 32 mM the following day and then chased with fresh growth medium for 15, 45, and 120 min. Before analysis, cells were fixed with 4% PFA, washed and immobilized with Prolong® Gold Antifade Agent.

Biotin-CB[7]-FITC uptake and localization

Confocal microscopy

L1210FR cells (5×10^5 cells/200 µL) were seeded in a 96-well plate and incubated with Dextran-647 (125 µg/mL) overnight at 37^0C. The following day, the cells were washed and incubated with 2 µM and 15 µM of biotin-CB[7]-FITC and CB[7]-FITC for 30 mins at 37^oC. Cells were washed 3 times, fixed with 4% PFA and stained with Hoechst33342. Cells were washed again and transferred to 3-well slides (Electron Microscopy Sciences) prior to confocal imaging. Experiments were repeated three times.

L1210FR cells (5×10^5 cells/200 µL) were seeded in a 96-well plate and incubated with 2 µM and 15 µM of biotin-CB[7]-FITC and CB[7]-FITC for 1.5 hrs at 4^oC. Cells were washed 3 times and chased with fresh media for 0, 15 and 30 mins at 37^oC. Cells were then fixed with 4% PFA and stained with Hoechst33342. Cells were washed again

and transferred to 3-well slides (Electron Microscopy Sciences) prior to confocal imaging. Experiments were repeated three times.

Flow Cytometry

5×10^5 cells/200 µL of L1210FR and L1210 cells were plated in 96-well plate (Corning) and treated with CB[7]–FITC and biotin-CB[7]-FITC at a concentration of 2 µM for 30 mins. Treatment was conducted at 37°C. Cells were washed 3 times with PBS and collected for analysis by Flow Cytometry. Each experiment consisted for two technical replicates and was repeated three times.

Similarly, for the biotin competition assay, 5×10^5 cells/200 µL of L1210FR and L1210 cells were plated in 96-well plate (Corning) and treated with increasing concentrations of Biotin (0.05-500 µM) for 30 mins. Cells were then washed twice and incubated with biotin-CB[7]-FITC at a concentration of 2 µM for 30 mins. Treatment was conducted at 37°C. Cells were washed 3 times and collected for analysis by Flow Cytometry. Each experiment consisted for two technical replicates and was repeated three times.

6.2.3 *In vitro* evaluation of drug efficacy upon loading into CB[7] and biotin-CB[7].

Ethambutol

RAW264.7 cells were seeded at 5×10^5 cells/mL in one well of a 24-well plate. As controls we examined untreated cells on day 0 and day 3. Each sample was tested in technical duplicates. Cells were infected with *M. smegmatis* at a multiplicity of infection (MOI) of 10:1 for 2 h and then incubated with chase media (infection media with varying

concentrations of EMB or CB[7]-EMB) for 3 days. The EMB and CB7-EMB were used at minimum inhibitory concentration (MIC) values of 0.1 (2.4 mM), 0.4 (9.6 mM), 0.8 (19.2 mM) and 1 (24 mM) [53] units during *M. smegmatis* treatment. On day 3, cells were lysed with 1 ml/well of distilled water/0.05%Tween-80. The cell lysate for each condition was added to 7H9 (DifcoH Middlebrook) media. These solutions were then serially diluted four times and plated in technical triplicates of 5 mL each on 7H10 (DifcoH Middlebrook) agar plates. Viable bacteria were quantified by calculating the number of colony forming units (CFU) per mL.

Oxaliplatin

5×10^5 cells/200 µL of L1210FR cells were seeded in a 96-well plate (Corning). Cells were treated with increasing concentrations of oxaliplatin, CB[7]-oxaliplatin, and biotin-CB7-oxaliplatin for 45 mins at 37°C. Cells were then washed twice with PBS and incubated with fresh growth medium for 24 hrs. The plate was treated with CellTiter One AQueous Solution® at a 60:80 v/v ratio for 3 hours after which time the data was collected using Bio-TEK Synergy HT plate reader at an absorbance of 490 nm. The data was normalized to percent cell viability using equation (**1**). Untreated samples were considered at 100% cell viability. This experiment included three technical replicates and was repeated three times.

6.2.4 Statistical Analysis.

Experimental data were presented as means ±SD except where otherwise stated. The results were analyzed using two-tailed Student's unpaired t-test with Graph Pad Prism Graph 5.0 software.

Chapter 7. PROJECT 2 RESULTS AND DISCUSSION

7.1 *In vitro* assessment of CB[7] biocompatibility

7.1.1 CB[7] is well tolerated in murine macrophage and human kidney and liver cell lines.

The MTS and AK assays for all three cell lines, HEK293, RAW264.7 and HepG2, were conducted after two days of incubation with the CB[7] at concentrations of 10 μM, 100 μM, and 1 mM (Figure 20). Relative absorbance and luminescence data was normalized to percent cell viability (MTS) and death (AK). In the MTS assay, the untreated samples were set at a 100% cell viability, while in the AK assay distilled water and CPT treated cells were set at a 100% cell death[145].

In the MTS assay conducted using HEK293 (Figure 20A) cells, CPT treatment resulted in an average 59% decrease in cell viability. CB[7] at a 1 mM dose resulted in an average 94% cell viability. In the AK assay (Figure 20B), the untreated HEK293 cell population indicated only an average 18% cell death and CB[7] at a concentration of 1 mM resulting in a comparable average of 9% cell death[145].

In studies conducted in the liver cell line, HepG2, the MTS assay (Figure 20C) for distilled water treated HepG2 population indicated a percent cell viability of an average of 0.28% while treatment with 1 mM of CB[7] resulted in an average 96% cell viability. In the AK assay (Figure 20D), the highest concentration of CB[7] resulted in an average 22% cell death in the HepG2 cell line.

In RAW264.7 cells, the MTS assay (Figure 20E) for the CPT treated cell population resulted in a decrease in cell viability by an average of 99%. At a 1 mM concentration, CB[7] produced an average 101% cell viability. The AK assay (Figure

20F) showed the untreated population cell death equal to an average of 38% and CB[7], at the highest dose of 1 mM, resulted in an average of 30% cell death[145].
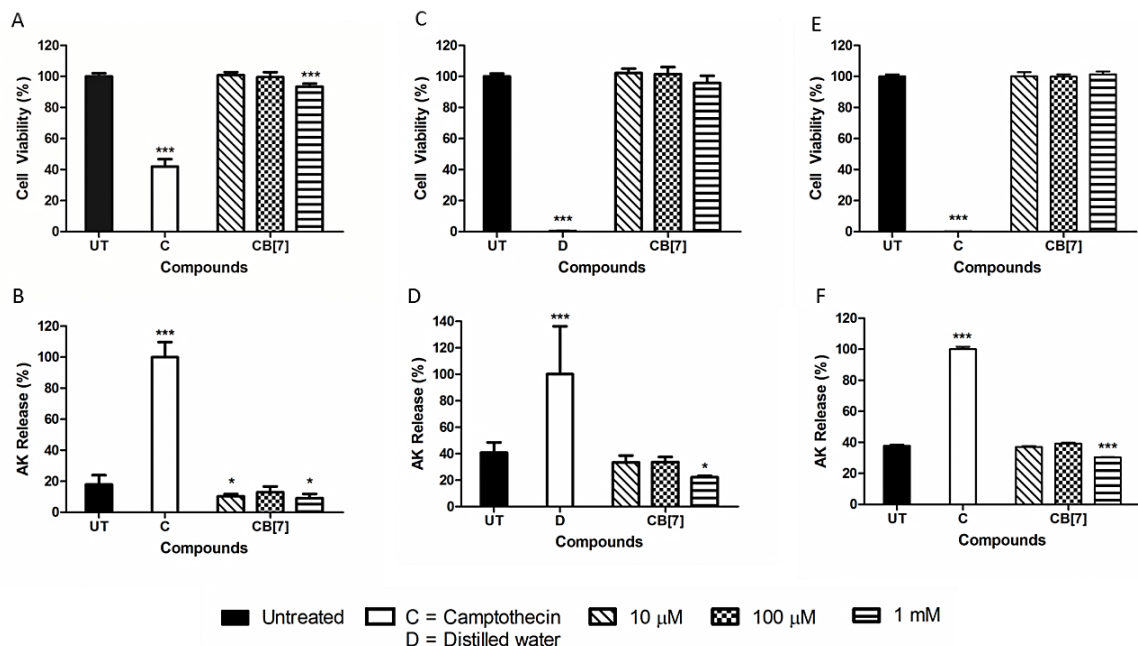
Figure 20: CB[7] is non-toxic in human kidney and liver cell lines and murine macrophages. Plots of cell viability (MTS assay; A C, E) and cell death (AK release assay; B, D, F) obtained for CB[7] (0.01 mM, 0.1 mM, 1 mM) after 48 hr incubation with three cell lines: HEK 293 cells (A, B), HepG2 cells (C, D) and RAW264.7 cells (E, F). Data presented in A-F are the average values obtained from triplicate experiments and the corresponding standard deviation values. Data represents the average and standard deviation values from three replicate experiments with four donors. For all panels, unpaired t-test analysis was used (*P = 0.01–0.05; **P = 0.001–0.01; ***P < 0.001) Work done by Gaya Hettiarachchi and Volker Briken[145].

7.1.2 Discussion

The first step towards establishing a proof-of-concept for using CB[n]s and their derivatives for targeted delivery of drugs is to evaluate host toxicity. The MTS and AK assays were used here to evaluate *in vitro* biocompatibility. Three different cell lines were used: human kidney (HEK293), liver (HepG2), and a murine macrophage (RAW264.7) cell line. The importance of using these cell lines were discussed before.

Both MTS and AK analysis of CB[7] revealed high cell viability and low cell death comparable to the untreated samples up to a concentration of 1 mM in HEK293 (Figure 20A and B), HepG2 (Figure 20C and D) and RAW264.7 (Figure 20E and F) cell lines. Within the scope of this study, up to a concentration of 1 mM, these results indicate that CB[7] is non-toxic to these cell lines. Several studies have been conducted into the safety of CB[7]. Several toxicity studies have been conducted using CB[7] in many different cell lines including Chinese hamster ovary cells, human blood tissue, mouse embryo cells and the human cancer cells up to a concentration of 100 mM [146]. Furthermore, *in vivo* experiments in mice have shown no adverse effects up to a concentration of 200 mg/kg [141].

Future studies in toxicology include assessment of biotin-CB[7] both *in vitro* and *in vivo*. Taking the biocompatibility of its individual components, biotin[50] and CB[7], it can be hypothesized that biotin-CB[7] may be fairly non-toxic within the parameters established above. However, it is still necessary to evaluate the delivery system as a whole, *in vivo,* so that a safe dosing schedule may be established for this targeted molecule. Collected data should be compared to other targeted drug delivery systems to determine its significance. If good efficacy is established *in vivo*, it will be necessary to

do a full spectrum of safety analysis as suggested for Motor1. This compound has a very long way to go before it can be considered for an IND.

7.2 Determination of the uptake and localization of CB[7] and biotin functionalized CB[7]

7.2.1 CB[7] is taken up through phagocytosis by murine macrophages and localizes in lysosomes.

The dose-dependent uptake of CB[7] was characterized via flow cytometry using 3.2 and a 32 mM of CB[7]-FITC (Figure 21). CB[7]-FITC was incubated with RAW264.7 cells for 20 min before analysis. A dose of 3.2 and 32 mM resulted in median fluorescence intensity (MFI) of 197 and 703 while the untreated sample was at a value of 131 (Figure 21A). Statistical analysis of the histograms showed the percentage of cells positive for CB[7]-FITC staining as an average of 5% for untreated cells, 24% for a concentration of 3.2 mM, and 86% for 32 mM (Figure 21C)[145].

To determine the intracellular stability of the CB[7]-FITC complex a time course assay was conducted. CB[7]-FITC was incubated with the cells for 20 min and then chased for 15, 45, and 120 min. This resulted in high MFIs of 743 after 15 min chase, 612 after 45 min, and 544 after 120 min chase time (Figure 21B). Further analysis determined that the percentage of cells positive for staining was 6% for untreated cells, 92% after 15 min chase, 91% after 45 min and finally 85% after a chase time of 120 min (Figure 21D)[145].
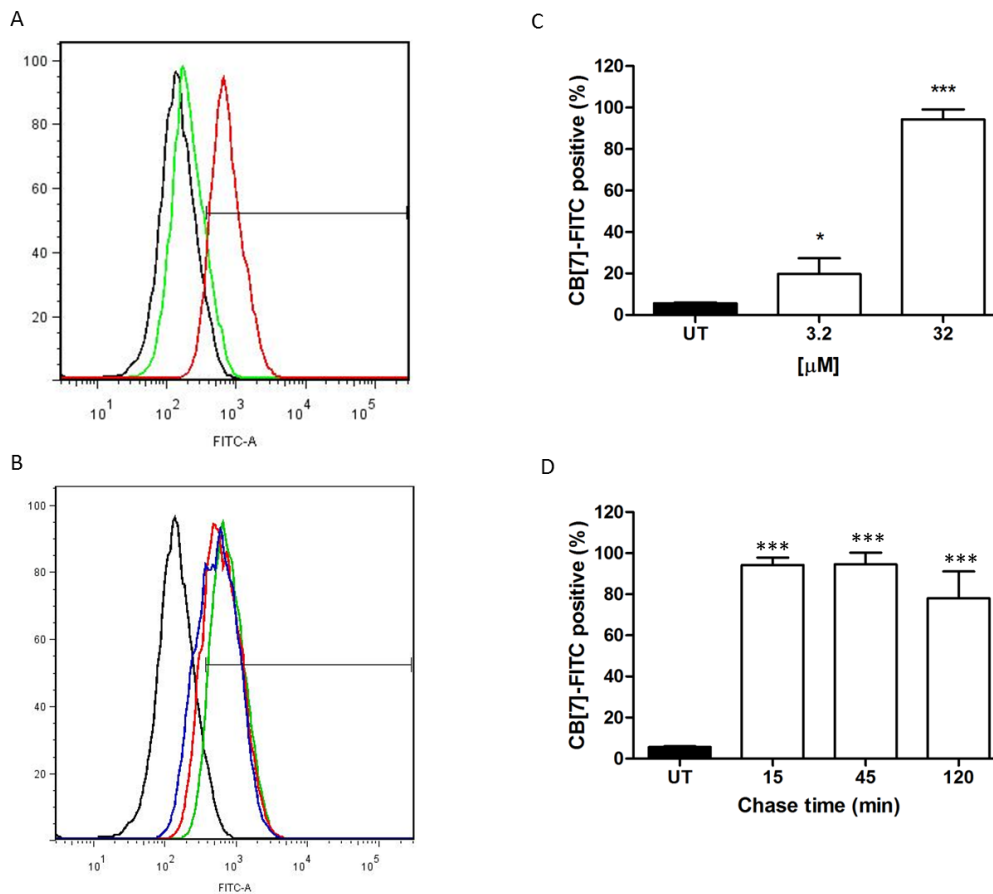
Figure 21: CB[7]-FITC is taken up by murine macrophages in a dose dependent manner. Both the dose titration and time course assays used RAW264.7cells incubated with CB[7]-FITC for 20 mins prior to analysis. (A) Dose titration assay used CB[7]-FITC concentrations of 3.2 (green) and 32 mM (red). (B) Statistical analysis of the percentage of cells positive for fluorescence. (C) Time course assay was conducted using 32 mM of CB[7]-FITC. After incubation with the fluorescent container, cells were chased for 15 (green), 45 (red) and 120 min (blue) (D) Statistical analysis of the percentage of cells positive for fluorescence. Unpaired t-test analysis was used (*P=0.01–0.05; **P=0.001–0.01; ***P<0.001)Work done by Gaya Hettiarachchi and Volker Briken[145].

Co-localization assays using fluorescence microscopy were conducted using Dextran-647, and CB[7]-Alexa555 in order to analyze the intracellular localization of the container. Dextran-647 was incubated with cells at a concentration of 125 mg/mL overnight to stain cell lysosomes. Cells were then pulsed with CB[7]-Alexa555 for 20 min and chased for 15, 45, 120 min. This analysis showed an initial uptake of CB[7]-Alexa555 and Dextran-647 at 15 min with little colocalization (Figure 22A), however, at 45 min, CB[7]-Alexa555 co-localization (indicated by arrows) with Dextran-647 was observed (Figure 22B)[145].
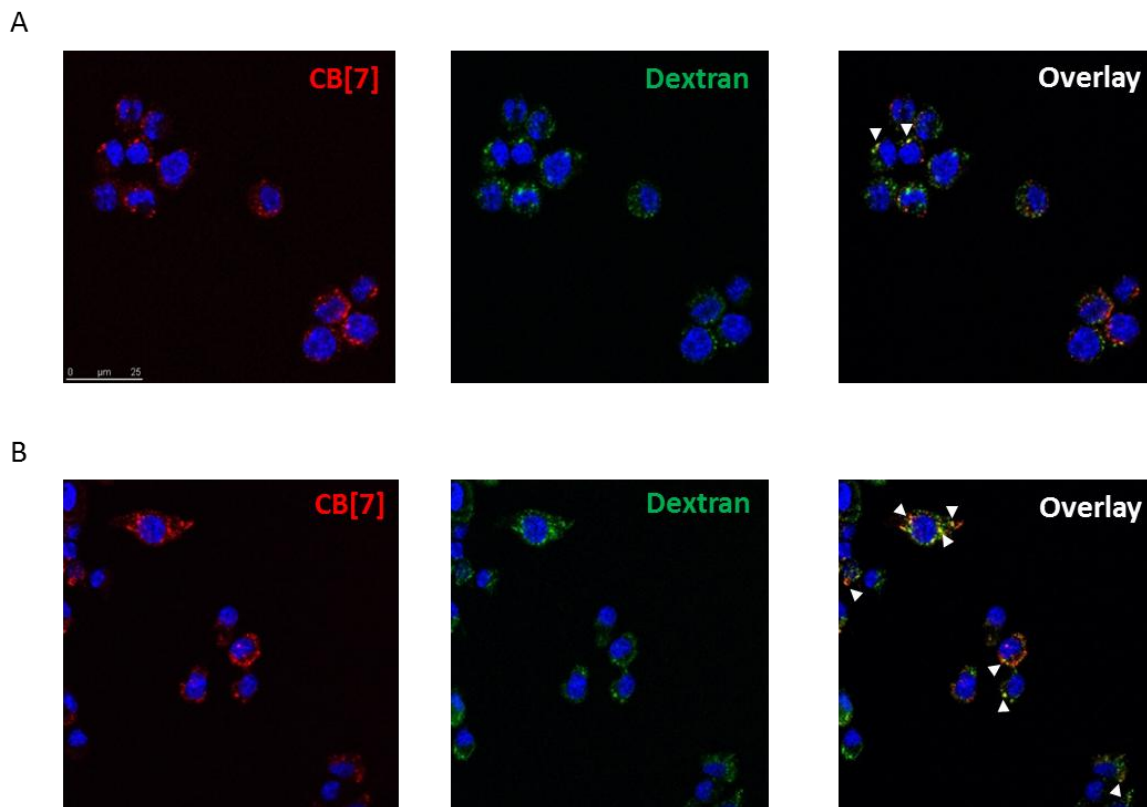
Figure 22: CB[7]-FITC are taken up by murine macrophages through phagocytosis and localizes in lysosome. Cell incubated with Dextran-647 (green) and CB[7]-FITC (red) showed intracellular localization of CB[7] through the endosomal pathway. RAW264.7cells were incubated with Dextran-647 (green) overnight and CB[7]-FITC (red) for 20 min the following day. Cells were chased for 15 (A), 45 (B) and 120 min (not shown) after incubation with CB[7]-FITC. Cells were imaged using confocal microscopy. Arrows indicate co-localization. Work done by Gaya Hettiarachchi and Volker Briken[145].

7.2.2 Biotin-CB[7] binds to and is taken up through receptor-mediated endocytosis in murine lymphocytic leukemia cells.

L1210 (Figure 23A; green) and L1210FR (Figure 23A; red and blue) cells were incubated with 2 µM of CB[7]-FITC (red) and biotin-CB[7]-FITC (green and blue) for 30 mins. Binding was quantified using flow cytometry at a reading of 10,000 cells/condition. Results showed an MFI of 1449 for CB[7]-FITC incubated with L1210FR cells (red), 1648 for biotin-CB[7]-FITC in L1210 cells (green), and finally an MFI of 5131 for biotin-CB[7]-FITC in L1210FR cells (blue).

A biotin competition assay (Figure 23B) was conducted using L1210 and L1210FR cells incubated first with increasing concentrations of free biotin (0, 0.05, 0.5, 5, 50 and 500 µM) for 30 mins followed by biotin-CB[7]-FITC (2 µM) for 30 mins. Quantification through flow cytometry indicated an average of 26.3%, 16.2%, 11.2%, 10.6%, 10.5%, and 8.9% of the L1210 cell population to be biotin-CB[7]-FITC positive with 0, 0.05, 0.5, 5, 50 and 500 µM free biotin pre-treatment respectively. An average 92.4%, 85.8%, 76.9%, 51.1%, 36.1%, and 27.3% of the L1210FR cell population was found to be biotin-CB[7]-FITC positive after 0, 0.05, 0.5, 5, 50 and 500 µM free biotin pre-treatment respectively.
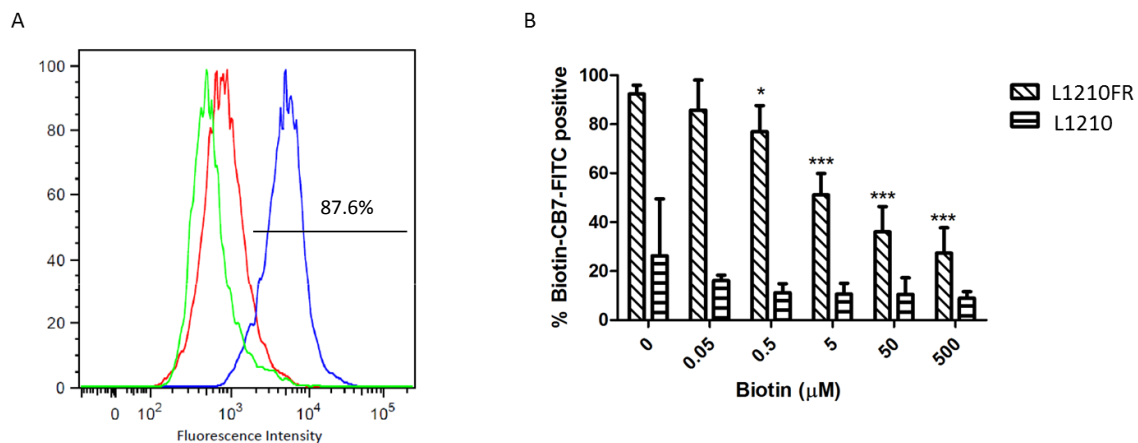
Figure 23: Biotin-CB[7]-FITC selectively binds to murine lymphocytic leukemia cells that overexpress the biotin receptor. L1210FR (red and blue) and L1210 (green) cells were incubated with 2 μM of CB[7]-FITC (red) and Biotin-CB[7]-FITC (green and blue) for 30 mins (A). Uptake was quantified with flow cytometry; 10,000 cells/sample were analyzed. This figure is representative of three experimental repeats. L1210FR and L1210 cells were incubated with increasing concentrations of biotin (0.05-500 μM) for 30 mins, washed, and then incubated with biotin-CB[7]-FITC (2 μM) for 30 mins (B). Cells were then collected for quantification with flow cytometry; 10,000 cells/sample were analyzed. This figure is the average of two experimental repeats, and standard deviation was calculated at n = 4. Unpaired t-test analysis was used for statistical analysis (*P=0.01–0.05;**P=0.001–0.01;***P<0.001). Work done by Gaya Hettiarachchi and Volker Briken[151].

Fluorescent microscopy conducted on L1210FR cells (Figure 24) showed high fluorescence in the FITC channel when incubated with biotin-CB[7]-FITC (green) for 30 mins at 37^oC. Colocalization (as indicated by arrows) of dextran-647 (red) and FITC (green) was also observed in these cells. This staining pattern was not observed in cells treated with CB[7]-FITC treated cells. A kinetics analysis of L1210FR cells treated with biotin-CB[7]-FITC (green) at 2 and 15 μM at 4^oC for 1.5 hrs indicated peripheral staining of L1210FR cells (Figure 25). At 30 mins chase time, staining was observed throughout the cells. These staining patterns were not observed in cells treated with CB[7]-FITC (green) at 37^oC or 4^oC.
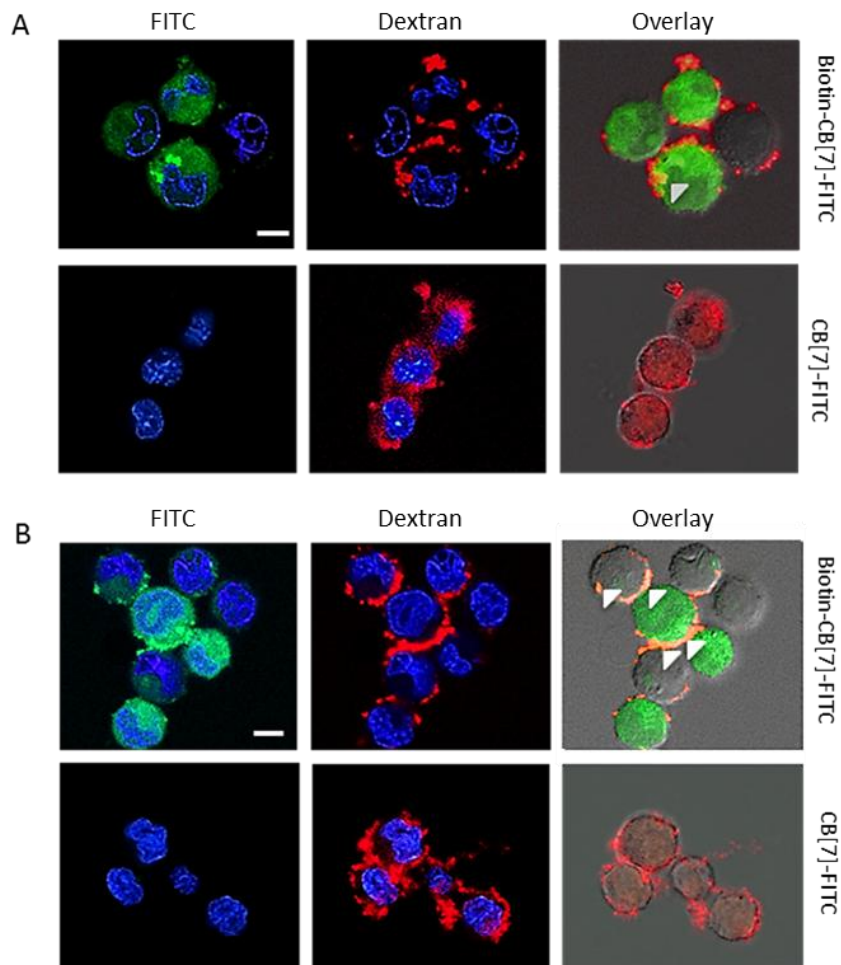
Figure 24: L1210FR cells incubated with 2 µM (A) and 15 µM (B) of Biotin-CB7-FITC and CB7-FITC. indicated receptor specific uptake. Cells were treated with Dextran-647 (red) overnight followed by targeted and untargeted CB[7]-FITC (green) the next day. Colocalization (indicated by arrows) of dextran-647 with targeted CB[7]-FITC in the bright field overlay indicated internalization of Biotin-CB[7]-FITC (green) through the endosomal pathway. Work done by Gaya Hettiarachchi and Volker Briken[151].
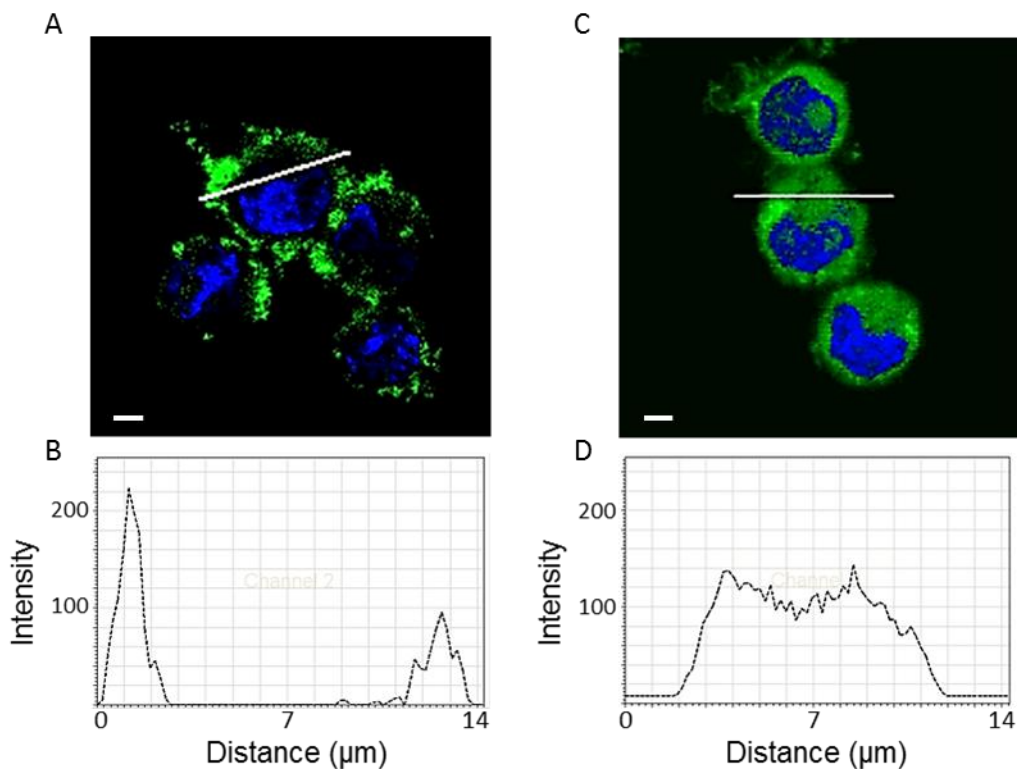
Figure 25: L1210FR showed receptor specific uptake of Biotin-CB[7]-FITC. L1210FR were incubated with 15 µM of biotin-CB7-FITC (green) for 1.5 hrs at 4°C, washed, and chased for 0 (A and B) and 30 mins (C and D) at 37°C. Confocal imaging showed peripheral FITC staining (A) at 0 min chase time indicating biotin-CB7-FITC binding and immobilization on the cell surface. Internalization of biotin-CB[7]-FITC was observed at 30 min chase time (C). Fluorescence intensity was quantified across the indicated line for each image confirming surface staining (B) and internalization (D). Work done by Gaya Hettiarachchi and Volker Briken[151].

7.2.3 Discussion

In order to elucidate if and where CB[7] would localize intracellularily, kinetics assays were conducted using Alexa-555 or FITC tagged CB[7] incubated with RAW264.7 cells. These cells were chosen because as macrophages, they have a high rate of endocytic and pinocytic activity thus maximizing the probability that the host molecules will be engulfed by the cells leading to intracellular localization (Figure 21 and 22).

The fluorescent CB[7] complexes used in these experiments were held together by non-covalent interactions through adamantaneamine linkages[145]. Accordingly, there is the possibility of an equilibrium between the free and bound dye forms. It is known, however, that CB[7] binds with adamantaneamine and its derivatives with extraordinarily high affinity CB[7] ($K_a \approx 10^{12}$ M^{-1}) which ensures that these complexes are thermodynamically and kinetically stable at the concentrations and times used in these confocal microscopy and flow cytometry experiments[139, 145]. As a result it can be concluded that the fluorescent signals collected in both flow cytometry and confocal microscopy is representative of the CB[7]-tag complex.

RAW264.7 cells incubated with 3.2 and 32 mM of CB[7]-FITC indicated dose dependent uptake by the cells as would be expected in these cells (Figure 21A and C). The kinetics assay showed increasing uptake of CB[7]-FITC with extended chase times indicating complex stability up to 120 mins (Figure 21B and D). These results were reflected in confocal microscopy studies conducted using CB[7]-FITC incubation followed by the same chase times: 15, 45, and 120 mins (Figure 22A, B and not shown respectively). In this study, dextran-647 (green) was used to label the endosomal pathway

prior to incubation with CB[7]-FITC (red). Co-localization (as indicated by arrows) for dextran-647 with CB[7]-FITC indicated that CB[7] is, in fact, take up through the endocytic pathway, and at 45 mins rests in lysosomes.

Similar studies have been published analyzing the uptake of fluorescently tagged CB[7] by different cell lines. CB[7] binds tightly to acridine orange and this complex was previously used to demonstrate the uptake of CB[7] by mouse muscle embryo cells (NIH/3T3)[197]. In addition, a CB[6] loaded with a FITC-spermine conjugate was shown to be internalized by HepG2 cells[198]. Both of these studies, however, did not quantify the uptake of the container nor did they investigate its intracellular localization but nevertheless they demonstrated that other cell types besides macrophages are able to take up CB[n] containers.

As a whole, these studies strongly suggest that untargeted CB[n]-type containers are able to cross into cells through the endocytic pathway and localize in the lysosomes of cells. This can be used for the controlled intracellular release of drugs under specific pH. CB[n] can be functionalized so that they release their guest molecules in the lysosomes at a pH of ~5. This, of course, requires that the released drug survive the harsh environment of the lysosomes.

L1210FR and L1210 were used to determine whether the biotin functionalized CB[7] is selectively bound to and taken up by cells overexpressing the biotin receptor (Figure 23-25). L1210FR cell line was used specifically because they overexpress the biotin receptor on the cell surface like many tumor cells do while L1210 cells have normal biotin receptor expression as normal healthy cells would[194, 199]. L1210 and L1210FR were incubated with CB[7]-FITC and biotin-CB[7]-FITC for 30 mins at 37°C

prior to analysis with flow cytometry (Figure 23A). Analysis showed similar MFI for CB[7]-FITC incubated with L1210FR (MFI = 1449) and biotin-CB[7]-FITC incubated with L1210 (MFI = 1648). This seems to indicate that there is little to no binding of untargeted CB[7]-FITC to cells overexpressing the biotin receptor and limited, though slightly higher, uptake of biotin-CB[7]-FITC to cells with normal biotin receptor expression. This slight increase in uptake should be excepted as the L1210 is not negative for the biotin receptor. There was, however, a significant increase in fluorescence intensity seen in the L1210FR cells treated with biotin-CB[7]-FITC (MFI = 5131). This seems to indicate that there is extensive binding of the biotin-CB[7]-FITC by the cells overexpressing biotin receptors (Figure 23A).

Selective targeting of biotin-CB[7]-FITC to cells overexpressing the biotin receptors was further validated in the biotin competition assay conducted using these same conditions after treatment with increasing concentrations of free biotin (Figure 23B). At high concentrations, free biotin binds to and occupies biotin receptors on the cell surface, thereby, limiting the binding of biotin-CB[7]-FITC through receptor saturation. This is indicated by the decrease in percent biotin-CB[7]-FITC positive cells following pretreatment with high concentrations of free biotin (at 0, 0.05, 0.5, 5, 50, 500 µM of free biotin, there is 92.4, 85.8, 76.9, 51.1, 36.1, and 27.3% biotin-CB[7]-FITC positive cells respectively). This phenomenon was not reflected in L1210 treated the same way. No significant increase or decrease in percent biotin-CB[7]-FITC positive cells was observed at any concentration of free biotin in this cell line. There results seem to indicate that there was no significant binding of biotin-CB[7]-FITC to the biotin

receptors on L1210, while there was significant binding of biotin-CB[7]-FITC to the L1210FR which overexpress the biotin receptor.

Selective receptor binding was visualized and quantified using confocal microscopy and flow cytometry. The first experiment involved continuous L1210FR incubation with CB[7]-FITC and biotin-CB[7]-FITC at 2 (Figure 24A) and 15 μM (Figure 24B) for 30 mins at 37°C. A clear and significant increase in fluorescence was observed in the FITC channel (green) at both concentrations (Figure 24) of biotin-CB[7]-FITC while no significant fluorescence was observed in the cells incubated with CB[7]-FITC. This significant difference in FITC staining suggests that biotin-CB[7]-FITC is binding to the overexpressed biotin receptors found on the surface of L1210FR cells while CB[7]-FITC is not. Because this experiment used confocal microscopy, this image is representative of a z-section of the middle of the cells which seems to show internalization of the biotin-CB[7]-FITC. Furthermore, colocalization (as indicated by arrows) of Dextran-647 (red) with biotin-CB[7]-FITC (green) treatment also seems to indicate internalization and localization in lysosomes of the biotin-CB[7]-FITC rather than simple surface staining.

A kinetics assay was conducted using these same treatments. L1210FR cells were incubated at 4°C for 1.5 hrs with biotin-CB[7]-FITC at 2 and 15 μM (Figure 25A and B). This allowed for the biotin-CB[7]-FITC to bind to the biotin receptors on the cell surface while the endosomal pathways had been temporarily halted. Following incubation at 4°C, cells were thoroughly washed to remove any unbound compounds. Cells were then chased for 0, 15 and 30 mins with fresh media to restart the endosomal pathway. This would allow for the receptor mediated internalization any receptor bound compounds.

This study revealed peripheral punctured staining of the cells at 0 mins chase time (Figure 25A) suggesting that biotin-CB[7]-FITC is bound to biotin receptors on the cell surface. At 30 min chase (Figure 25B), a hazy, all around staining was observed indicating internalization of the targeted delivery system. This experiment further confirmed that biotin-CB[7]-FITC is, in fact, being internalized through selective receptor mediated endocytosis. One drawback of these two experiments is the difficulty with which it is to see the cytosolic or lysosomal staining sometime. This is most likely due to the fact that these cells are non-adherent and, therefore, rounded with limited visible cytosols. These binding an uptake experiments seem to lend towards the hypothesis that biotin-CB[7] can be targeted to and selectively taken up by cells overexpressing the biotin receptor (like many tumor cells) while being excluded by healthy cell with normal biotin receptor expression. This suggests that this system can be used to specifically delivery anti-cancer drugs to tumors while leaving healthy cells alive.

It should be noted here that the heterogynous staining observed in Figure 25 could be due to different factors. One such explanation could be that these non-adherent cells were in a clump during the staining process thus limiting the biotin-CB[7]-FITC and dextran-647 access to cells in the middle of the clump. It may also be possible that because these are non-adherent cells, they are on different planes on the z-axis thus limiting the visibility of the staining. Finally, it may also be possible that the unstained cells are unhealthy and, therefore, have limited receptor-mediated uptake either during the time of staining. There are several ways to improve these confocal microscopy studies. One way would be to decrease the number of cells used in the experiment while increasing the amount of agitation during the staining process so as to minimize

clumping. Finally, to further support the idea that biotin-CB[7]-FITC is, in fact, internalized, this experiment could be repeated with an extracellular quenching agent to eliminate extracellular fluorescence or to present the images using full z-stack, 3D image of the cells.

A primary future study would be to evaluate whether the selective binding and uptake of biotin-CB[7] can be translated *in vivo*. There are many problems that arise when translating ligand targeted therapeutics into the animal model. This is a primary reason why there are limited compounds currently in advanced stages of development. One important obstacle is the rapid clearance of targeted DDSs. In fact, many studies have shown that the pharmacokinetics and biodistribution of ligand targeted particles do not usually differ significantly from free drug due rapid clearance from the body[200]. Furthermore, if a targeted DDS is too small to induce the EPR effect, it may likely be filtered out of the tumors fairly quickly, giving the targeting ligands limited time to bind to receptors on tumor cells [200]. These particles will then be back in general circulation and be cleared from the system through renal filtration. This rapid filtration and systemic clearance could limit cell uptake of the drug and render the therapy ineffective. Therefore, it is clear that ligand targeted delivery of drugs may not be enough.

PEGylation of a DDS could both extend circulation time and promote retention of DDSs by inducing the EPR effect[95], however, PEGylation alone is also not enough to produce an effective targeted DDS. There are several reasons for this. For the EPR effect to be efficient, the DDS must remain in circulation at high concentrations for more than 6 hrs[100, 201]. Furthermore, the EPR effect only allows for the accumulation of the drug in the tumor tissue, and does not imply that the drug is actually released from the

nanoparticle or that the drug or DDS is taken up by the tumor cells[199]. This uptake can, however, be guaranteed by using a targeting ligand like biotin.

Therefore, it may be prudent to include a targeting ligand in addition to PEGylating a delivery system as it is clear that both methods of targeting may be necessary for effective delivery[200]. This system would theoretically 1) reach the tumor successfully with limited to no phagocytosis and inactivation by macrophages and blood proteins, 2) accumulate within the tissue as a result of the EPR effect, 3) bind to tumor specific receptors through their targeting ligands thus retaining the drugs in the tumor and 4) allow for the DDS to be taken up into the cell through receptor mediated endocytosis.

There are several targeted delivery systems that are currently in clinical trials that utilize both these components to enhance drug delivery. One such example is BIND-014 which is a PSMA aptamer targeted PEG/PLGA nanoparticle loaded with the anticancer docetaxel[188].

7.3 *In vitro* evaluation of drug efficacy upon loading into targeted and untargeted CB[7].

7.3.1 Ethambutol (EMB) retains its efficacy upon coupling with CB[7]

RAW264.7 cells were infected with *M. smegmatis* and then treated with EMB and CB[7]-EMB for 3 days after which time the amount of viable bacteria was determined (Figure 26). At day 3, untreated cells provided high bacterial survival with a CFU of 1.24×10^7 ($\pm 5.4 \times 10^6$) CFU/mL. At a MIC of 0.1 units, cells treated with EMB resulted in 4×10^5 ($\pm 2.3 \times 10^5$) CFU/mL and cells treated with CB[7]-EMB resulted in 8.6×10^5 ($\pm 6 \times 10^5$) CFU/mL. CFU values between EMB and CB[7]-EMB at a MIC value of 0.4

units were found to be 3.6×10^4 ($\pm1.7\times10^3$) CFU/mL and 4.3×10^4 ($\pm1.7\times10^3$) CFU/mL respectively. At a MIC of 0.8 units, EMB was 1×10^3 ($\pm4\times10^2$) CFU/ mL and CB[7]-EMB was 6×10^2 ($\pm3.3\times10^2$) CFU/mL. Finally at a MIC of 1 units, CFU values for EMB and CB[7]-EMB were 8×10^2 ($\pm6.6\times10^2$) CFU/mL and 1.4×10^3 ($\pm1.1\times10^3$) CFU/mL respectively. The values of CFUs within each MIC dose for free EMB or CB[7]-EMB were not significantly different from each other (unpaired t-test).
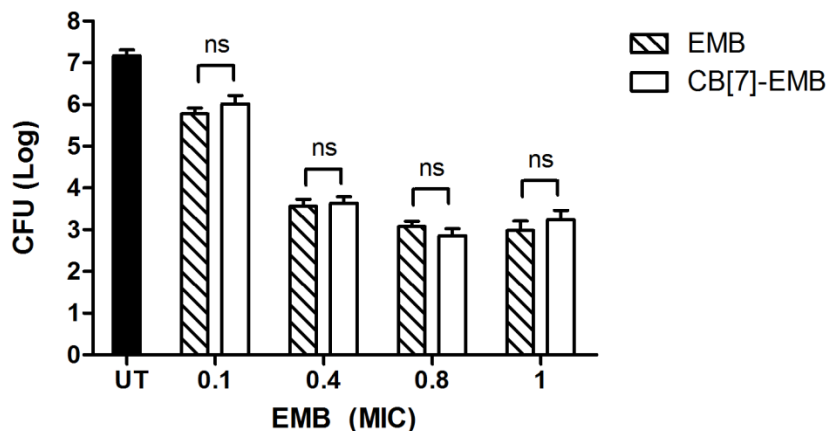
Figure 26: *M. smegmatis* **treatment using the TB drug EMB loaded into CB[7] (CB[7]-EMB, white bars) were equally effective in treating** *M. smegmatis* **infected RAW264.7 cells as free EMB (patterned bars).** RAW264.7cells were incubated with M. smegmatis for two hours and then chased for three days with EMB and CB[7]-EMB. Varying MIC values for EMB and CB[7]-EMB were used: 0.1, 0.4, 0.8, and 1 units. Viable bacteria were quantified using CFU/ml. This figure is representative of two replicate experiments, unpaired student t-test was conducted. Work was done by Gaya Hettiarachchi and Volker Briken[145].

7.3.2 Increased oxaliplatin efficacy is observed as a result of increased drug uptake due to targeted delivery by biotin-CB[7].

In this study, oxaliplatin was loaded into untargeted CB[7] (CB[7]-Oxaliplatin), and targeted biotin-CB[7] (biotin-CB[7]-oxaliplatin) (Figure 27). These compounds were used to treat L1210FR and L1210 cells along with the oxaliplatin alone at increasing concentrations (0, 0.5, 5, 15, 25, 50, 150 and 250 μM) (Figure 27A). MTS analysis revealed that L1210FR treated with oxaliplatin resulted in an average of 100%, 95%, 107%, 106%, 106%, 83%, 59%, and 59% cell viability respectively. CB[7]-oxaliplatin resulted in an average of 100%, 108%, 125%, 110%, 96%, 83%, 60% and 57% cell viability and an average of 100%, 107%, 96%, 55%, 60%, 36%, 48%, and 44% cell viability was observed with increasing concentrations of biotin-CB[7]-Oxaliplatin.

In the L1210 cell line, the same concentrations of oxaliplatin resulted in 100%, 87%, 93%, 90%, 94%, 93%, 51%, and 49% cell viability. CB[7]-oxaliplatin resulted in 100%, 102%, 104%, 111%, 100%, 111%, 74%, and 52% cell viability while biotin-CB[7]-oxaliplatin resulted in 100%, 89%, 89%, 78%, 65%, 55%, 38%, and 34% cell viability. (Figure 27B)
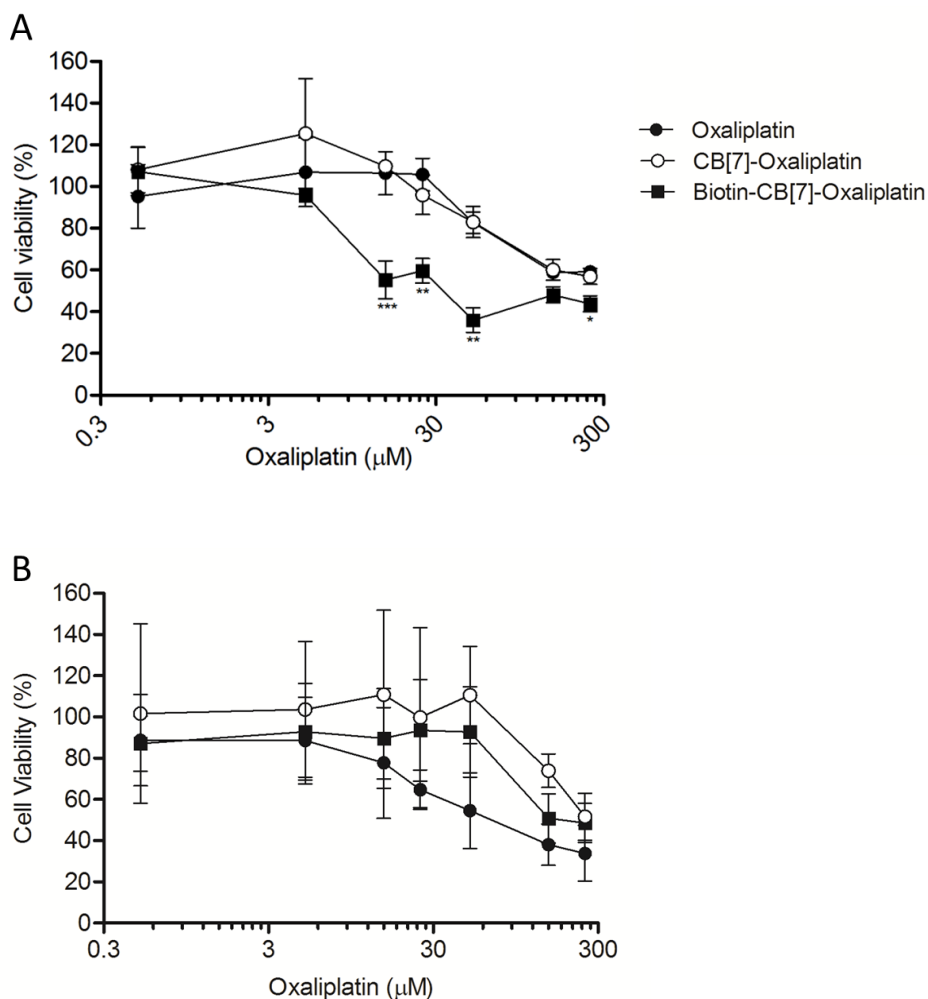
Figure 27: Biotin-CB[7]-Oxaliplatin results in target specific decrease in cell viability in the biotin receptor positive murine lymphocytic leukemia cell line (L1210FR). L1210(B) and L1210FR (A) cells were incubated with Oxaliplatin (black circle), CB[7]-Oxaliplatin (open circle), and Biotin-CB[7]-Oxaliplatin (black square) for 45 mins. Cells were then washed and incubated in fresh media for 24 hrs prior to analysis with the MTS assay. These figures are representative of three experimental repeats (n = 3) (A) and two experimental repeats (n=4) (B). The unpaired student t-test was conducted. *P = 0.01–0.05; **P = 0.001–0.01; ***P < 0.001. Work was done by Gaya Hettiarachchi[151].

7.3.3 Discussion

In order to assess whether CB[7] binding would inhibit the activity of an encapsulated drug, EMB loaded CB[7] was used to treat *M. smegmatis* infected RAW264.7 cells (Figure 26). EMB was specifically chosen because it is a widely used anti-tuberculosis drug with high efficacy and minimum side effects. Therefore, any inhibition of the drug's activity by CB[7] would be readily observable upon treatment. *M. smegmatis* is a non-virulent mycobacterium often used as a model for tuberculosis infections[202] and is treatable with EMB. Treatment of infected RAW264.7 cells with free EMB and CB[7]-EMB revealed equal and efficient killing of bacteria by both with increasing doses of the drug. No significant difference in efficacy was found between the free and encapsulated drug, therefore, suggesting that CB[7] does not inhibit the activity of EMB. It has been shown previously, that CB[7] loaded with the anticancer drug oxaliplatin reduced the activity of the drug by 5–10 fold depending on the specific cancer cell line used for treatment[146]. In contrast, no to moderate decrease of activity upon loading into CB[7] has been reported for a dinuclear platinum complex[203]. The latter finding could be confirmed in an *in vivo* cancer model using Balb/c mice bearing human ovarian cancer[196]. Thus it seems that potential inhibitory effects of loading drugs into CB[7] have to be determined for each individual drug. This experiment also further perpetuates the idea that CB[n]-type molecular compounds can be used across therapeutic fields and not just in the field of cancer.

Next we attempted to elucidate whether a biologically active anti-cancer drug could be delivered specifically to tumor cells overexpressing the biotin receptor and, as a result, cause specific cell death. For this purpose, a biotin-CB[7]-oxaliplatin complex

was used in the treatment of L1210 and L1210FR cells (Figure 27). Oxaliplatin is a very potent and efficacious drug with problems with severe toxicity and would, therefore, benefit from the targeted drug delivery system. Cell viability results using this system indicate a significant decrease in cell viability (55 and 47% cell viability) in L1210FR cells at only 15 µM of biotin-CB[7]-oxaliplatin. However, treatment with the oxaliplatin or CB[7]-oxaliplatin alone in these cells did not result in a significant decrease in cell viability until a concentration of 150 and 50 µM which resulted in 59 and 60% cell viability respectively (Figure 27A). In contrast, no significant differences was detected between targeted and untargeted CB[7]-oxaliplatin in the treatment of L1210 cells where a decrease in cell viability was not detected until a concentration of 50 µM (Figure 27B). These results suggests that oxaliplatin loaded into biotin-CB[7] allows for the specific binding to and cytotoxicity in cells overexpressing the biotin receptor while leaving cells with normal receptor expression healthy. Furthermore, this study suggests the need for lower drug concentrations to induce greater cytotoxicity in L1210FR cells when oxaliplatin is delivered using the biotin-CB[7] system. Both these factors combined can lead to significantly diminished side effects in chemotherapy. Finally, cell death results suggests that oxaliplatin is, in fact, internalized and released from the delivery system so that it can bind to DNA and induce cell death through its mechanism of action.

The significant differences in cell death between oxaliplatin, and CB[7] encapsulated drug systems in the L1210 cell line could be attributed to the fact that CB[7] may be limiting oxaliplatin bioactivity (Figure 27B). This phenomenon was demonstrated by the Kim group [146] in a variety of different cell lines *in vitro* stating that this could be due to inadequate uptake of CB[7]-oxaliplatin. It is important to note here though, that

this behavior is not reflected in the L1210FR cell line upon treatment with biotin-CB[7]-oxaliplatin thus further validating the receptor specific uptake of the targeted DDS and eventual release of the drug with the cell. This also seems to suggest that limited harm can be done to "healthy" cells with untargeted or targeted CB[7]-oxaliplatin while free oxaliplatin results in high cell death. This again validates the need to use a targeted drug delivery system like biotin-CB[7] to delivery oxaliplatin.

An essential future study to evaluate the plausibility of a targeted CB[n] is to translate this system *in vivo* as mentioned previously. As previously stated, these biotin-CB[7]-oxaliplatin particles could be cleared from the blood quickly with limited access to the tumor, however, there are other considerations in the practical use of this compound and the CB[n]s as targeting molecules to also consider. One factor is that DDSs like liposomes and dendrimers are able to carry and delivery large numbers of drug molecules/nanoparticle[108, 111, 193], however, the CB[7] is limited to one drug molecule/CB[7] at best. One way researchers have somewhat circumvented this problem in CDs is by using CD-polymer nanoparticles that allow for the loading of more than one drug particle at a time. An example of this is CRLX101 which is a PEG-CD based nanoparticle that can bind to and protect CPT[163]. In clinical trials, this compound has demonstrated improved pharmacokinetics and efficient protection and passive targeting of active CPT to tumors. Nanoparticles with repeating CB[n] units have been constructed before, however, an ideal chemical balance in necessary to properly encapsulate and actually delivery drug particles effectively *in vivo*[204].

Another problem that is prominent with targeted drug delivery is drug leakage. For a targeted DDS to be effective, the drug must be maintained, at its original

concentration, within the delivery system until it reaches the tumor. However, the problem with many targeted DDSs is the leakage of drug from the DDS leading to high levels of toxicity and ineffective treatment. This is a more prominent problem with the CB[n] family, because like the CDs, these macromolecules are at an equilibrium between bound and unbound drug. As explained before, this means that any changes to this equilibrium, like high dilutions upon i.v. administration, would release the drug from the CB[n]. This could render any targeted CB[n] ineffective and would lead to high toxicity. PEGylating a compound has been demonstrated to provide some added encapsulation time of drugs within liposomes, but it may not be the ideal solution for CB[n]s. One possible solution might be to use Motor2 as a targeted delivery system. As stated before Motor2 binds to certain drugs, like CPT, with very high binding affinity and may retain the drug until the system reaches the tumor. It should also be noted that Motor2's ability to tightly bind drug compounds may also lead to problems with releasing the drug when it does reach the tumor. A second solution to this problem may be to construct a prodrug system that would result in the controlled and specific release of the drug at the tumor vasculature or within tumor cells. One stimulus that could trigger the cleavage of a prodrug and the release of the active drug would be the low pH of tumor vasculature.

One such targeted DDS that uses passive and active targeting in addition to a prodrug system is synthesized and extensively tested in Dr. Farokhad's lab (Harvard Medical School, Boston, MA)[74]. This compound is a PLGA-*b*-PEG, PSMA aptamer targeted nanoparticle that has a prodrug formulation of a potent platinum (Pt) based anticancer drug. Preclinical studies established the MTD values of this compound in rats was established at twice the dose of Pt alone (40 mg/kg vs. 20 mg/kg) and this targeted

compound was found to have significantly extended systemic circulation time, decreased accumulation in the kidney (less toxicity), and only about a third of the drug was need to elicit the same response as cisplatin delivered through conventional methods. Furthermore, the prodrug holds the drug in within the nanoparticle in an inactive form.

Due to these proposed limitations and those mentioned in the previous discussion section, it is clear that targeted CB[n] and CB[n]-type compounds have a long way to go before reaching the FDA approval process. Extensive formulation and *in vivo* studies will need to be done in close collaboration with Dr. Isaacs' lab in order to design the ideal targeting molecule using the cucurbit[n]uril family of macromolecules. As part of this developing project, different CB[n]-type molecules with the ability to significantly increase the solubility of drugs, such as with Motor2, should be tested as alternative carriers for targeting. And finally, new targeting ligands like folate, anti-PSMA particles, or antibodies should also be considered.

Chapter 8. THESIS CONCLUSION and FUTURE IMPLICATIONS

The wellbeing of the public greatly depends on the discovery and development of novel drugs, however, the productivity of the drug development pipeline has significantly decreased over the past few years. In fact, for every 10,000 drug candidates that enter the drug development pipeline, only one is eventually approved by the FDA and marketed in addition to significantly rising costs/drug[10, 12]. This decline in productivity within the development pipeline is referred to as drug development attrition. The highest contributors to developmental attrition are high drug toxicity (11% of all failed drugs), low efficacy (30%) and low drug bioavailability (39%)[12].

One solution to alleviate attrition rates is to use excipients and DDSs to improve drug bioavailability by enhancing drug solubility or improve drug toxicity through the targeted drug delivery[63, 80, 82, 98]. There are many different kinds of excipients and DDSs currently being studied and marketed including polymers, liposomes and CDs[92, 122, 180]. A new family of macromolecules proposed for these uses is the CB[n] family[138]. Despite the fact that there are so many different kinds of successful excipients and DDSs both under research and being marketed, there is a continuous need to expand this toolbox. The reason for this is that no one host molecule can solubilize and help deliver every drug compound.

As a result, here, we have introduced and evaluated three new CB[n]-type molecules. Motor1, Motor2 and functionalized CB[7] were synthesized and their chemical properties analyzed in Dr. Lyle Isaacs' lab. Their work demonstrated that Motor1 and 2 can increase the solubility of a large variety of drugs across therapeutic fields, many of which HP-β-CD could not (Table1). Some of the most striking were PBS-

1086 (7.5 mM increase with Motor1), PTX (~2750 fold increase with Motor1), melphalan (~1690-fold increase with Motor1 and 2), CPT (~580-fold with Motor2), and cinnarizine (~308-fold increase with Motor1). There are many drugs, currently being investigated, abandoned or marketed, that cannot be formulated with other excipients without inducing high toxicity but it may be improved by using Motor1. The re-formulation and approval of these drugs can have an immense impact on improving public health by increasing the diversity and availability of drugs in the market, not just in the field of cancer, but across therapeutic fields. Of course there are several compounds that are not compatible with Motor1 or 2, like the anticancer drug doxorubicin, therefore, here we do not necessarily strive to replace established excipients like CDs and liposomes. Instead we hope to add to the expanding toolbox currently available and provide a wider range of alternatives for solubilizing drugs.

In vitro and *in vivo* analysis of Motor1 suggested that it was highly biocompatible and is able to solubilize a large variety of drugs without inhibiting drug activity. Some of the most pressing studies that will need to be conducted with this compound in the near future include adequate *in vivo* evaluation of Motor1-drug complexes. This not only entails further evaluation of Motor1-drug efficacy, but also Motor1-drug pharmacokinetics to clearly establish the bioavailability, biodistribution and clearance of these compounds. The information collected from studies conducted in rodent models (like rats) will provide a clear idea of how useful Motor1 will be in the clinical setting and will also allow for us to establish adequate dosage and dosing schedules for translation into non-rodent models. Following the outcome of these *in vivo* experiments, further development of Motor1 can be pursued by conducting a more in-depth analysis of

Motor1 toxicity in accordance with requirements and guidelines set forth by the FDA such as evaluating genetic toxicity, immunotoxicity, reproductive/developmental etc. It is essential to establish these in rodent and non-rodent models. The most immediate and relevant toxicity study may be *in vitro* genetic toxicity testing and evaluating *in vivo* immunotoxicity as detailed in the discussion of Motor1 biocompatibility. Furthermore, it may be essential to begin to establish the long-term repeat dose effects of Motor1. An MTD study of Motor1 and 2 in rats is already underway in a collaboration with Dr. Matthias Eikermann (Massachusetts General Hospital, Harvard Medical School, Boston, MA). Another avenue that may be interesting to explore further down the road, once essential parameters have been established, is to investigate whether Motor1 can be used for the oral administration of drugs. Additionally, other fields of therapy should also be explored given Motor1's ability to increase the solubility of drugs across therapeutic fields (Table1). Both of these investigations would significantly expand the therapeutic reach of this delivery system and increase the impact Motor1 has on public health. Finally, biologically evaluation of Motor2 should commence in the near future to establish its potential use as a drug delivery system.

Dr. Isaacs' lab was also able to successfully ligate biotin to the surface of CB[7] in order to create a delivery system that could deliver drugs specifically to tumors that overexpress the biotin receptor on the cell surfaces. This kind of targeted drug delivery system would help alleviate severe side effects associated with cancer therapy. This system was shown to be effective in *in vitro* treatment against cell lines overexpressing the biotin receptor, however, the practical translation of this system into the *in vivo* model and then into humans will need extensive thought and research as detailed in the

discussion sections. There are several disadvantages to this system that may need to be improved upon before further study can be conducted into targeted tumor treatment. One disadvantage is that, because of its small size, it may be cleared for tumor vasculature very quickly thus limiting the time biotin-CB[7] has to bind to its receptors on cancer cells. Furthermore it can also be cleared from systemic circulation very quickly, thus limiting its bioavailability. One possible option towards improving circulation and retention time is to PEGylate the targeted compound. It may also be possible to form nanoparticles from targeted CB[n] and PEG like with CRLX101. This is a CD-PEG based nanoparticle that can delivery active CPT to tumors very effectively. It is currently in clinical trials[162]. A nanoparticle such as this also demonstrates the added advantage of being able to delivery multiple drug molecules in one nanoparticle. However, the restructuring of biotin-CB[7] and plausibility of these solutions will have to be carefully evaluated by Dr. Isaacs.

A second disadvantage to biotin-CB[7] is the fact that the CB[n]-drug system works on an equilibrium between bound and unbound drug much like the CD family. This system takes advantage of factors, like high dilutions, that can shift this equilibrium to release and retain free drug from the CB[n]. When targeting a drug molecule to a tumor, the drug must be maintained within the carrier until it reaches and binds to the tumor; with the current biotin-CB[n] system, this is not the case. Theoretically, when the biotin-CB[7]-drug compound reaches a high dilution in the blood upon i.v dosing, the drug will be released before the system reaches the tumor. One potential solution to this may be to explore Motor2 as a targeted DDS due to its high affinity towards drug compounds like CPT. However, drug release will have to be closely monitored to ensure

drug efficacy is maintained. A second option would be design a prodrug system that would allow for the retention and controlled release of the drug specifically at the tumor. One example that uses all three elements of an ideal targeted drug delivery system is the PSMA aptamer targeted PLGA-*b*-PEG nanoparticle encapsulating the Pt (IV) prodrug that was discussed previously[74].

In an effort to understand what would happen to the biotin-CB[7] *in vivo* it may be conducive to quantify and visualize the biodistribution of biotin-CB[7] through live animal imaging. This would give practical information about whether tumor targeting with this compound is plausible and what problems we can expect to run into with targeted *in vivo* drug delivery. If encouraging results are collected, *in vivo* treatment of biotin overexpressing tumors can be conducted to evaluate whether a drug can be delivered to tumors while maintaining efficacy. Following these studies, further investigation into the pharmacokinetics and safety profile of this targeted compound can be conducted in a similar manner to that of Motor1.

Despite their limitations and the need for further investigation, the results presented in this thesis provide an encouraging proof-of-principle towards the use of CB[n]-type compounds for enhancing the solubility and targeting the delivery of many drugs. By improving drug solubility and toxicity profiles, these compounds may be able to help get essential therapies marketed and as a result help reduce attrition rates within the drug development pipeline. These CB[n]-type compounds may be able to help enhance public health and the quality of life for many.

BIBLIOGRAPHY

1. Lipp, R., *The innovator Pipeline: Bioavailability Challenges and Advanced Oral Drug Delivery Opportunities.* American Pharmaceutical Review, 2013.

2. U.S. Department of Health and Human Services, F.D.A. *F.D.A. History- Origins and Functions*. 2013; Available from: http://www.fda.gov/AboutFDA/WhatWeDo/History/default.htm.

3. U.S. Department of Health and Human Services, F.D.A. *Significant Dates in U.S. Food and Drug Law History*. 2013; Available from: http://www.fda.gov/AboutFDA/WhatWeDo/History/Milestones/ucm128305.htm.

4. Dickson, M. and J.P. Gagnon, *Key factors in the rising cost of new drug discovery and development.* Nat Rev Drug Discov, 2004. **3**(5): p. 417-29.

5. Pritchard, J.F., et al., *Making better drugs: Decision gates in non-clinical drug development.* Nat Rev Drug Discov, 2003. **2**(7): p. 542-53.

6. Wehling, M., *Assessing the translatability of drug projects: what needs to be scored to predict success?* Nat Rev Drug Discov, 2009. **8**(7): p. 541-6.

7. Teitelbaum, Z., et al., *Risk assessment in extrapolation of pharmacokinetics from preclinical data to humans.* Clin Pharmacokinet, 2010. **49**(9): p. 619-32.

8. Scannell, J.W., et al., *Diagnosing the decline in pharmaceutical R&D efficiency.* Nat Rev Drug Discov, 2012. **11**(3): p. 191-200.

9. Cuatrecasas, P., *Drug discovery in jeopardy.* J Clin Invest, 2006. **116**(11): p. 2837-42.

10. U.S. Department of Health and Human Services, N.I.H. *Therapeutic Developmental Process*. 2013; Available from: http://www.ncats.nih.gov/research/reengineering/process.html.

11. Mahajan, R. and K. Gupta, *Food and drug administration's critical path initiative and innovations in drug development paradigm: Challenges, progress, and controversies.* J Pharm Bioallied Sci, 2010. **2**(4): p. 307-13.

12.   Kola, I. and J. Landis, *Can the pharmaceutical industry reduce attrition rates?* Nat Rev Drug Discov, 2004. **3**(8): p. 711-5.

13.   Booth, B. and R. Zemmel, *Prospects for productivity.* Nat Rev Drug Discov, 2004. **3**(5): p. 451-6.

14.   U.S. Department of Health and Human Services, F.D.A. *Innovation or Stagnation: Challenge and Opportunity on the Critical Path to New Medical Products*. 2004; Available from: http://www.fda.gov/oc/initiatives/criticalpath/whitepaper.html.

15.   van de Waterbeemd, H. and E. Gifford, *ADMET in silico modelling: towards prediction paradise?* Nat Rev Drug Discov, 2003. **2**(3): p. 192-204.

16.   Bowes, J., et al., *Reducing safety-related drug attrition: the use of in vitro pharmacological profiling.* Nat Rev Drug Discov, 2012. **11**(12): p. 909-22.

17.   W.H.O. *Cancer Mortality and Morbidity* 2013; Available from: http://www.who.int/gho/ncd/mortality_morbidity/cancer/en/index.html.

18.   Cho, K., et al., *Therapeutic nanoparticles for drug delivery in cancer.* Clin Cancer Res, 2008. **14**(5): p. 1310-6.

19.   Muller, P.Y. and M.N. Milton, *The determination and interpretation of the therapeutic index in drug development.* Nat Rev Drug Discov, 2012. **11**(10): p. 751-61.

20.   Houck, K.A. and R.J. Kavlock, *Understanding mechanisms of toxicity: insights from drug discovery research.* Toxicol Appl Pharmacol, 2008. **227**(2): p. 163-78.

21.   Eichler, H.G., et al., *Balancing early market access to new drugs with the need for benefit/risk data: a mounting dilemma.* Nat Rev Drug Discov, 2008. **7**(10): p. 818-26.

22.   Park, S.B., et al., *Oxaliplatin-induced neurotoxicity: changes in axonal excitability precede development of neuropathy.* Brain, 2009. **132**(Pt 10): p. 2712-23.

23. Alcindor, T. and N. Beauger, *Oxaliplatin: a review in the era of molecularly targeted therapy.* Curr Oncol, 2011. **18**(1): p. 18-25.

24. Alian, O.M., A.S. Azmi, and R.M. Mohammad, *Network insights on oxaliplatin anti-cancer mechanisms.* Clin Transl Med, 2013. **1**(1): p. 26.

25. Guengerich, F.P., *Mechanisms of drug toxicity and relevance to pharmaceutical development.* Drug Metab Pharmacokinet, 2010. **26**(1): p. 3-14.

26. U.S. Department of Health and Human Services, F.D.A., *Preclinical safety evaluation of biotechnology-derived pharmaceuticals S6(R1)* 1997.

27. U.S. Department of Health and Human Services, F.D.A., Center for Drug Evaluation and Research (CDER), Center for Biologics Evaluation and Research (CBER), *Guidance for Industry S6 Preclinical Safety Evaluation of Biotechnology-Derived Pharmaceuticals*. 1997.

28. U.S. Department of Health and Human Services, F.D.A., Center for Drug Evaluation and Research (CDER), *Guidance for Industry: Immunotoxicology Evaluation of Investigational New Drugs*. 2002.

29. Weiss, R.B., et al., *Hypersensitivity reactions from taxol.* J Clin Oncol, 1990. **8**(7): p. 1263-8.

30. Szebeni, J., F.M. Muggia, and C.R. Alving, *Complement activation by Cremophor EL as a possible contributor to hypersensitivity to paclitaxel: an in vitro study.* J Natl Cancer Inst, 1998. **90**(4): p. 300-6.

31. Gelderblom, H., et al., *CremophorEL: the drawbacks and advantages of vehicle selection for drug formulation.* Eur J Cancer, 2001. **37**(13): p. 1590-8.

32. Lin, J.H. and A.Y. Lu, *Role of pharmacokinetics and metabolism in drug discovery and development.* Pharmacol Rev, 1997. **49**(4): p. 403-49.

33. Tang, W. and A.Y. Lu, *Drug metabolism and pharmacokinetics in support of drug design.* Curr Pharm Des, 2009. **15**(19): p. 2170-83.

34. James, L.P., P.R. Mayeux, and J.A. Hinson, *Acetaminophen-induced hepatotoxicity.* Drug Metab Dispos, 2003. **31**(12): p. 1499-506.

35. James, L.P., et al., *Effect of N-acetylcysteine on acetaminophen toxicity in mice: relationship to reactive nitrogen and cytokine formation.* Toxicol Sci, 2003. **75**(2): p. 458-67.

36. Liu, X. and L. Jia, *The conduct of drug metabolism studies considered good practice (I): analytical systems and in vivo studies.* Curr Drug Metab, 2007. **8**(8): p. 815-21.

37. U.S. Department of Health and Human Services, F.D.A., Center for Drug Evaluation and Research (CDER), Center for Biologics Evaluation and Research (CBER). *Guidance for Industry In Vivo Drug Metabolism/Drug Interaction Studies — Study Design, Data Analysis, and Recommendations for Dosing and Labeling*. 1999.

38. Biagini, C.P., et al., *Investigation of the hepatotoxicity profile of chemical entities using Liverbeads and WIF-B9 in vitro models.* Toxicol In Vitro, 2006. **20**(6): p. 1051-9.

39. U.S. Department of Health and Human Services, F.D.A., Center for Drug Evaluation and Research (CDER), Center for Biologics Evaluation and Research (CBER), *Guidance for Industry: S1B Testing for Carcinogenicity of Pharmaceuticals*. 1997.

40. U.S Department of Health and Human Services, N.I.H., National Toxicology Program, *Report on Carcinogens (RoC), 12th Edition*. 2011.

41. Elespuru, R.K., et al., *Current and future application of genetic toxicity assays: the role and value of in vitro mammalian assays.* Toxicol Sci, 2009. **109**(2): p. 172-9.

42. Eastmond, D.A., et al., *Mutagenicity testing for chemical risk assessment: update of the WHO/IPCS Harmonized Scheme.* Mutagenesis, 2009. **24**(4): p. 341-9.

43. Mahadevan, B., et al., *Genetic toxicology in the 21st century: reflections and future directions.* Environ Mol Mutagen, 2011. **52**(5): p. 339-54.

44.   Myhr, B.C., *Validation studies with Muta Mouse: a transgenic mouse model for detecting mutations in vivo.* Environ Mol Mutagen, 1991. **18**(4): p. 308-15.

45.   Lloyd, A.L., *The Mouse Lymphoma Assay.* Methods in Molecular Biology, 2012. **817**.

46.   U.S Department of Health and Human Services, F.D.A., *Guideline for Industry: Detection of Toxicity to Reproduction for Medicinial Products.* 1994.

47.   U.S. Department of Health and Human Services, F.D.A., Center for Drug Evaluation and Research (CDER). *Guidance for Industry Reproductive and Developmental Toxicities — Integrating Study Results to Assess Concerns.* 2011.

48.   Farombi, E.O., et al., *Tetracycline-induced reproductive toxicity in male rats: effects of vitamin C and N-acetylcysteine.* Exp Toxicol Pathol, 2008. **60**(1): p. 77-85.

49.   E.P.A, U.S.E.P.A., *Guidelines for Developmental Toxicity Risk Assessment.* 1991.

50.   Fiume, M.Z., *Final report on the safety assessment of biotin.* Int J Toxicol, 2001. **20 Suppl 4**: p. 1-12.

51.   Sharma, S.V., D.A. Haber, and J. Settleman, *Cell line-based platforms to evaluate the therapeutic efficacy of candidate anticancer agents.* Nat Rev Cancer, 2010. **10**(4): p. 241-53.

52.   Swinney, D.C., *Biochemical mechanisms of drug action: what does it take for success?* Nat Rev Drug Discov, 2004. **3**(9): p. 801-8.

53.   Eichler, H.G., et al., *Bridging the efficacy-effectiveness gap: a regulator's perspective on addressing variability of drug response.* Nat Rev Drug Discov, 2011. **10**(7): p. 495-506.

54.   Novac, N., *Challenges and opportunities of drug repositioning.* Trends Pharmacol Sci, 2013. **34**(5): p. 267-72.

55.   Mullard, A., *Drug repurposing programmes get lift off.* Nat Rev Drug Discov, 2012. **11**(7): p. 505-6.

56.   U.S. Department of Health and Human Services, N.I.H. *Rescuing and Repurposing Drugs*. 2013; Available from: http://www.ncats.nih.gov/research/reengineering/rescue-repurpose/rescue-repurpose.html.

57.   Huang, R., et al., *The NCGC pharmaceutical collection: a comprehensive resource of clinically approved drugs enabling repurposing and chemical genomics.* Sci Transl Med, 2011. **3**(80): p. 80ps16.

58.   U.S. Department of Health and Human Services, F.D.A. *Designating an Orphan Product: Drugs and Biologics*. 2013; Available from: http://www.fda.gov/ForIndustry/DevelopingProductsforRareDiseasesConditions/HowtoapplyforOrphanProductDesignation/default.htm.

59.   U.S. Department of Health and Human Services, F.D.A., Center for Drug Evaluation and Research (CDER). *Guidance for Industry: Bioavailability and Bioequivalence Studies for Orally Administered Drug Products — General Considerations*. 2003.

60.   Williams, H.D., et al., *Strategies to address low drug solubility in discovery and development.* Pharmacol Rev, 2013. **65**(1): p. 315-499.

61.   Lombardo, F., E. Gifford, and M.Y. Shalaeva, *In silico ADME prediction: data, models, facts and myths.* Mini Rev Med Chem, 2003. **3**(8): p. 861-75.

62.   Goldberg, M. and I. Gomez-Orellana, *Challenges for the oral delivery of macromolecules.* Nat Rev Drug Discov, 2003. **2**(4): p. 289-95.

63.   Savjani, K.T., A.K. Gajjar, and J.K. Savjani, *Drug solubility: importance and enhancement techniques.* ISRN Pharm, 2012. **2012**: p. 195727.

64.   Stegemann, S., et al., *When poor solubility becomes an issue: from early stage to proof of concept.* Eur J Pharm Sci, 2007. **31**(5): p. 249-61.

65.   Hedaya, M.A., *Drug Pharmacokinetics Following Single Oral Drug Administration: The Rate of Drug Absorption*, in *Basic Pharmacokinetics*. 2012, CRC Press Taylor and Francis Group: Boca Raton. p. 125-145.

66.   Hedaya, M.A., *Drug Pharmacokinetics Following Single Oral Drug Administration: The Extent of Drug Absorption*, in *Basic Pharmacokinetics*. 2012, CRC Press Taylor and Francis Group: Boca Raton. p. 151-171.

67.   Hedaya, M.A., *Drug Pharmacokinetics Following a Single IV Bolus Administration: Drug Distribution*, in *Basic Pharmacokinetics*. 2012, CRC Press Taylor and Francis Group: Boca Raton. p. 23-37.

68.   Hedaya, M.A., *Drug Pharmacokinetics Following a Single IV Bolus Administration: The Rate of Drug Elimination*, in *Basic Pharmacokinetics*. 2012, CRC Press Taylor and Francis Group: Boca Raton. p. 49-68.

69.   Hedaya, M.A., *Drug Pharmacokinetics Following a Single IV Bolus Administration: Drug Clearance*, in *Basic Pharmacokinetics*. 2012: Boca Raton. p. 39-47.

70.   Lindenberg, M., S. Kopp, and J.B. Dressman, *Classification of orally administered drugs on the World Health Organization Model list of Essential Medicines according to the biopharmaceutics classification system.* Eur J Pharm Biopharm, 2004. **58**(2): p. 265-78.

71.   McConnell, E.L., H.M. Fadda, and A.W. Basit, *Gut instincts: explorations in intestinal physiology and drug delivery.* Int J Pharm, 2008. **364**(2): p. 213-26.

72.   Pade, V. and S. Stavchansky, *Link between drug absorption solubility and permeability measurements in Caco-2 cells.* J Pharm Sci, 1998. **87**(12): p. 1604-7.

73.   Smith, D.A., L. Di, and E.H. Kerns, *The effect of plasma protein binding on in vivo efficacy: misconceptions in drug discovery.* Nat Rev Drug Discov, 2010. **9**(12): p. 929-39.

74.   Dhar, S., et al., *Targeted delivery of a cisplatin prodrug for safer and more effective prostate cancer therapy in vivo.* Proc Natl Acad Sci U S A, 2011. **108**(5): p. 1850-5.

75.   Hedaya, M.A., *Metabolite Pharmacokinetics*, in *Basic Pharmacokinetics*. 2012, CRC Press Taylor and Francis Group: Boca Raton. p. 253-276.

76. Mahato, A.S.N.a.R.I., *Site-Specific Prodrug Activation Strategies for Targeted Drug Action*, in *Targeted Delivery of Small and Macromolecular Drugs*, A.S.N.a.R.I. Mahato, Editor. 2010, CRC Press Taylor and Francis Group: Boca Raton. p. 283-294.

77. Hedaya, M.A., *Renal Drug Excretion*, in *Basic Pharmacokinetics*. 2012, CRC Press Taylor and Francis Group: Boca Raton. p. 233-249.

78. Merisko-Liversidge, E.M. and G.G. Liversidge, *Drug nanoparticles: formulating poorly water-soluble compounds.* Toxicol Pathol, 2008. **36**(1): p. 43-8.

79. Rosen, H. and T. Abribat, *The rise and rise of drug delivery.* Nat Rev Drug Discov, 2005. **4**(5): p. 381-5.

80. Allen, T.M. and P.R. Cullis, *Drug delivery systems: entering the mainstream.* Science, 2004. **303**(5665): p. 1818-22.

81. Farokhzad, O.C. and R. Langer, *Impact of nanotechnology on drug delivery.* ACS Nano, 2009. **3**(1): p. 16-20.

82. Wang, A.Z., et al., *Biofunctionalized targeted nanoparticles for therapeutic applications.* Expert Opin Biol Ther, 2008. **8**(8): p. 1063-70.

83. Davis, M.E., Z.G. Chen, and D.M. Shin, *Nanoparticle therapeutics: an emerging treatment modality for cancer.* Nat Rev Drug Discov, 2008. **7**(9): p. 771-82.

84. Garcia-Bennett, A., M. Nees, and B. Fadeel, *In search of the Holy Grail: Folate-targeted nanoparticles for cancer therapy.* Biochem Pharmacol, 2011. **81**(8): p. 976-84.

85. Chen, S., et al., *Mechanism-based tumor-targeting drug delivery system. Validation of efficient vitamin receptor-mediated endocytosis and drug release.* Bioconjug Chem. **21**(5): p. 979-87.

86. Lyass, O., A. Hubert, and A.A. Gabizon, *Phase I study of doxil-cisplatin combination chemotherapy in patients with advanced malignancies.* Clin Cancer Res, 2001. **7**(10): p. 3040-6.

87.   Devi, G.R., *siRNA-based approaches in cancer therapy.* Cancer Gene Ther, 2006. **13**(9): p. 819-29.

88.   Gabizon, A.A., *Pegylated liposomal doxorubicin: metamorphosis of an old drug into a new form of chemotherapy.* Cancer Invest, 2001. **19**(4): p. 424-36.

89.   Webster, D.M., P. Sundaram, and M.E. Byrne, *Injectable nanomaterials for drug delivery: carriers, targeting moieties, and therapeutics.* Eur J Pharm Biopharm, 2013. **84**(1): p. 1-20.

90.   Singh, R. and J.W. Lillard, Jr., *Nanoparticle-based targeted drug delivery.* Exp Mol Pathol, 2009. **86**(3): p. 215-23.

91.   Duncan, R., *The dawning era of polymer therapeutics.* Nat Rev Drug Discov, 2003. **2**(5): p. 347-60.

92.   Liechty, W.B., et al., *Polymers for drug delivery systems.* Annu Rev Chem Biomol Eng, 2010. **1**: p. 149-73.

93.   Ishida, T., et al., *Injection of PEGylated liposomes in rats elicits PEG-specific IgM, which is responsible for rapid elimination of a second dose of PEGylated liposomes.* J Control Release, 2006. **112**(1): p. 15-25.

94.   Matsumura, Y. and H. Maeda, *A new concept for macromolecular therapeutics in cancer chemotherapy: mechanism of tumoritropic accumulation of proteins and the antitumor agent smancs.* Cancer Res, 1986. **46**(12 Pt 1): p. 6387-92.

95.   Fang, J., H. Nakamura, and H. Maeda, *The EPR effect: Unique features of tumor blood vessels for drug delivery, factors involved, and limitations and augmentation of the effect.* Adv Drug Deliv Rev, 2010. **63**(3): p. 136-51.

96.   Maeda, H., *Tumor-selective delivery of macromolecular drugs via the EPR effect: background and future prospects.* Bioconjug Chem, 2010. **21**(5): p. 797-802.

97.   Yuan, F., et al., *Vascular permeability in a human tumor xenograft: molecular size dependence and cutoff size.* Cancer Res, 1995. **55**(17): p. 3752-6.

98.   Torchilin, V., *Tumor delivery of macromolecular drugs based on the EPR effect.* Adv Drug Deliv Rev, 2010. **63**(3): p. 131-5.

99.   Jain, R.K., *Transport of molecules, particles, and cells in solid tumors.* Annu Rev Biomed Eng, 1999. **1**: p. 241-63.

100.   Hamidi, M., A. Azadi, and P. Rafiei, *Pharmacokinetic consequences of pegylation.* Drug Deliv, 2006. **13**(6): p. 399-409.

101.   Moghimi, S.M., et al., *Complement activation cascade triggered by PEG-PL engineered nanomedicines and carbon nanotubes: the challenges ahead.* J Control Release, 2010. **146**(2): p. 175-81.

102.   Andersen, A.J., et al., *Complement activation by PEG-functionalized multi-walled carbon nanotubes is independent of PEG molecular mass and surface density.* Nanomedicine. **9**(4): p. 469-73.

103.   Kim, T.Y., et al., *Phase I and pharmacokinetic study of Genexol-PM, a cremophor-free, polymeric micelle-formulated paclitaxel, in patients with advanced malignancies.* Clin Cancer Res, 2004. **10**(11): p. 3708-16.

104.   Torchilin, V.P., *Recent advances with liposomes as pharmaceutical carriers.* Nat Rev Drug Discov, 2005. **4**(2): p. 145-60.

105.   Mufamadi, M.S., et al., *A review on composite liposomal technologies for specialized drug delivery.* J Drug Deliv, 2011. **2011**: p. 939851.

106.   Nagayasu, A., K. Uchiyama, and H. Kiwada, *The size of liposomes: a factor which affects their targeting efficiency to tumors and therapeutic activity of liposomal antitumor drugs.* Adv Drug Deliv Rev, 1999. **40**(1-2): p. 75-87.

107.   Moghimi, S.M. and J. Szebeni, *Stealth liposomes and long circulating nanoparticles: critical issues in pharmacokinetics, opsonization and protein-binding properties.* Prog Lipid Res, 2003. **42**(6): p. 463-78.

108.   Gabizon, A.A., *Stealth liposomes and tumor targeting: one step further in the quest for the magic bullet.* Clin Cancer Res, 2001. **7**(2): p. 223-5.

109.   Gramatikoff, K. *Liposomes for Drug Delivery*. 1999; Available from: http://en.wikipedia.org/wiki/File:Liposome.jpg#filelinks.

110.   Szebeni, J., et al., *Liposome-induced complement activation and related cardiopulmonary distress in pigs: factors promoting reactogenicity of Doxil and AmBisome.* Nanomedicine, 2011. **8**(2): p. 176-84.

111.   Allen, T.M., *Liposomes. Opportunities in drug delivery.* Drugs, 1997. **54 Suppl 4**: p. 8-14.

112.   Sharma, A., et al., *Activity of paclitaxel liposome formulations against human ovarian tumor xenografts.* Int J Cancer, 1997. **71**(1): p. 103-7.

113.   Barenholz, Y., *Doxil(R)--the first FDA-approved nano-drug: lessons learned.* J Control Release, 2012. **160**(2): p. 117-34.

114.   Wu, Z.H., et al., *Hypoglycemic efficacy of chitosan-coated insulin liposomes after oral administration in mice.* Acta Pharmacol Sin, 2004. **25**(7): p. 966-72.

115.   Postma, N.S., et al., *Treatment with liposome-bound recombinant human tumor necrosis factor-alpha suppresses parasitemia and protects against Plasmodium berghei k173-induced experimental cerebral malaria in mice.* J Pharmacol Exp Ther, 1999. **288**(1): p. 114-20.

116.   Vyas, S.P., et al., *Design of liposomal aerosols for improved delivery of rifampicin to alveolar macrophages.* Int J Pharm, 2004. **269**(1): p. 37-49.

117.   Sioud, M. and D.R. Sorensen, *Cationic liposome-mediated delivery of siRNAs in adult mice.* Biochem Biophys Res Commun, 2003. **312**(4): p. 1220-5.

118.   Shi, G., et al., *Efficient intracellular drug and gene delivery using folate receptor-targeted pH-sensitive liposomes composed of cationic/anionic lipid combinations.* J Control Release, 2002. **80**(1-3): p. 309-19.

119.   Pan, X.Q., H. Wang, and R.J. Lee, *Boron delivery to a murine lung carcinoma using folate receptor-targeted liposomes.* Anticancer Res, 2002. **22**(3): p. 1629-33.

120.   Kobayashi, T., et al., *Effect of transferrin receptor-targeted liposomal doxorubicin in P-glycoprotein-mediated drug resistant tumor cells.* Int J Pharm, 2007. **329**(1-2): p. 94-102.

121.   Mamot, C., et al., *EGFR-targeted immunoliposomes derived from the monoclonal antibody EMD72000 mediate specific and efficient drug delivery to a variety of colorectal cancer cells.* J Drug Target, 2006. **14**(4): p. 215-23.

122.   Uekama, K., F. Hirayama, and T. Irie, *Cyclodextrin Drug Carrier Systems.* Chem Rev, 1998. **98**(5): p. 2045-2076.

123.   Loftsson, T. and M.E. Brewster, *Pharmaceutical applications of cyclodextrins: basic science and product development.* J Pharm Pharmacol, 2010. **62**(11): p. 1607-21.

124.   Stella, V.J. and Q. He, *Cyclodextrins.* Toxicol Pathol, 2008. **36**(1): p. 30-42.

125.   Loftsson, T. and M.E. Brewster, *Pharmaceutical applications of cyclodextrins. 1. Drug solubilization and stabilization.* J Pharm Sci, 1996. **85**(10): p. 1017-25.

126.   *Cyclodextrins*. 2006; Available from: http://en.wikipedia.org/wiki/File:Cyclodextrin.svg.

127.   Loftsson, T. and D. Duchene, *Cyclodextrins and their pharmaceutical applications.* Int J Pharm, 2007. **329**(1-2): p. 1-11.

128.   Irie, T. and K. Uekama, *Pharmaceutical applications of cyclodextrins. III. Toxicological issues and safety evaluation.* J Pharm Sci, 1997. **86**(2): p. 147-62.

129.   Frank, D.W., J.E. Gray, and R.N. Weaver, *Cyclodextrin nephrosis in the rat.* Am J Pathol, 1976. **83**(2): p. 367-82.

130.   Gould, S. and R.C. Scott, *2-Hydroxypropyl-beta-cyclodextrin (HP-beta-CD): a toxicology review.* Food Chem Toxicol, 2005. **43**(10): p. 1451-9.

131.   Captisol. *Captisol A Ligand Technology*. 2013; Available from: http://www.captisol.com/partnerships-collaborations/.

132.   Rao, V.M. and V.J. Stella, *When can cyclodextrins be considered for solubilization purposes?* J Pharm Sci, 2003. **92**(5): p. 927-32.

133.   Muller, B.W. and U. Brauns, *Hydroxypropyl-beta-cyclodextrin derivatives: influence of average degree of substitution on complexing ability and surface activity.* J Pharm Sci, 1986. **75**(6): p. 571-2.

134.   Loftsson, T. and M.E. Brewster, *Pharmaceutical applications of cyclodextrins: effects on drug permeation through biological membranes.* J Pharm Pharmacol. **63**(9): p. 1119-35.

135.   Davis, M.E. and M.E. Brewster, *Cyclodextrin-based pharmaceutics: past, present and future.* Nat Rev Drug Discov, 2004. **3**(12): p. 1023-35.

136.   Center, N.I.H.C. *Hydroxypropyl Beta Cyclodextrin for Niemann-Pick Type C1 Disease*. 2013; Available from: http://clinicaltrials.gov/ct2/show/NCT01747135.

137.   Kim, K., et al., *Functionalized cucurbiturils and their applications.* Chem Soc Rev, 2007. **36**(2): p. 267-79.

138.   Lagona, J., et al., *The cucurbit[n]uril family.* Angew Chem Int Ed Engl, 2005. **44**(31): p. 4844-70.

139.   Isaacs, L., *Cucurbit[n]urils: from mechanism to structure and function.* Chem Commun (Camb), 2009(6): p. 619-29.

140.   Pourgholami, M.H., K.T. Wangoo, and D.L. Morris, *Albendazole-cyclodextrin complex: enhanced cytotoxicity in ovarian cancer cells.* Anticancer Res, 2008. **28**(5A): p. 2775-9.

141.   Uzunova, V.D., et al., *Toxicity of cucurbit[7]uril and cucurbit[8]uril: an exploratory in vitro and in vivo study.* Org Biomol Chem, 2010. **8**(9): p. 2037-42.

142.   Zhao, Y., et al., *Solubilisation and cytotoxicity of albendazole encapsulated in cucurbit[n]uril.* Org Biomol Chem, 2008. **6**(24): p. 4509-15.

143.   Hennig, A., G. Ghale, and W.M. Nau, *Effects of cucurbit[7]uril on enzymatic activity.* Chem Commun (Camb), 2007(16): p. 1614-6.

144. Saleh, N., A.L. Koner, and W.M. Nau, *Activation and stabilization of drugs by supramolecular pKa shifts: drug-delivery applications tailored for cucurbiturils.* Angew Chem Int Ed Engl, 2008. **47**(29): p. 5398-401.

145. Hettiarachchi, G., et al., *Toxicology and drug delivery by cucurbit[n]uril type molecular containers.* PLoS One, 2010. **5**(5): p. e10514.

146. Jeon, Y.J., et al., *Novel molecular drug carrier: encapsulation of oxaliplatin in cucurbit[7]uril and its effects on stability and reactivity of the drug.* Org Biomol Chem, 2005. **3**(11): p. 2122-5.

147. Dong, N., et al., *Cucurbit[n]urils (n = 7, 8) binding of camptothecin and the effects on solubility and reactivity of the anticancer drug.* Supramolecular Chemistry, 2007. **20**(7): p. 659-665.

148. Plumb, J.A., et al., *Cucurbit[7]uril encapsulated cisplatin overcomes cisplatin resistance via a pharmacokinetic effect.* Metallomics, 2012. **4**(6): p. 561-7.

149. Wyman, I.W. and D.H. Macartney, *Host-guest complexations of local anaesthetics by cucurbit[7]uril in aqueous solution.* Org Biomol Chem, 2009. **8**(1): p. 247-52.

150. Ma, D., et al., *Acyclic cucurbit[n]uril molecular containers enhance the solubility and bioactivity of poorly soluble pharmaceuticals.* Nat Chem, 2012. **4**(6): p. 503-10.

151. Cao, L., et al., *Targeted Cucurbit[7]uril Containers Delivery Oxaliplatin to Cancer Cells.* Angew Chem Int Ed Engl, 2013.

152. Fabre, C., et al., *Dual inhibition of canonical and noncanonical NF-kappaB pathways demonstrates significant antitumor activities in multiple myeloma.* Clin Cancer Res, 2012. **18**(17): p. 4669-81.

153. Karin, M., et al., *NF-kappaB in cancer: from innocent bystander to major culprit.* Nat Rev Cancer, 2002. **2**(4): p. 301-10.

154. Liebmann, J.E., et al., *Cytotoxic studies of paclitaxel (Taxol) in human tumour cell lines.* Br J Cancer, 1993. **68**(6): p. 1104-9.

155.   U.S Department of Health and Human Services, F.D.A., *TAXOL[®] (paclitaxel) INJECTION* 2011.

156.   U.S. Department of Health and Human Services, F.D.A., *ABRAXANE® for Injectable Suspension (paclitaxel protein-bound particles for injectable suspension) (albumin-bound)* 2005.

157.   Sparreboom, A., et al., *Comparative preclinical and clinical pharmacokinetics of a cremophor-free, nanoparticle albumin-bound paclitaxel (ABI-007) and paclitaxel formulated in Cremophor (Taxol).* Clin Cancer Res, 2005. **11**(11): p. 4136-43.

158.   Ibrahim, N.K., et al., *Phase I and pharmacokinetic study of ABI-007, a Cremophor-free, protein-stabilized, nanoparticle formulation of paclitaxel.* Clin Cancer Res, 2002. **8**(5): p. 1038-44.

159.   Hertzberg, R.P., M.J. Caranfa, and S.M. Hecht, *On the mechanism of topoisomerase I inhibition by camptothecin: evidence for binding to an enzyme-DNA complex.* Biochemistry, 1989. **28**(11): p. 4629-38.

160.   Venditto, V.J. and E.E. Simanek, *Cancer therapies utilizing the camptothecins: a review of the in vivo literature.* Mol Pharm, 2010. **7**(2): p. 307-49.

161.   Guarino, A.M., et al., *Pharmacologic studies of camptothecin (NSC-100880): distribution, plasma protein binding, and biliary excretion.* Cancer Chemother Rep, 1973. **57**(2): p. 125-40.

162.   Young, C., et al., *CRLX101 (formerly IT-101)-A Novel Nanopharmaceutical of Camptothecin in Clinical Development.* Curr Bioact Compd, 2011. **7**(1): p. 8-14.

163.   Svenson, S., et al., *Preclinical to clinical development of the novel camptothecin nanopharmaceutical CRLX101.* J Control Release, 2011. **153**(1): p. 49-55.

164.   Pourgholami, M.H., et al., *Antitumor activity of albendazole against the human colorectal cancer cell line HT-29: in vitro and in a xenograft model of peritoneal carcinomatosis.* Cancer Chemother Pharmacol, 2005. **55**(5): p. 425-32.

165. Pourgholami, M.H., et al., *Albendazole: a potent inhibitor of vascular endothelial growth factor and malignant ascites formation in OVCAR-3 tumor-bearing nude mice.* Clin Cancer Res, 2006. **12**(6): p. 1928-35.

166. Pourgholami, M.H., et al., *Phase I clinical trial to determine maximum tolerated dose of oral albendazole in patients with advanced cancer.* Cancer Chemother Pharmacol, 2009. **65**(3): p. 597-605.

167. Isaacs, L., et al., *Molecular Container to Enhance Aqueous Solubility of Drugs*, U.o. Maryland, Editor. 2010: U.S.A.

168. Ma, D., et al., *Acyclic cucurbit[n]uril-type molecular containers bind neuromuscular blocking agents in vitro and reverse neuromuscular block in vivo.* Angew Chem Int Ed Engl, 2012. **51**(45): p. 11358-62.

169. Velmurugan, K., et al., *Mycobacterium tuberculosis nuoG is a virulence gene that inhibits apoptosis of infected host cells.* PLoS Pathog, 2007. **3**(7): p. e110.

170. Promega, *CellTiter 96® AQueous One Solution Cell Proliferation Assay*. 2012.

171. Lonza, *ToxiLight™ bioassay kit Non destructive cytotoxicity assay*. 2013.

172. Danhier, F., et al., *Paclitaxel-loaded PEGylated PLGA-based nanoparticles: in vitro and in vivo evaluation.* J Control Release, 2009. **133**(1): p. 11-7.

173. Hine, C.M., A. Seluanov, and V. Gorbunova, *Rad51 promoter-targeted gene therapy is effective for in vivo visualization and treatment of cancer.* Mol Ther, 2011. **20**(2): p. 347-55.

174. Chen, Q., et al., *Pharmacologic doses of ascorbate act as a prooxidant and decrease growth of aggressive tumor xenografts in mice.* Proc Natl Acad Sci U S A, 2008. **105**(32): p. 11105-9.

175. Zhang, X., et al., *Anti-tumor efficacy and biodistribution of intravenous polymeric micellar paclitaxel.* Anticancer Drugs, 1997. **8**(7): p. 696-701.

176. Hobbs, S.K., et al., *Regulation of transport pathways in tumor vessels: role of tumor type and microenvironment.* Proc Natl Acad Sci U S A, 1998. **95**(8): p. 4607-12.

177. Gref, R., et al., *Poly(ethylene glycol)-coated nanospheres: potential carriers for intravenous drug administration.* Pharm Biotechnol, 1997. **10**: p. 167-98.

178. Klibanov, A.L., et al., *Amphipathic polyethyleneglycols effectively prolong the circulation time of liposomes.* FEBS Lett, 1990. **268**(1): p. 235-7.

179. Torchilin, V.P., et al., *New synthetic amphiphilic polymers for steric protection of liposomes in vivo.* J Pharm Sci, 1995. **84**(9): p. 1049-53.

180. Immordino, M.L., F. Dosio, and L. Cattel, *Stealth liposomes: review of the basic science, rationale, and clinical applications, existing and potential.* Int J Nanomedicine, 2006. **1**(3): p. 297-315.

181. Ishida, T., et al., *The accelerated clearance on repeated injection of pegylated liposomes in rats: laboratory and histopathological study.* Cell Mol Biol Lett, 2002. **7**(2): p. 286.

182. Hatakeyama, H., et al., *Development of a novel systemic gene delivery system for cancer therapy with a tumor-specific cleavable PEG-lipid.* Gene Ther, 2007. **14**(1): p. 68-77.

183. Akhtar, N.H., et al., *Prostate-specific membrane antigen-based therapeutics.* Adv Urol, 2011. **2012**: p. 973820.

184. Kularatne, S.A., et al., *Prostate-specific membrane antigen targeted imaging and therapy of prostate cancer using a PSMA inhibitor as a homing ligand.* Mol Pharm, 2009. **6**(3): p. 780-9.

185. Galsky, M.D., et al., *Phase I trial of the prostate-specific membrane antigen-directed immunoconjugate MLN2704 in patients with progressive metastatic castration-resistant prostate cancer.* J Clin Oncol, 2008. **26**(13): p. 2147-54.

186. Zhao, Y., et al., *Prodrug strategy for PSMA-targeted delivery of TGX-221 to prostate cancer cells.* Mol Pharm, 2012. **9**(6): p. 1705-16.

187. Kolishetti, N., et al., *Engineering of self-assembled nanoparticle platform for precisely controlled combination drug therapy.* Proc Natl Acad Sci U S A, 2010. **107**(42): p. 17939-44.

188. N.I.H, B.T., *A Study of BIND-014 Given to Patients With Advanced or Metastatic Cancer.* 2013.

189. Gabizon, A., et al., *In vivo fate of folate-targeted polyethylene-glycol liposomes in tumor-bearing mice.* Clin Cancer Res, 2003. **9**(17): p. 6551-9.

190. Kukowska-Latallo, J.F., et al., *Nanoparticle targeting of anticancer drug improves therapeutic response in animal model of human epithelial cancer.* Cancer Res, 2005. **65**(12): p. 5317-24.

191. Said, H.M., *Cellular uptake of biotin: mechanisms and regulation.* J Nutr, 1999. **129**(2S Suppl): p. 490S-493S.

192. Kim, J.H., et al., *Synthesis and evaluation of biotin-conjugated pH-responsive polymeric micelles as drug carriers.* Int J Pharm, 2012. **427**(2): p. 435-42.

193. Yellepeddi, V.K., A. Kumar, and S. Palakurthi, *Biotinylated poly(amido)amine (PAMAM) dendrimers as carriers for drug delivery to ovarian cancer cells in vitro.* Anticancer Res, 2009. **29**(8): p. 2933-43.

194. Chen, S., et al., *Mechanism-based tumor-targeting drug delivery system. Validation of efficient vitamin receptor-mediated endocytosis and drug release.* Bioconjug Chem, 2010. **21**(5): p. 979-87.

195. Syrigou, E.I., et al., *Hypersensitivity reactions to oxaliplatin: a retrospective study and the development of a desensitization protocol.* Clin Colorectal Cancer, 2009. **8**(2): p. 106-9.

196. Wheate, N.J., *Improving platinum(II)-based anticancer drug delivery using cucurbit[n]urils.* J Inorg Biochem, 2008. **102**(12): p. 2060-6.

197. Montes-Navajas, P., et al., *Cucurbituril complexes cross the cell membrane.* Photochem Photobiol Sci, 2009. **8**(12): p. 1743-7.

198.   Kim, J., et al., *Carbohydrate wheels: cucurbituril-based carbohydrate clusters.* Angew Chem Int Ed Engl, 2007. **46**(39): p. 7393-5.

199.   Russell-Jones, G., K. McTavish, and J. McEwan, *Preliminary studies on the selective accumulation of vitamin-targeted polymers within tumors.* J Drug Target, 2010. **19**(2): p. 133-9.

200.   Pirollo, K.F. and E.H. Chang, *Does a targeting ligand influence nanoparticle tumor localization or uptake?* Trends Biotechnol, 2008. **26**(10): p. 552-8.

201.   Veronese, F.M. and G. Pasut, *PEGylation, successful approach to drug delivery.* Drug Discov Today, 2005. **10**(21): p. 1451-8.

202.   Shenoi, S. and G. Friedland, *Extensively drug-resistant tuberculosis: a new face to an old pathogen.* Annu Rev Med, 2009. **60**: p. 307-20.

203.   Wheate, N.J., et al., *Multi-nuclear platinum complexes encapsulated in cucurbit[n]uril as an approach to reduce toxicity in cancer treatment.* Chem Commun (Camb), 2004(12): p. 1424-5.

204.   Park, K.M., et al., *Cucurbituril-based nanoparticles: a new efficient vehicle for targeted intracellular delivery of hydrophobic drugs.* Chem Commun (Camb), 2009(1): p. 71-3.